Chapter

An Overview of Polymer-Dispersed Liquid Crystal Composite Films and Their Applications

Anuja Katariya Jain and Rajendra R. Deshmukh

Abstract

Inherent and incredible properties of liquid crystals (LC) such as optical and dielectric anisotropy make them special candidates for flat-panel display devices; bi-stable reflective displays; high-definition spatial light modulators; switchable windows; haze-free normal- and reverse-mode light shutter devices; projectors; optical, thermal and strain sensors; tuneable lenses; etc. Non-linear response of LC material to the applied electric field is very useful in the above-mentioned applications. When a low molecular weight LC material is doped in a high molecular weight polymer matrix to obtain polymer-dispersed liquid crystal (PDLC) films, it offers flexibility and mechanical strength (structural stabilization) to the composite films—PDLC devices. Depending upon the concentration of monomer/polymer, these composite films are classified as polymer-stabilized liquid crystal (PSLC), PDLC and holographic PDLC (HPDLC) films. Depending upon the process conditions, we get phase-separated randomly dispersed micron-sized LC droplets in a continuous polymer matrix. These nematic LC droplets exhibit light scattering transmission properties depending on their orientation, which can be controlled by external electric field. This chapter gives deep insight about operating principle, phase separation techniques involved, alignment of LC and controlling LC droplet morphology of PDLC films to obtain desired properties. In order to improve the optical efficiency and to obtain the desired result from PDLC films, various guest entities such as dye and nanomaterials are doped in the host LC material. This chapter also accounts for various possible LC dopants desired for improving the electro-optic (EO) and dielectric properties of PDLC devices. Various applications of PDLC composite films are also described in this chapter.

Keywords: nematic liquid crystal, polymer-stabilized liquid crystal, polymer-dispersed liquid crystal, holographic polymer-dispersed liquid crystal, phase separation techniques, electro-optic and dielectric properties of PDLC

1. Definition and history of liquid crystals

Liquid crystal (LC) is a thermodynamic phase of a condensed matter, intermediate of (in between) conventional isotropic liquid and three dimensionally ordered solid crystal with only orientational order but no positional order [1]. It holds

properties of liquid such as fluidity, coalescence and formation of droplets as well as crystalline properties such as order and anisotropy in optical, electrical and magnetic properties (as summarized in **Table 1**) [2]. The difference between molecular arrangement of solid, liquid crystal and liquid is shown in **Figure 1**.

This phase of matter was discovered by the Austrian botanist Friedrich Reinitzer in the year 1888 while he was studying the compounds cholesteryl benzoate and cholesteryl acetate. He observed colored phenomena occurring in melts of cholesteryl acetate and cholesteryl benzoate. In addition, he reported that the compound cholesteryl benzoate has two distinct melting points. Its crystal transforms into hazy liquid at a temperature 145.5°C, and with the further increase in temperature, it suddenly turns into isotropic liquid at a temperature 178.5°C [3]. The word "liquid crystal" for this unusual phase of material was coined by German Physicist, Otto Lehmann, a specialist in polarizing optical microscopy [4]. Friedrich Reinitzer's and Otto Lehmann's studies revealed that liquid crystals (LCs) can rotate the direction of polarization of light and reflect circularly polarized light [5]. The history of the development of LCs can be divided into three phases: the first phase is from the discovery of LC (1888) to the acceptance of its existence (1925). Friedel's article about classification of LC, along with the publications on synthesis and studies of new LC materials by organic chemists in Germany, notably Vorlander [6, 7], provided a firm basis for the development of the subject. In the period from 1925 to about 1960, research in the field of LC was at a low level; however contribution of some devoted researcher has been summarized here: Vorlander synthesized a number of compounds forming LC phases, some of them showing up to three different mesophases. A lamellar and tilted lamellar structure was found by Herrmann for some thallium soaps [8]. In this period, the effect of external electric or magnetic field on the LC has been recognized, modifications of surface to orient LC has been done, and significance of anisotropic physical properties of aligned LC has been understood, which was the foundation of display technology of the future world. Synthesis of new LC materials and their structure–property

Solid	Liquid crystal	Liquid
Anisotropic	Anisotropic	Isotropic
Rigidity	Fluidity	Fluidity
Ordered	Ordered	Disordered
3-D lattice	0/1/2 lattice	No lattice

Table 1.
Properties of solid, liquid crystal and liquid.

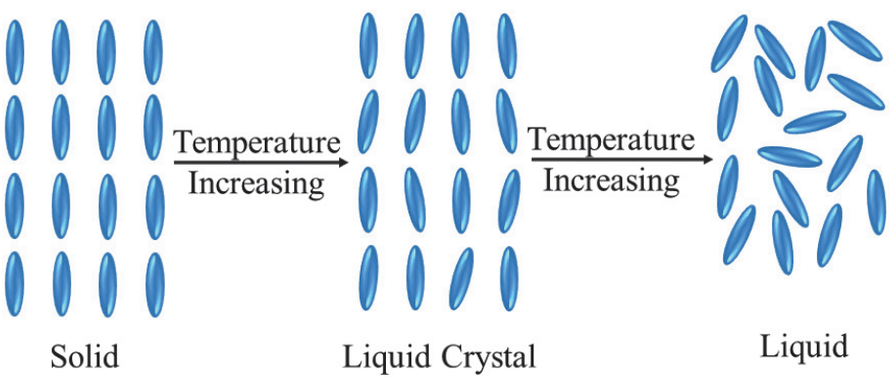

Figure 1.
Molecular arrangement of solid, liquid crystal and liquid.

relationships has been explained using principles commencing from swarm theory to continuum theory. Identification of mesophases, determination of transition temperatures and awareness about defect textures through polarizing optical microscope (POM) appreciably helped in developing a new era of LC applications [9]. The beginning of the third period (1960 to the present time) gives us a famous statistical Maier and Saupe mean field theory which states about the isotropic-nematic phase transition [10, 11]. Synthesis of new LC materials is ongoing. Classification, molecular structure and properties of LCs, defects characterizing microscopic textures of LC phases and existence of blue phases are some topics, which are now well understood [12–14]. The decade of 1970 is known for announcing application of LCs as display devices. Expansion of theories and their employment in practical applications give rise to new LC science from display world to beyond display technology as well. Having high resolution and high brightness and being lightweight, flexible and an energy saver make LC devices attractive and competitive in the high-tech world. LC science has been now well acknowledged and documented, but it is still thriving. Liquid crystal displays (LCDs) are like a milestone for the future world, but a continuous evolution via dedicated research is still anticipated.

2. Types and phases of liquid crystals

This special class of materials are moderate-sized organic molecules, composed of flat segments like benzene rings, double bonds, strong dipole and easily polarizing groups [15]. Depending upon the molecular structure, LC compounds may have one or many phases (polymorphism), characterized by order and symmetry. LCs can be broadly classified into two generic classes: thermotropic and lyotropic [1]. Commonly found LCs from either group possess a remarkable polymorphism and give rise to various mesophases such as nematic, smectic, cholesteric, columnar and blue phases in thermotropic LC and discontinuous, hexagonal, lamellar, bicontinuous, reverse hexagonal and inverse cubic phases in lyotropic LC, depending upon the type, amount and proportion of ordering in it [16]. Sometimes, thermotropic LCs are also cataloged as rod-like (calamatic) and disk-like (discotic). Thermotropic LC are single compounds, whereas lyotropic LC are always mixtures. The LiqCryst database accounts for more than 39,000 nematic phase compounds, about 18,000 chiral compounds and more than 6000 ferroelectric SmecticC* phase compounds [17]. Some day-to-day life examples of LCs are soap solution, tobacco mosaic virus, protein and cell membrane.

2.1 Thermotropic liquid crystals

Thermotropic LCs are comprised of rod-like organic molecules and exhibit phase transition into the LC phase as a function of temperature. At very low temperature, most LC materials are in anisotropic phase, but with the increase in temperature, these LC materials acquire isotropic phase along with so many intermediate phases such as smectic, nematic, cholesteric etc., which are described below [1, 15].

2.1.1 Nematic phase

As the temperature of isotropic phase (no positional or orientation order) is lowered, the LC material undergoes a transition to the nematic phase. It is a transparent or translucent low-viscosity liquid and a stable LC phase in a particular

temperature range. It is the most common LC phase of calamatic or rod-shaped organic molecules, as shown in **Figure 2(a)** [4].

The structure of a typical nematic LC is shown in **Figure 2(b)**, and each entity has exclusive function. The terminal group (e.g. $(C_6H_{13})_n$) determines dielectric constant and anisotropy, and benzene rings provide short-range molecular forces which affect electrical and elastic properties; the linkage group stabilizes LC against moisture, UV radiation and chemicals, and the side chain (e.g. cyano group) influences the elastic constants and transition temperature of LC. **Figure 2(c)** represents example of nematic LC. Nematic LCs lack positional order, but have self-aligning long-range directional order with their long axes almost parallel, characterized by a nematic director $\hat{n}$, which is the average direction of the ensemble of molecules [15]. The director $\hat{n}$ is a function of space with unit magnitude and $\hat{n} = -\hat{n}$. Thus, the LC molecules in nematic phase are free to flow with three translational degrees of freedom, and their centre of mass positions is randomly distributed as in a liquid, but still maintains their long-range directional order. In nematic phase of LC, one axis is generally longer and preferred than the other two, i.e., they are uniaxial and can be approximated as cylinders and rods. The easy alignment of these uniaxial nematic LC using electric or magnetic field makes them optically uniaxial and prominent in display devices. However, some LCs are biaxial nematic, i.e., in addition to orienting along their long axis, they also orient along a secondary axis [1, 18]. As the nematic LC is relatively a low-viscosity fluid, it easily gets deformed by small external forces. In a deformed LC, the director direction $\hat{n}$ changes from point to point. These LC deformations can be explained using three basic deformations: splay, twist and bend,

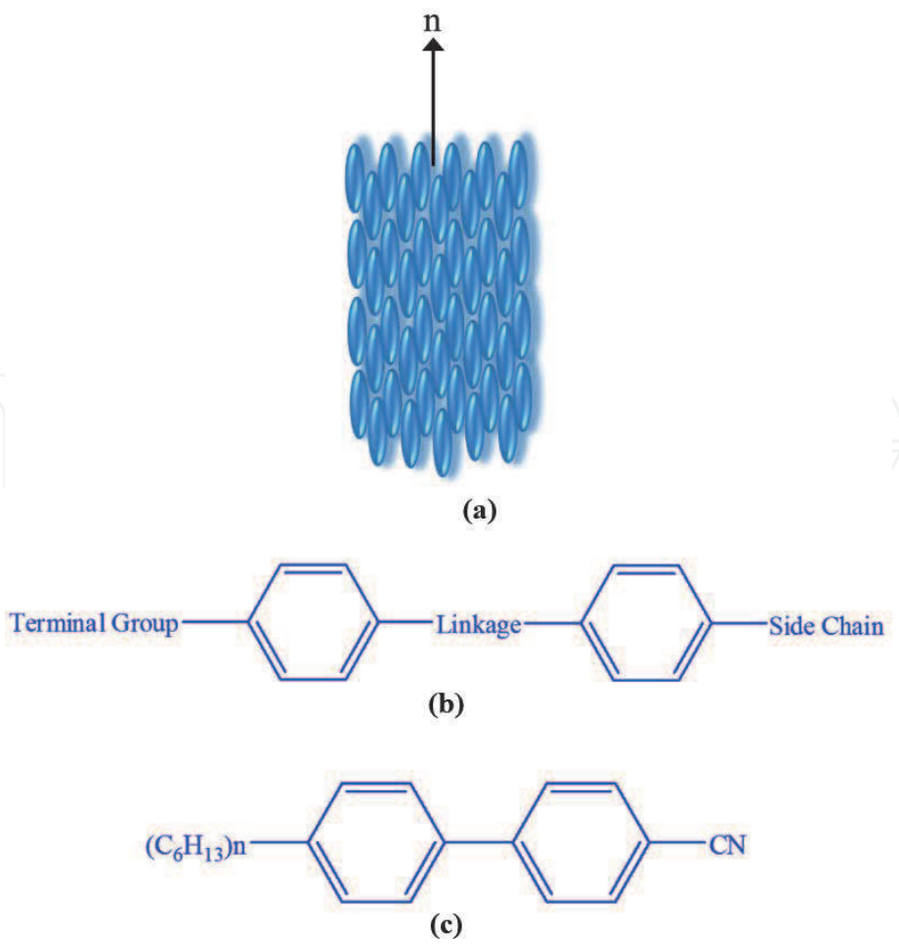

Figure 2.
(a) Molecular arrangement, (b) general chemical structure and (c) example of nematic liquid crystal.

and their associated elastic constants are K_{11}, K_{22} and K_{33}, respectively. The free energy of distortions of nematic LC is given by Eq. (1) [19]:

$$F = \frac{1}{2}\left[K_{11}\left(\nabla.\vec{n}\right)^2 + K_{22}\left(\vec{n}.\nabla\times\vec{n}\right)^2 + K_{33}\left(\vec{n}\times\nabla\times\vec{n}\right)^2\right] \quad (1)$$

2.1.2 Cholesteric phase

The cholesteric LC phase is typically composed of nematic mesogenic molecules containing chiral centres. Chiral molecules have no internal planes of symmetry and produce a twist in the nematic structure by inducing intermolecular forces which favour alignment between molecules at a slight angle to one another. They are composed of quasi-nematic layers. Their individual directors are turned by a fixed angle on proceeding from one layer to the next as shown in **Figure 3(a)**. The rotation is constrained in a plane perpendicular to the pitch direction. The pitch (p) is the distance over which the director of LC molecules undergoes a full twist of 2π angle. As the phase directors at 0° and 180° are equivalent, the arrangement of molecules in the chiral nematic phase repeats at every half pitch (p/2). Due to this strong twisting effect, in a definite spectral range, cholesteric phase shows a selective reflection of the circularly polarized light of wavelength equal to pitch length. The pitch length p can be altered by varying temperature or adding other materials in LC host. With the increase in temperature, the angle at which the director changes increases, which in turn decreases the pitch length and vice versa [4, 20, 21]. The free energy of distortions in cholesteric LC is given by Eq. (2)

$$F = \frac{1}{2}\left[K_{11}\left(\nabla.\vec{n}\right)^2 + K_{22}\left(\vec{n}.\nabla\times\vec{n}+q_0\right)^2 + K_{33}\left(\vec{n}\times\nabla\times\vec{n}\right)^2\right] \quad (2)$$

where $q_0 = \frac{2\pi}{p}$ corresponds to the intrinsic twist of the system. For nematics p is infinite; therefore q_0 vanishes from free energy equation of nematic LC [22]. **Figure 3(b)** represents example of cholesteric LC.

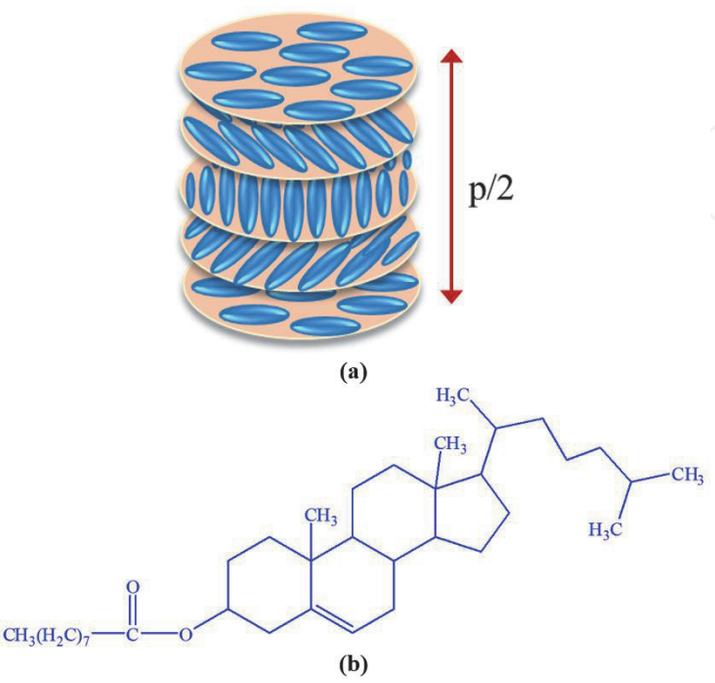

Figure 3.
(a) Molecular arrangement and (b) example of cholesteric LC phase.

2.1.3 Blue phase

The blue phases are a set of thermodynamically distinct phases that occur at the boundary of the helical phase and isotropic phase of highly chiral LCs within a small temperature range. It was first observed by Reinitzer in 1888 as an unstable phase, and after a century (in 1975), they were shown to be stable and distinct thermodynamic phase by Armitage and Price [23, 24]. In the absence of electric fields, in the order of increasing temperature, there can be three blue phases: BPI*, BPII* and BPIII*. BPI* has body-centred cubic symmetry, BPII* possess simple cubic symmetry and BPIII* is with a local cubic lattice only. BPI* and BPII* reflect blue light, as their name suggest, whereas BPIII* phase is observed at highest temperature and appears fogy because of which it is called as fog phase or blue fog [25, 26]. The building structure element of BPI* and BPII* phase is double-twist cylinders (**Figure 4(a)**). The double-twist cylinder is a local structure of minimum free energy with local director rotating around any given radius of the cylinders. Free energy of blue phases is lower than the free energy of chiral nematic phase because here molecules twist in two dimensions simultaneously (**Figure 4(b)**). As the local twist is increased, the cylinder becomes strained and distorted. Therefore, blue phase cannot have a single, large double-twist structure; instead it consists of many of these double-twist structures arranged in a lattice with cubic symmetry. But for elastic reasons, it is only possible by introducing a lattice of topological defects [27, 28] as shown in **Figure 4(c)**.

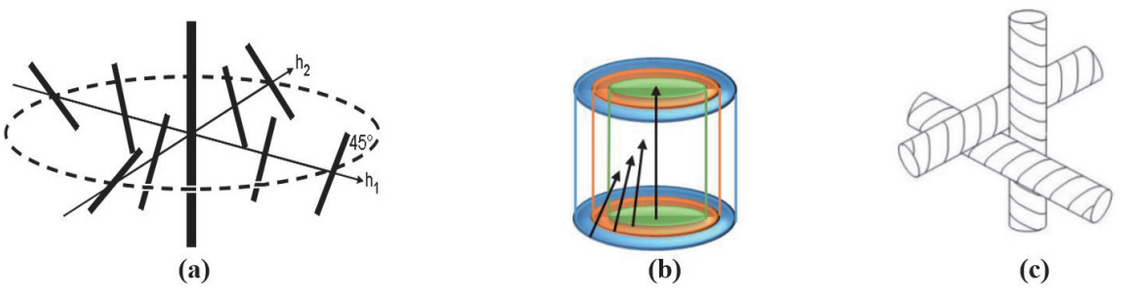

Figure 4.
(a) Double twisted structure with two helical axes, h1 and h2 in a blue phase LC, the directors perform a rotation of 90° across the diameter. (b) Perspective view of the double twist cylinder, the angle of directors at the outer edge of the cylinder is 45°, relative to the central axis. (c) Local arrangement of three double twist cylinders forming a defect region, which eventually leads to the three-dimensional, cubic lattice of defects observed in blue phases.

2.1.4 Smectic phase

Upon cooling, nematic phase LC transforms into smectic phase. The distinguished feature of smectic phase LC is their stratification. In addition to the orientational order, their molecules form well-defined layers which can slide over one another. Thus, they are positionally ordered along one direction with two translational degrees of freedom. The increased order indicates that the smectic phase is more solid-like than the nematic. Several different smectic classes (phases) have been discovered so far, and some of them are discussed here. In the smectic A (SmA) phase, on average, the molecules are parallel to one another possessing orientational order and are arranged in layers, with the long axes perpendicular to the layer plane. The orientational order is characterized by the director $\hat{n}$ analogous to the nematic LC but restricted within a specific layer/plane. Within the layers the centre of mass of the molecules is ordered at random and has no correlation between intra-plane centres of masses. Thus, the SmA phase (**Figure 5(a)**) possesses the one-dimensional quasi long-range positional order, and within the layers,

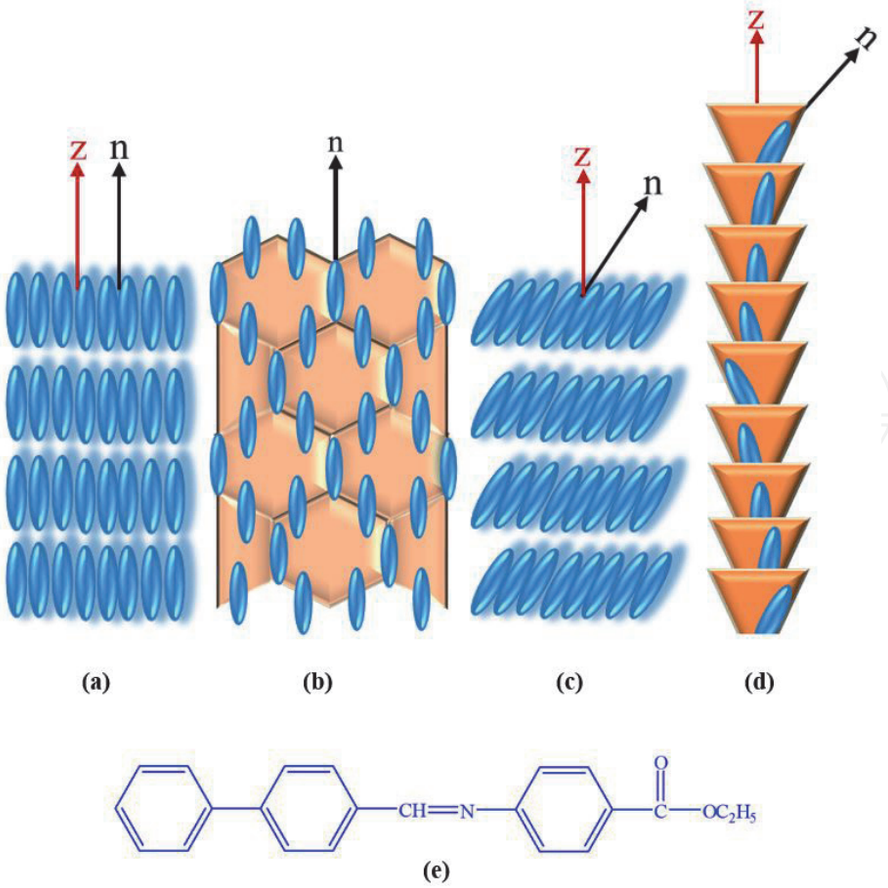

Figure 5.
Molecular arrangement in (a) smectic A phase, (b) smectic B phase, (c) smectic C phase, (d) smectic C phase and (e) example of smectic phase.*

molecules show relatively high mobility. The thickness of layer is equal to molecular length. The SmA LCs are optically positive and uniaxial with the optic axis parallel to the molecular long axes. The layers of the SmA LC can be bended in a way causing splay deformation. Bend and twist deformations are prohibited in this LC phase. The free energy density equation is given by Eq. (3)

$$F = \frac{1}{2}\left[K_{11}\left(\nabla.\vec{n}\right)^2\right] \tag{3}$$

Upon further cooling, the smectic B (SmB) (**Figure 5(b)**) and smectic C (SmC) (**Figure 5(c)**) phases are formed. The SmB mesophase orients with the director perpendicular to the smectic plane, but the molecules are arranged into a network of hexagons within the layer. In the SmC mesophase, molecules are arranged as in the SmA mesophase, but the director is at a constant tilt angle measured normally to the smectic plane. For some material the tilt angle is constant, but for others it is temperature dependent. The centre of mass of the molecules is randomly oriented/ordered, and the molecules are free to rotate around their long axes. SmC phases are optically biaxial. If the molecules of SmC LC are in chiral state, then they are designated as smectic C* (SmC*) (**Figure 5(d)**) state, and the direction of the director projection is rotated from layer to layer forming a helix. Therefore, these phases appear optically positive uniaxial and show optical activity and selective reflection similar to the cholesteric phase. The SmC* shows ferroelectric properties if their molecules have permanent dipole moment perpendicular to their long axes.

In some smectic phases (e.g. Smectic G phase), the molecules are affected by the various layers above and below them. Therefore, a small amount of

three-dimensional order is observed in them [1, 2, 15, 21]. **Figure 5(a–d)** shows the molecular arrangement in all types of smectic phases, and **Figure 5(e)** is an example of smectic phase.

2.1.5 Discotic phase

Apart from the rod-like molecules, more advanced-shaped LCs are possible such as disk-like (**Figure 6(a)**) which can give rise to other types of ordering. They were first discovered in carbon precursor compounds with a transient existence by Brooks and Taylor in stable low molecular weight systems [29, 30].

Disk-shaped LC molecules can orient themselves in a layer-like manner termed as the discotic nematic phase. This phase is called as a discotic columnar, if their disks pack into stacks/columns. Again, these columns may organize themselves into rectangular or hexagonal arrays [31]. Discotic LCs are composed of an aromatic core surrounded by flexible chains as shown in **Figure 6(b)**. The aromatic cores allow charge transfers in the stacking direction through the π conjugate system, due to which these LCs become electrically semiconducting along the stacking direction.

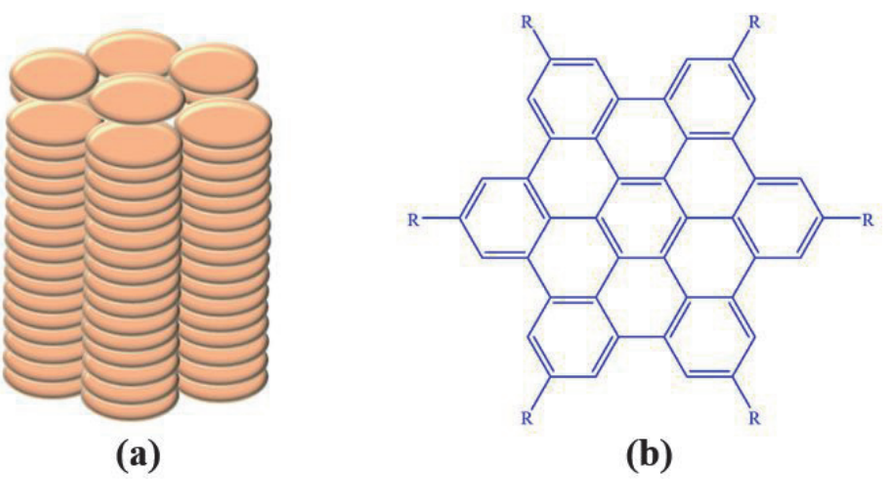

Figure 6.
(a) Molecular arrangement and (b) example of disk-shaped LC.

2.1.6 Banana-shaped LC

Sterically induced packing of bent core (banana-shaped) LC molecules (**Figure 7(a)**) is interesting from many viewpoints. These are the first ferroelectric and anti-ferroelectric LCs, which contain no chiral carbon atoms; however they can introduce chirality to the system [32]. One example of banana-shaped LC is shown in **Figure 7(b)**.

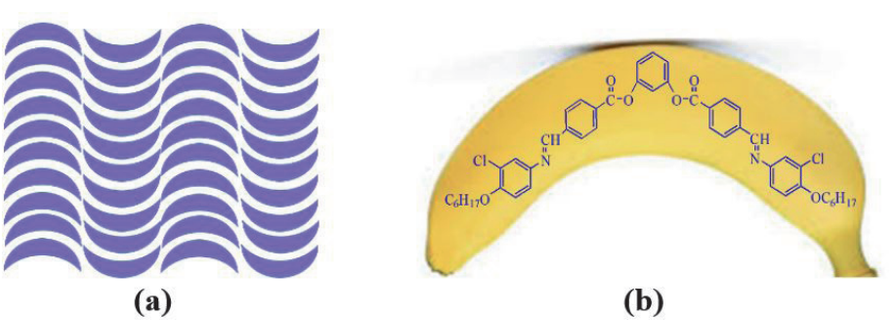

Figure 7.
(a) Molecular arrangement and (b) example of banana-shaped LC.

2.2 Lyotropic liquid crystals

Another class of LCs is named as lyotropic LCs, having two distinct parts/building blocks—hydrophobic and hydrophilic. Their properties depend on the concentration in the solvent and the shape of the molecule. Soaps and detergents are some common examples of lyotropic LCs. It consists of two or more components that exhibit phase transition into the LC phase as a function of both temperature and concentration of the molecules in a solvent (generally water). The solvent molecules fill the space around the compounds and provide fluidity to the system. In lyotropics, along with temperature, concentration is another degree of freedom that enables them to induce a variety of different phases. A compound which has two immiscible hydrophobic and hydrophilic parts within the same molecule is termed as an amphiphilic molecule. Depending on the volume balances between the hydrophobic part and hydrophilic part, many amphiphilic molecules show lyotropic liquid-crystalline phase sequences. These structures are formed because of the micro-phase segregation of two incompatible components on a nanometre scale. At very low amphiphile concentration, the molecules are randomly dispersed in a solvent without any order. At slightly higher concentration, amphiphilic molecules spontaneously assemble into micelles or vesicles. This is done to "hide" the hydrophobic tail of the amphiphile inside the micelle core, exposing a hydrophilic (water-soluble) surface to aqueous solution. However, these spherical objects do not order themselves in solution. At higher concentration, the assemblies are well ordered. An example of such phase is a hexagonal columnar phase (**Figure 8(a)**). In this phase, the amphiphiles form long cylinders (again with a hydrophilic surface) that arrange themselves into a roughly hexagonal lattice. This is called the middle soap phase. At further higher concentration, a lamellar phase (**Figure 8(c)**) (neat soap phase) may form. In this phase extended sheets of amphiphiles are separated by thin layers of water. For some systems in between the hexagonal and lamellar phases, a cubic phase (**Figure 8(b)**) (viscous isotropic) may exist. In this phase spheres are formed that create a dense cubic lattice. These spheres may also be connected to one another, forming a bicontinuous cubic phase. The objects created by amphiphiles are usually spherical (as in the case of micelles), but sometimes disk-like (bicelles), rod-like or biaxial (all three micelle axes are distinct) objects are also possible. These anisotropic self-assembled nanostructures can then order themselves in similar way as thermotropic LCs do, forming large-scale versions of all the thermotropic phases (such as a nematic phase of rod-shaped micelles). For some systems, at high concentrations, inverse phases are observed, i.e., one may generate an inverse hexagonal columnar phase (columns of water encapsulated by amphiphiles) or an inverse

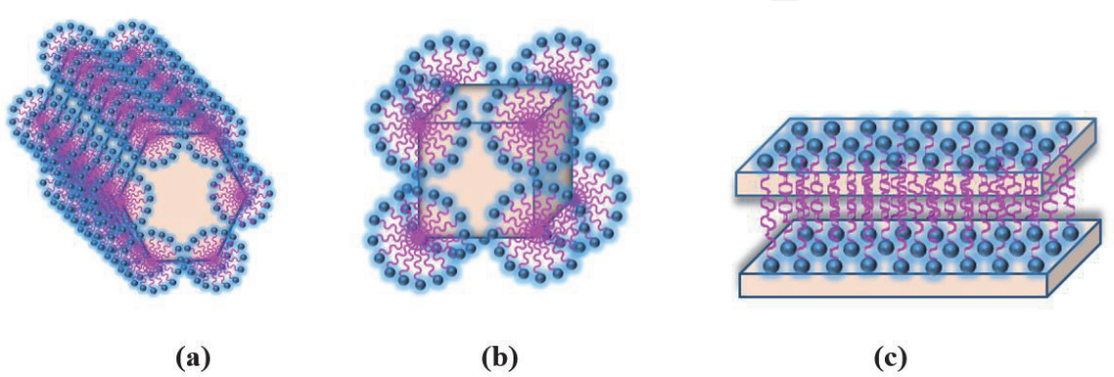

Figure 8.
Molecular arrangement of (a) hexagonal phase, (b) micellar cubic phase and (c) lamellar phase of lyotropic LC.

micellar phase (a bulk LC sample with spherical water cavities) [33, 34]. Different lyotropic phases are listed below:

1. Hexagonal phase (hexagonal columnar phase) (middle phase) (**Figure 8(a)**)

2. Discontinuous cubic phase (micellar cubic phase) (**Figure 8(b)**)

3. Lamellar phase (**Figure 8(c)**)

4. Bicontinuous cubic phase

5. Reverse hexagonal columnar phase

6. Inverse cubic phase (inverse micellar phase)

By varying concentration, even within the same phases, their self-assembled structures can be tuned. For example, in lamellar phases, distance between the layers increases with the solvent volume. Since lyotropic LCs indirectly depend on a subtle balance of intermolecular interactions, it is difficult to analyse their properties and structures as compared to those of thermotropic LCs. Similar type of phases and properties has been observed in immiscible diblock copolymers.

3. Properties of liquid crystals

3.1 Order parameter

To quantify amount of the orientational order in the LC phase, the term order parameter has been introduced; it is a second-rank symmetric traceless tensor defined as

$$S = \frac{1}{2}\left\langle 3\cos^2\theta - 1\right\rangle; \text{For nematic phase } 0.5 < S < 0.7 \tag{4}$$

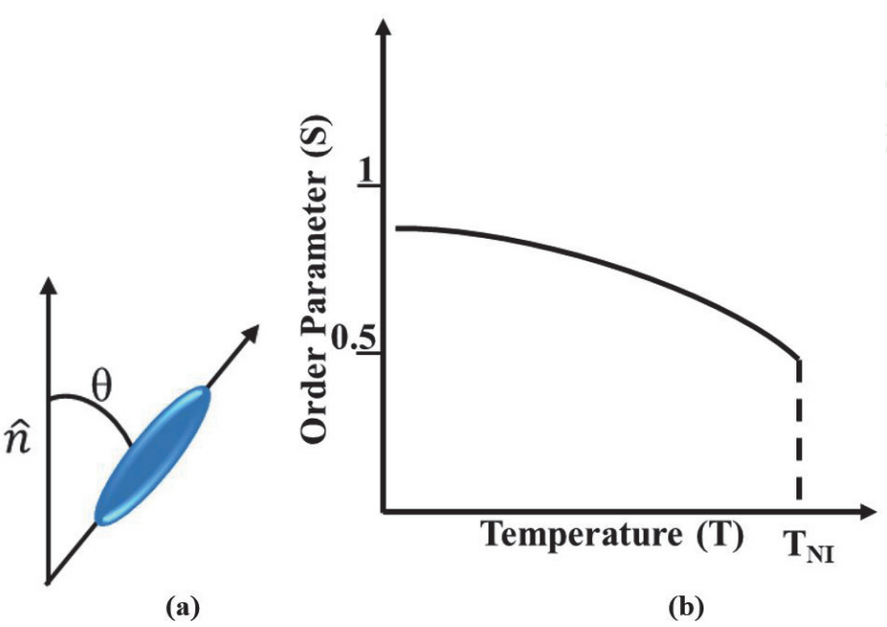

Figure 9.
(a) Liquid crystal director direction and (b) temperature dependence of order parameter.

where θ is the angle between the axis of an individual molecule and the local director $\hat{n}$ as shown in **Figure 9(a)**. It is the preferred direction in a volume element of a LC, and the average is taken over the complete ensemble. The bracket denotes both temporal and spatial average. For a completely isotropic sample, S = 0, whereas for a perfectly aligned sample, S = 1. For a typical LC sample, the value of S is 0.3 to 0.9, and for nematic LC, it is 0.5–0.7. **Figure 9(b)** shows the temperature dependence of order parameter (S), which follows an inverse relation [11, 35, 36].

3.2 Anisotropy in liquid crystals

LCs exhibit uniaxial symmetry around the director, which gives them shape anisotropy. The shape anisotropy of LC and their resulting interactions with the surrounding environment (applied fields) leads to an anisotropy in many other physical properties such as refractive index (RI), dielectric permittivity, magnetic susceptibility, viscosity and conductivity.

3.2.1 Optical anisotropy

LCs are optically anisotropic materials and show birefringence. LCs have two direction-dependent refractive indices, ordinary RI (n_o) and extraordinary RI (n_e) with birefringence:

$$\Delta n = n_e - n_o. \tag{5}$$

Also, the average RI is given by

$$n_{av} = \sqrt{\frac{1}{3}\left(n_e^2 + 2n_o^2\right)} \tag{6}$$

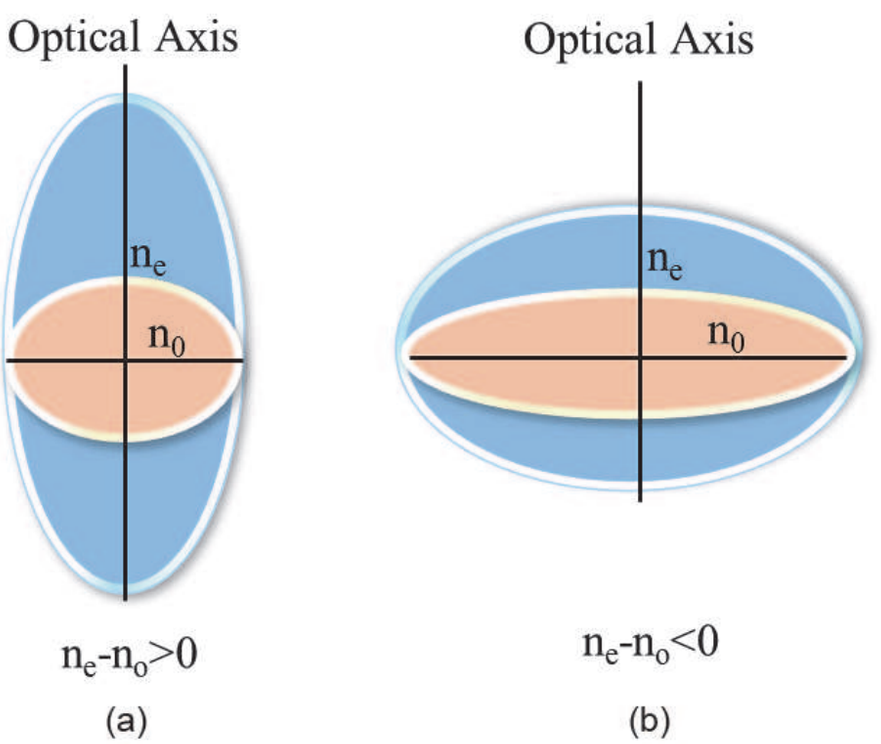

Figure 10.
Indicatrix of optically uniaxially material: (a) positive birefringent material and (b) negative birefringent material.

The value of Δn may be positive or negative, which can be represented by indicatrix as shown in **Figure 10**. For uniaxial crystal, it is ellipsoid where the rotational axis is identical to the optical axis [34, 37, 38].

For rod-like molecules (Nematic LC) $n_e > n_o$, where Δn is positive and between 0.02 and 0.4. For discotic and chiral nematic molecules $n_e < n_o$, and thus negative birefringence is associated with the discotic or columnar phase.

The values of optical anisotropy Δn can be increased [39]:

1. by replacing saturated aromatic rings with the unsaturated ones
2. with the elongation of the conjugation chain parallel to the long molecular axis
3. by increasing the values of the order parameter S or decreasing the value of temperature
4. by shortening the alkyl chain of the end molecular groups in homologous series in the form of even-odd alternation

In general, birefringence Δn of LCs decreases as the wavelength of the incident light or the temperature increases. Also, if the temperature of the LC material is raised up to its clearing point/nematic-isotropic temperature (T_{NI}), its internal order gets destroyed, and it behaves like an isotropic liquid with RI n_{iso} as shown in **Figure 11**.

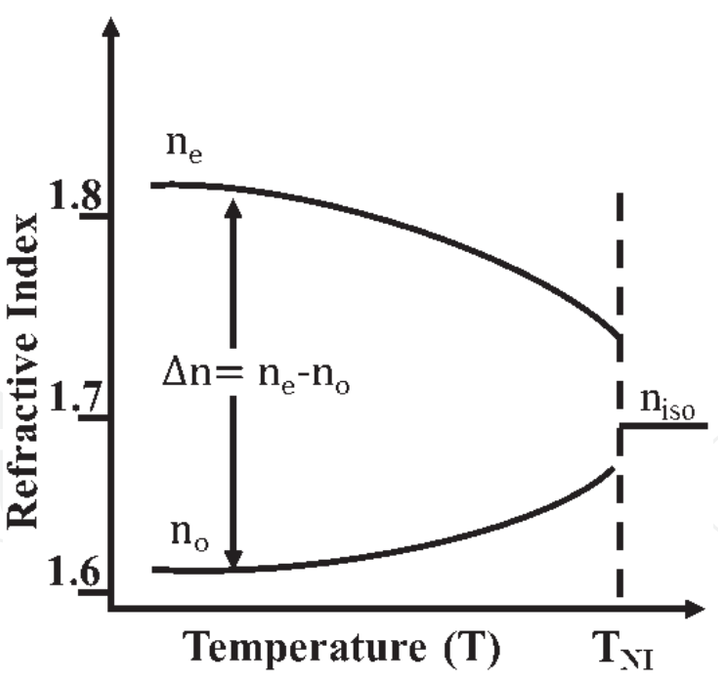

Figure 11.
Temperature dependence of refractive index (RI).

3.2.2 Dielectric anisotropy

Dielectric properties of LCs are related to the response of LC molecules upon application of an electric field. Permittivity is a property of a material that determines how dielectric medium affects and is affected by an electric field. It is determined by the capability of a material to polarize upon application of an electric field and in turn partially cancels the field induced inside the material [40, 41].

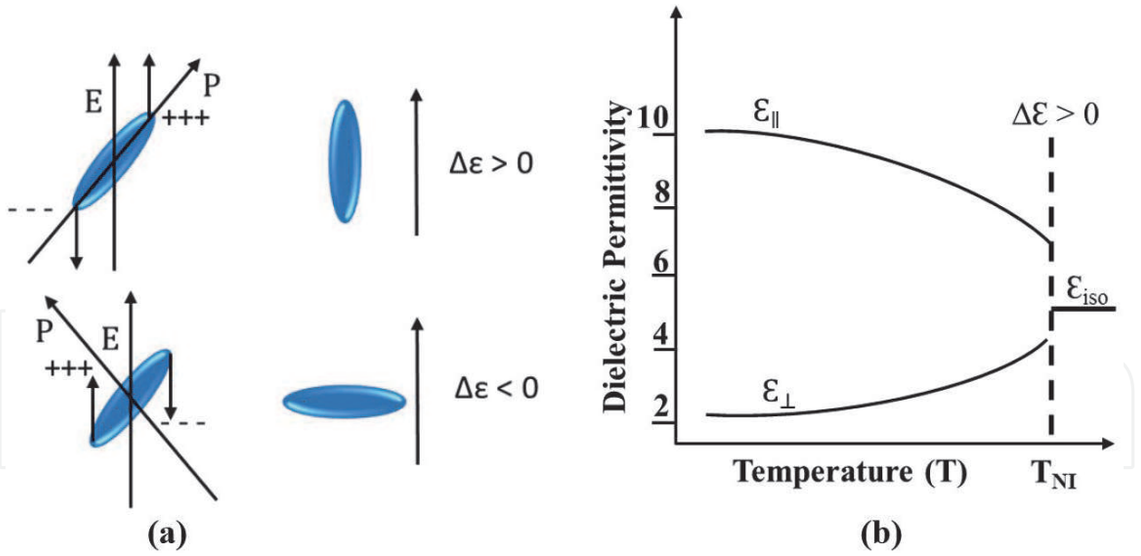

Figure 12.
(a) Alignment of positive and negative dielectric anisotropic LCs in external field, (b) temperature dependence of dielectric constant.

In the LC materials, consisting of non-polar molecules, there is only an induced polarization, which consists of two parts: the electronic polarization (which is also present at optical frequencies) and the ionic polarization. In the LCs with polar molecules, the orientational polarization exists along with the above-mentioned polarization. Considering the uniaxial LC phases in a macroscopic coordinate system, x, y and z, with the z-axis parallel to the director $\hat{n}$, it is possible to distinguish two principal permittivities, parallel to the director $\varepsilon_{\parallel} = \varepsilon_{zz}$ and perpendicular to the director $\varepsilon_{\perp} = 1/2(\varepsilon_{xx} + \varepsilon_{yy})$. $\varepsilon_{\parallel}$ is the characteristic of nematic LCs, as it corresponds to the polarization contribution related to the molecules. Then the dielectric anisotropy $\Delta\varepsilon = \varepsilon_{\parallel} - \varepsilon_{\perp}$ can take positive or negative values. If the value of $\Delta\varepsilon > 0$, then LC molecules align parallel to the field, whereas if the value of $\Delta\varepsilon < 0$, then the LC molecules tend to align perpendicular to the field (**Figure 12(a)**). The graph of temperature dependence of dielectric permittivity for a typical LC (**Figure 12(b)**) shows that magnitude of $\Delta\varepsilon$ usually depends on temperature. With the increase in temperature, liquid crystal material behaves as isotropic liquid with dielectric permittivity ε_{iso} [15].

The mean dielectric permittivity $\bar{\varepsilon}$ is temperature and frequency dependent, which can be described as

$$\bar{\varepsilon} = \frac{1}{3}(\varepsilon_{\parallel} - \varepsilon_{\perp}) \tag{7}$$

3.3 Elastic properties

The behaviour of LCs in an external electric field is highly dependent on their viscoelastic properties. While dealing with the elasticity of the nematic LC, we assume that the order parameter S remains invariable throughout the volume of LC at a constant temperature T and only director $\hat{n}$ changes with external field. The elastic constants of LCs associated with the restoring torques become apparent when the system is perturbed from its equilibrium configuration. These are of the order of 10^{-11} N (especially for nematic and fluid smectic phases), which suggests that a LC can be easily deformed by external forces, such as mechanical, electric or magnetic. The resistance of the LC to the external field gives rise to deformation. Final deformation pattern depends on the contribution of the associated elastic

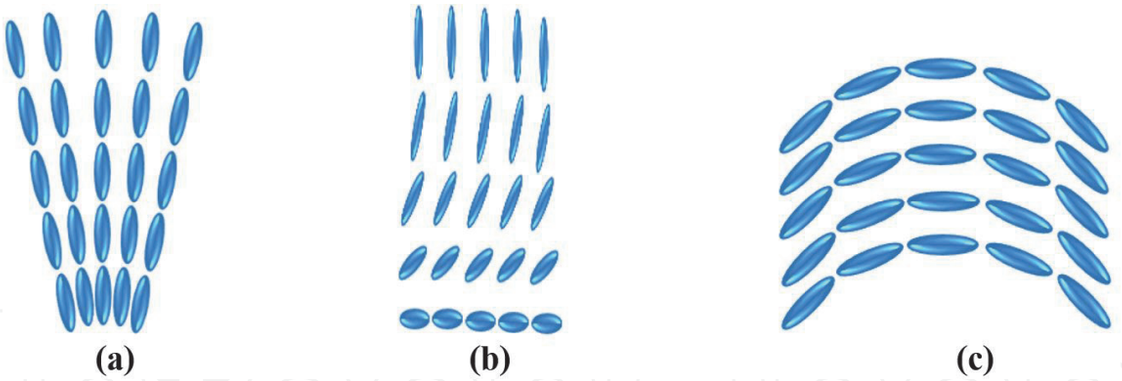

Figure 13.
(a) Splay, (b) twist and (c) bend deformation.

constants in elastic energy. For nematic LCs, it is assumed that change in elastic energy is only due to splay, twist and bend type deformation (**Figure 13**). The increase of free energy F due to these deformations is described by the continuum theory. This theory was first developed by Oseen and Zocher and later reformulated by Frank. It was based on the balance laws for linear and angular momentum [4, 42]. The contribution of each deformation to the overall energy F is given by

$$F = \frac{1}{2}\left[K_{11}(\nabla.n)^2 + K_{22}(n.\nabla \times n)^2 + K_{33}(n \times \nabla \times n)^2\right] \tag{8}$$

where K_{11}, K_{22} and K_{33} are proportionality constants of splay, twist and bend deformations, respectively, often known as Frank elastic constants [19]. They were forced to splay, twist and bend until equilibrium. When the system is in equilibrium, it is in minimum energy state [15]. Other types of deformation are forbidden due to the symmetry and absent polarity.

3.4 Viscosity

The dynamics of LC is described by (i) velocities of the centres of the molecules v and (ii) director field $\hat{n}$. Generally, these variables obey equation of continuity in incompressible liquids, Navier–Stokes equation in anisotropic viscous liquid and the equation of rotation of director in nematic LC. While dealing with the rotation of director, backflow effect should be considered, which states that the rotation of molecules (after removing external field) induces a macroscopic translational motion in LCs. However, the mathematics associated with the above-mentioned equations is insufficient to explain the viscosity behaviour of different LC substances and their mixtures. But in order to develop new liquid crystalline low-viscosity materials, the following phenomenological rules should be remembered [39]:

1. Alkyl end groups provide lower values of viscosity than alkoxy and acyloxy end groups.

2. The viscosity is lower for shorter molecules.

3. Introducing the rings with heteroatoms increases viscosity compared to phenyl analogues.

4. The most viscous bridging groups are the ester group –COO–, the simple bond (as in biphenyls) and the ethane group –CH=CH–.

5. Replacement of phenyl ring by a trans-cyclohexane ring results in reduced viscosity values.

The most useful compounds for reducing viscosity in LC materials are cyclohexane derivatives due to their high clearing temperature, good solubility and low viscosity.

3.5 LC in electric and magnetic field

The dependence of the free energy "*F*" of nematic LC on gradients of the director field is a unique property of LC. Therefore, the measurement of elastic constants in LC is a very crucial part in LC studies. The idea behind K_{ii} measurement is related to the registration of spatial distortions in structure induced by different factors such as electric field, magnetic field and thermal and surface fluctuations for which the following methods can be employed:

1. Optical method (Freedericksz transition)

2. Light scattering

3. Alignment inversion walls

4. Cholesteric-nematic transition

Out of which the optical method based on Freedericksz transition is the simplest and most significant from the application point of view [40].

3.5.1 Freedericksz transition

In the absence of any surface alignment or external field, LC directors of nematic molecules are free to point in any direction. However, it is possible to force the director to point in a specific direction by introducing an outside agent to the system. For example, when a thin layer of polymer (usually a polyimide (PI)) is coated on a glass substrate and rubbed in a single direction with a velvet cloth, it is observed that LC molecules in contact with that surface get aligned along the rubbing direction and achieve uniform director configuration. Upon application of magnetic or electric field for any distortion to occur (to overcome the elastic and viscoelastic forces of LC), the strength of the applied field has to be larger than certain threshold value [21]. Initially, when electric field is low, no change in alignment occurs. However, as we increase electric field above threshold, the LC director changes its orientation from one molecule to the next, and deformation occurs. This threshold is called the Freedericksz threshold, and the transition from a uniform director configuration to deformed director configuration is named as Freedericksz transition. To find out various elastic constants, we need to understand geometry of confined LC molecules and applied external field. The external field may be either electric or magnetic; it is more convenient and accurate to record electric field because measurement of magnetic field near to the sample is a tricky procedure due to the field inhomogeneity, and temperature dependence of Hall probe, etc.

Consider two, coated and rubbed (along *X* direction), conducting glass plates, separated by a distance "*d*". Due to this, LC director tends to align along the direction parallel to the flat surface (*X* direction). Now we consider the following cases which give rise to splay, bend and twist geometries [20].

3.5.1.1 Twist geometry

An electric field is applied perpendicular to the x-axis. Let this be the y-axis. If the anisotropy of the dielectric susceptibility is positive, then the director tends to align along the direction of electric field, rotating away from the x-axis towards the y-axis. Let us call the angle between the director and the x-axis be θ. If we consider the dimensions of the flat pieces of glass to be much larger than the separation, then θ should not be a function of x or y but should depend on z (an axis normal to the surfaces of the glass). This geometry is illustrated in **Figure 14**.

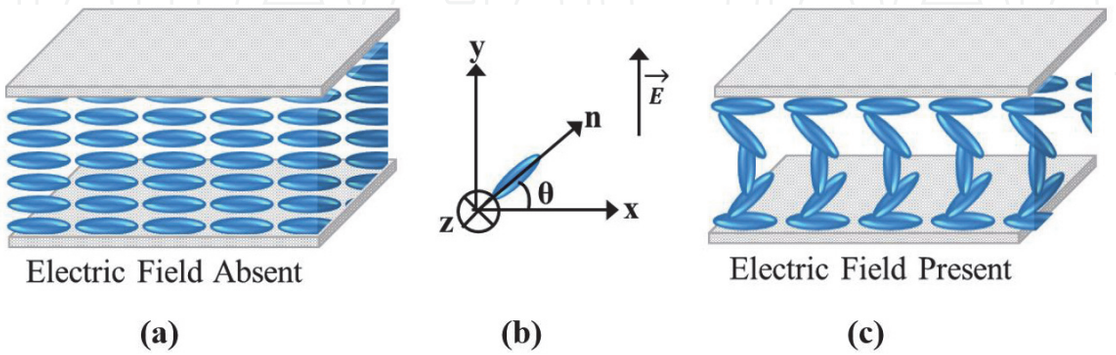

Figure 14.
Twist deformation in nematic LC molecules: (a) initially oriented planar cell, (b) sketch of molecular reorientation, and (c) deformation induced by electric field.

3.5.1.2 Splay geometry

A director is oriented along the x-axis, but now the electric field is applied in the z direction. The director now has x and z components, and $\theta(z)$ is measured from the x-axis to the director in the xz plane as shown in **Figure 15**.

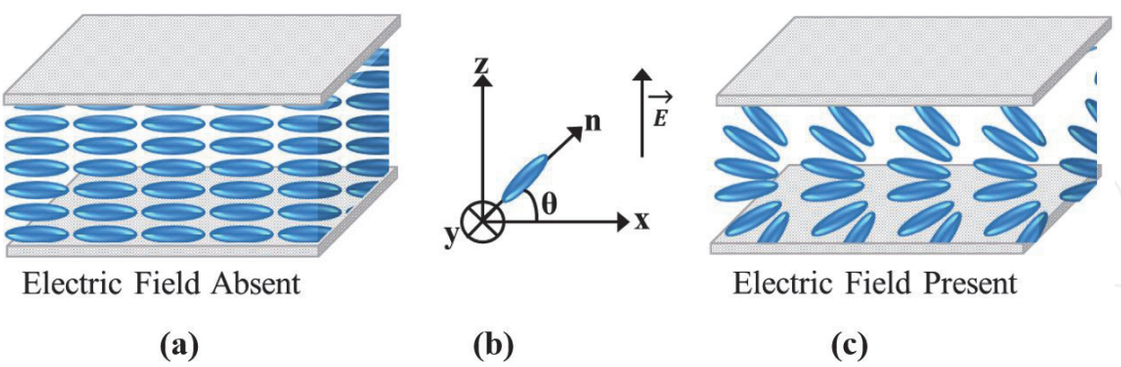

Figure 15.
Splay deformation in nematic LC molecules: (a) initially oriented planar cell, (b) sketch of molecular reorientation, and (c) deformation induced by electric field.

3.5.1.3 Bend geometry

The last geometry also involves both splay and bend. As shown in **Figure 16**, the boundary conditions are such that the undistorted director points along the z-axis and the electric field is applied along the x-axis. The angle $\theta(z)$ now is measured from the z-axis to the director in the xz plane.

The threshold value for deformations of the director $\hat{n}$ in the electric (E_t) and magnetic field (B_t) is given by

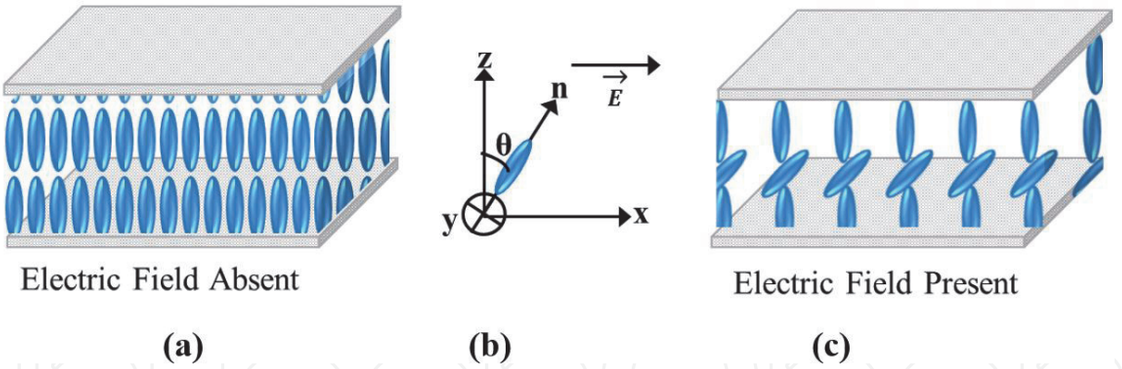

Figure 16.
Bend deformation in nematic LC molecules: (a) initially oriented homeotropic cell, (b) sketch of molecular reorientation, (c) deformation induced by electric field.

$$E_t = \frac{\pi}{d}\sqrt{\frac{K_{ii}}{\varepsilon_0 \Delta\varepsilon}} \tag{9}$$

$$B_t = \frac{\pi}{d}\sqrt{\frac{K_{ii}}{\mu_0^{-1}\Delta\chi}} \tag{10}$$

where K_{ii} is elastic constant; ii = 11, 22, 33 corresponds to splay, bend and twist deformations respectively; μ_0 is permeability of free space and $\Delta\chi$ is anisotropic diamagnetic susceptibility.

3.6 Alignment of liquid crystals

To manufacture LC device with desired electro-optic (EO) effect, confinement and alignment of LC molecules in a specific direction is very essential. Mauguin reported that LC domains could be aligned by placing them in contact with a crystal surface. The structure of LC nearby interface is different from that in the bulk. The interfacial LC molecules change the boundary conditions and influence the LC in bulk. By controlling the LC directors at the surface, reproducible director orientations can be obtained. The different interaction (anchoring) conditions of LC molecules with their neighboring phase (solid substrate) give rise to different types of liquid crystal display (LCD) devices with varied properties [4, 31, 38, 43–46]. Various types of LC molecule alignment can be induced by treating the supporting substrate differently. The most common types of alignment are homogeneous (planar) and homeotropic.

3.6.1 Homogeneous alignment

This is also called as planar alignment (**Figure 17(a)**). Here, directors of LC molecules are oriented parallel to the electrode surface. Homogeneous alignment refers to the unidirectional orientation of the molecular axis in the planar mode and displays birefringence with excellent optical quality [47]. It can be achieved using surface treatment methods, such as obliquely evaporated SiO*x* layers, Langmuir–Blodgett films, photoalignment and rubbed polymer films [48–50]. Out of which photoalignment and mechanical rubbing are more promising techniques. In photoalignment, materials like polyvinyl alcohol (PVA) or polyvinyl cinnamate (PVC) are coated on indium tin oxide (ITO)-coated glass plates. These materials are illuminated with polarized ultraviolet light, which forces the LC directors to align parallel to the specific surface direction. Another method is rubbing, invented by Mauguin in 1911; in this method electrode is coated with transparent polymeric

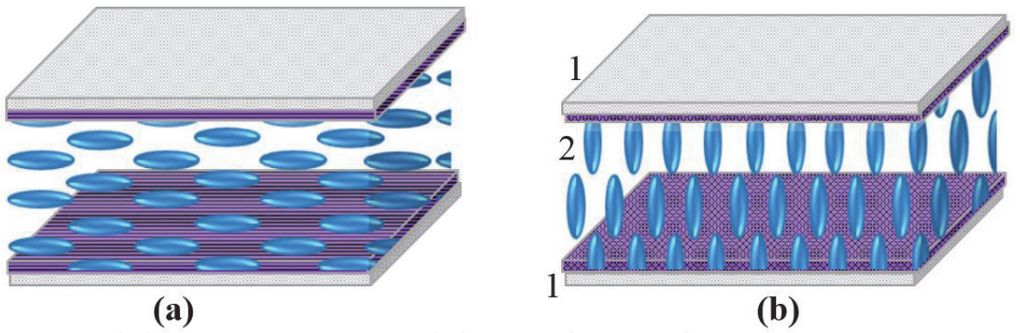

Figure 17.
(a) Homogeneous and (b) homeotropic alignment of liquid crystals. [1, PI coated ITO glass plate; 2, LC molecules].

material (generally PI), followed by baking and rubbing [45, 51]. The thin layer of PI is known for its exceptionally strong and outstanding heat, mechanical and chemical resistivity [52]. The mechanical treatment such as unidirectional rubbing modifies surface topography by breaking the symmetry and creating linear micro-grooves on the polymer surface [48, 53, 54]. The rubbing direction on one ITO plate is 0° or 90° with respect to other depending upon the parallel/antiparallel or twisted mode, respectively [55, 56].

3.6.2 Homeotropic alignment

In homeotropic alignment the LC molecule directors are oriented perpendicular to the electrode surface (**Figure 17(b)**). It can be achieved by treating the surface with a surfactant such as hexadecyltrimethylammonium bromide (HTAB), lecithin and polymers [57]. The polar head of a surfactant chemically attaches to the substrate, and the hydrocarbon tail points out, perpendicular to its surface. At this point maximum intermolecular interaction between LC molecules and surfactant promotes perpendicular anchoring of the nematic LC director. However, surfactant-based homeotropic alignment is not stable against humidity and heat [58, 59].

Apart from these two standard alignments, there are many other variations such as hybrid, twisted, supertwisted, fingerprint, multidomain vertically aligned, etc. which are employed in various LCD devices.

4. Applications of liquid crystals

LC science and applications now permeate almost all segments of the society from display technology to beyond display front. LCD is a well-known and leading application of LC [60] in the information display industry. They are used in small-sized displays such as smart phones, calculators, wearable displays and digital cameras, medium-sized displays such as desktop and laptop computers and large-sized displays such as data projectors and direct view TVs. They have the advantages of having high brightness and high resolution and being flat paneled, energy saving, light weight and even flexible in some cases [61]. To select the appropriate LCD for application and to tailor their optical performance, we need to understand broad classification (**Figure 18**) of LCD and their basic mechanism [62]. Till date mainly three types of LCD have been developed: transmissive, reflective and trans-reflective.

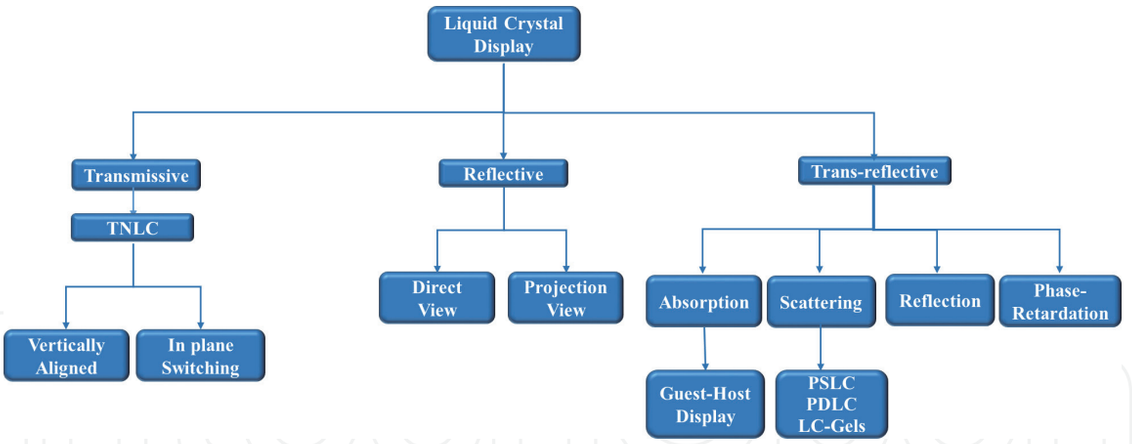

Figure 18.
Classification of LCD.

4.1 Transmissive LCD

A transmissive LCD transmits a backlight for illuminating the LCD panel, which results in high contrast ratio and high brightness. As their viewing angle is limited, they are more suitable for single-viewer applications, such as games and notebook computers. To make them applicable for multiple viewers, such as televisions and desktop computers, a phase compensation film should be introduced in them. They can also be used for projection displays, for which a high-power arc lamp or a light-emitting diode (LED) array is used as a light source. The most common and finest example of transmissive LCD is twisted nematic liquid crystal (TNLC) cells which are extensively used for notebook computers, where viewing angle is not critical. Its operating principle is based on the ability of the nematic LC to rotate the polarization of light beams passing through it [43, 63].

4.1.1 Twisted nematic liquid crystal cell

It was first invented by Schadt and Helfrich and demonstrated by Fergason in 1971 [64, 65]. It consists of two ITO-coated glass substrates, additionally coated with transparent alignment layers, usually PI. These PI-coated glass plates are rubbed with velvet cloth in one direction; as a result, the LC molecules orient parallel to the rubbing direction. The rubbing directions on two substrates are perpendicular to each other. These glass plates are arranged in such a way that a 90° twist of director from one substrate to the other is formed inside the cell. The cell is kept in between two crossed polarisers in such a way that their polarization is parallel to the rubbing direction of the same glass substrate. In the absence of electric field, the top LC alignment is parallel to the optical axis of the top polarizer, while the bottom LC directors are rotated 90° and parallel to the optical axis of the bottom polarizer (analyzer) as shown in **Figure 19(a)**. When $d\Delta n \gg 0.5\lambda$ (the Gooch-Tarry's first minimum condition) is satisfied, the incoming linearly polarized light will follow closely the molecular twist and transmit the crossed analyzer. Here Δn is the birefringence of LC, d is the cell gap, and λ is the wavelength of the light. This is called the normally white (NW) mode, since light is transmitted without application of any voltage. In the voltage-on state (**Figure 19(b)**), the LC molecules undergo a Freedericksz transition. In this state, the director of the nematic LC is parallel to the field and no longer twisted. When polarized light enters a cell in such a configuration, it is not twisted and is absorbed/blocked by the analyser, resulting in a dark state. Regions where an electric field is applied appear dark against a bright

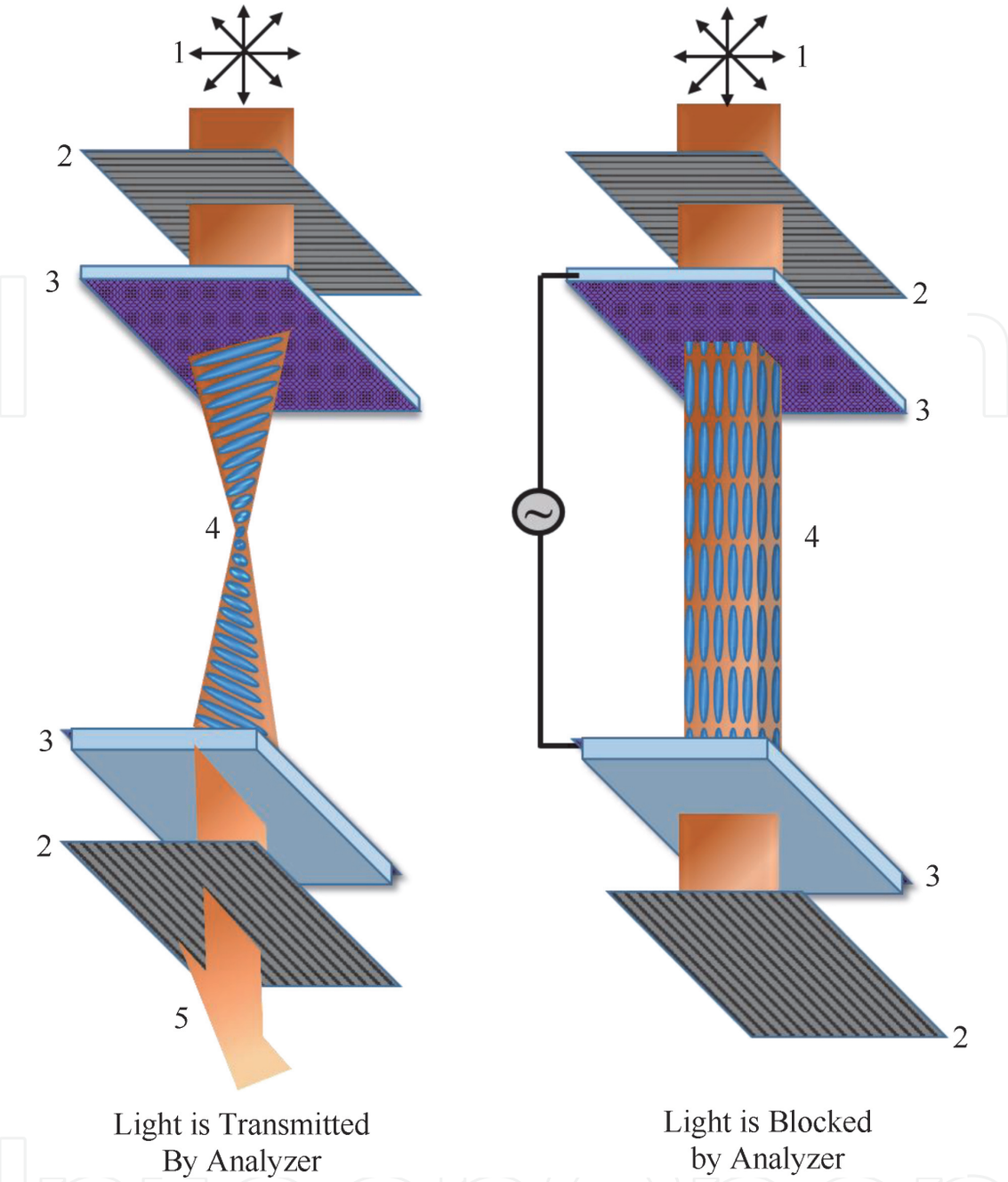

Figure 19.
Twisted nematic LCD in (a) OFF state and (b) ON state. [1, unpolarised light; 2, polarizer; 3, PI coated ITO glass plates; 4, LC droplets; 5, polarized light].

background. Because of the orthogonality of boundary layers, the dark state is achieved at relatively lower voltage. Depending on the field strength, twisted nematic displays can switch between light and dark states, or somewhere in between (greyscale.) How the LC molecules respond to applied field is the important characteristic of this type of display. However, every device has some shortcoming, in TNLC is its narrow viewing angle and poor color production. To overcome these problems, new technologies such as in-plane switching and vertical alignment mode have been introduced [61].

4.2 Reflective LCD

In R-LCDs, the necessity of backlight source (as in transmissive-type LCD) has been seized. They reflect ambient light for displaying images. Therefore, they

consume low power, are lighter in weight and have good readability in outdoor environment, but are inapplicable under low or dark ambient conditions.
The R-LCDs are of two types: direct view and projection view.

4.3 Trans-reflective LCD

In order to overcome the drawbacks and to take advantage of both transmissive as well as reflective LCDs, trans-reflective LCDs have been developed, which use both ambient light and backlight to display images based on availability and necessity. It has a semi-reflective film in the back of LCD screen, the backlight can transmit through it so that it may work as a transmissive mode, but the front light cannot pass through it and get reflected, and it simultaneously works as a reflective mode. Broadly, trans-reflective LCDs are classified into four categories: (a) absorption, (b) scattering, (c) reflection and (d) phase retardation. As the name suggests, the first category absorbs light, and the corresponding device is referred to as guest-host (GH) display. The second one scatters light, and polymer-dispersed liquid crystal (PDLC), polymer-stabilized liquid crystal (PSLC) and LC gels are related technologies. The third category is based on reflection of light. The fourth one modulates the phase of an incident light. Here we will discuss operating principle of PSLC, PDLC and holographic PDLC (HPDLC).

4.3.1 Guest-host display

These types of display systems were first introduced by Heilmeier and Zanoni [66]. As the name suggests, in these systems light is absorbed by the guest material, which are generally dichroic dye molecules, dissolved in a host LC material. Dichroic dye molecules are rod-shaped molecules, which absorb light of certain wavelength more along one axis than the other. Dye molecules get dissolved in LC and orient along with LC molecule. Upon application of external field, the rotation of absorption axis of dye molecule along with LC molecule modulates light transmission. Mainly, there can be three types of GH displays exist: the Heimeier type, the double-layer type and the PDLC type, which uses 1, 2 and zero polarizers, respectively [15, 67].

4.3.2 Polymer-liquid crystal composites

Polymer-LC composites are thin films prepared from phase-separated high molecular weight polymer and low molecular weight LCs. The polymer, which is homogenously mixed into LC, provides mechanical and structural stabilization to LC devices. Polymer-LC composites have been used in a wide range of applications such as high-definition spatial light modulators; switchable windows; flat-panel large area flexible displays; light valves; color projectors; thermal, optical and strain sensors; bi-stable reflective displays and haze-free normal- and reverse-mode light shutter devices [68–71]. The confinement of LC material in both dense polymer matrix and moderate polymer networks modifies the bulk LC phase. Depending upon the concentration of monomer unit, they are classified as polymer-stabilized liquid crystal or polymer-dispersed liquid crystal or holographic polymer-dispersed liquid crystal (HPDLC). In PSLC, polymer forms a sponge-like structure in a continuous LC medium. The concentration of LC is much higher than the polymer concentration. In PDLC, the LC is in the form of micron- and submicron-sized droplets, which are dispersed in a continuous polymer matrix. The concentration of polymer is comparable to the LC [61]. In HPDLC the polymer concentration is high around 60–70 wt%. As droplet size is much smaller than the visible wavelength,

HPDLC films are free of light scattering. These films have faster response time and require higher switching voltages. In PDLC and HPDLC films, no surface alignment layer is needed [72].

5. Polymer-stabilized liquid crystal

Polymer-stabilized liquid crystal is a thin composite film prepared from the homogenous mixture of LC and monomer. Typically, the monomer concentration in PSLC is less than 10% of the total weight. The small amount of monomer is used to stabilize/lock the oriented LC structure at different optical states and to reduce the switching time and operating voltage [73]. The homogenous mixture of LC and polymer is prepared and filled into the prefabricated cells made of transparent ITO-coated electrodes for photopolymerization using PIPS technique [51]. For improved display performance, LCs should be homogenously and uniformly aligned inside the cell. To control the orientation of LC, the inner face of electrodes is coated with a transparent polymeric material (generally PI) followed by baking and rubbing [53]. A thin layer of PI is known for its excellent strong and outstanding heat, mechanical, and chemical resistivity [53]. The mechanical treatment such as unidirectional rubbing modifies surface topography by breaking the symmetry and creating linear microgrooves on the polymer surface [48, 54, 56]. The rubbing direction on one ITO plate is 0° or 90° with respect to the other depending upon the parallel/antiparallel or twisted mode, respectively [55, 74]. This induced anisotropic surface diffuses monomer molecules preferentially along the rubbing direction. Due to strong interaction and anchoring between LC and monomer, the polymer network formed during/after polymerization keeps the LC director in a definite direction [75]. Along with the surface alignment layer, the configuration and orientation of LC can also be controlled by application of external field and/or temperature during photopolymerization. Even low electric field is sufficient to align the LC director along the field by fixing torque on it. After establishing the proper combination of surface treatment and applied field, the sample is irradiated by ultraviolet (UV) light to induce photopolymerization to obtain the desired texture. Since the monomer concentration is very small, a continuous LC texture along with interconnected, interpenetrating and mitigated polymer network can be obtained after polymerization [61, 76–78] as shown in **Figure 20**.

Because of application of electric field during photopolymerization, oriented LC domains are formed. Also, this controlled alignment of the LC molecules between polymer networks has significant effect on the transmittance, absorbance, response time, and dielectric properties of PSLC films [79].

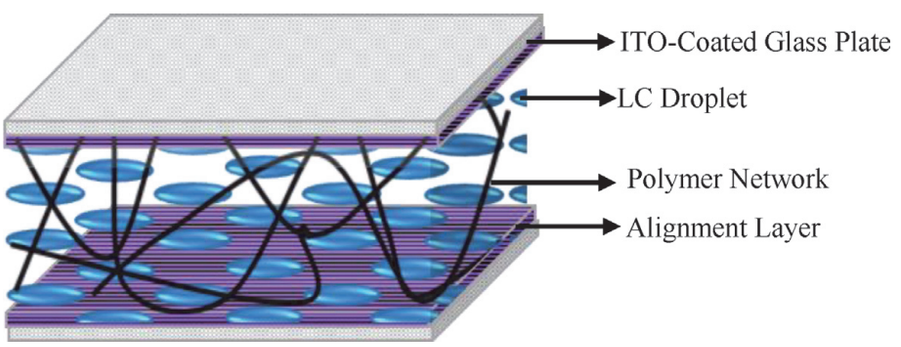

Figure 20.
Polymer stabilized liquid crystal.

5.1 Morphological analysis

Figure 21 shows POM images of PSLC films which are prepared using LC BL036 and prepolymer NOA-65 in 95/5 wt/wt% ratio under different rubbing directions and in the absence and presence of electric field [80].

Figure 21 shows the POM image of four types of PSLC films named as "A" (antiparallel rubbing; electric field absent), "B" (antiparallel rubbing; electric field present), "C" (twisted rubbing; electric field absent) and "D" (twisted rubbing; electric field present). On the acute observation of these images in all the four samples, complex geometrical structures of LC and polymer network were found. Samples A and C which were prepared without applying any electric field during polymerization showed rectilinear alignment. Since polymer network has a strong aligning effect on the LC, therefore it tends to keep LC in the aligned state [81]. In these films, polymer chains move throughout the sample parallel to the rubbing direction; therefore shorter chains with smaller domains entrapped between them were observed. In the case of samples B and D, which were prepared by applying electric field during polymerization, bigger LC domains were formed. Upon application of electric field during sample preparation, LC material orients and often indefinitely retains the alignment imposed by an electric field [82]. Because of the adsorption of LC droplets at the polymer wall, polymer network grows in the direction of field. Due to which cross linked, thicker and topologically defective polymeric walls were formed. Also, diffraction of light was observed from polymer nodules.

The effect of electric field on the orientation and confirmation of the LC material between the boundaries of polymer network gives deep insight in understanding PSLC film behaviour.

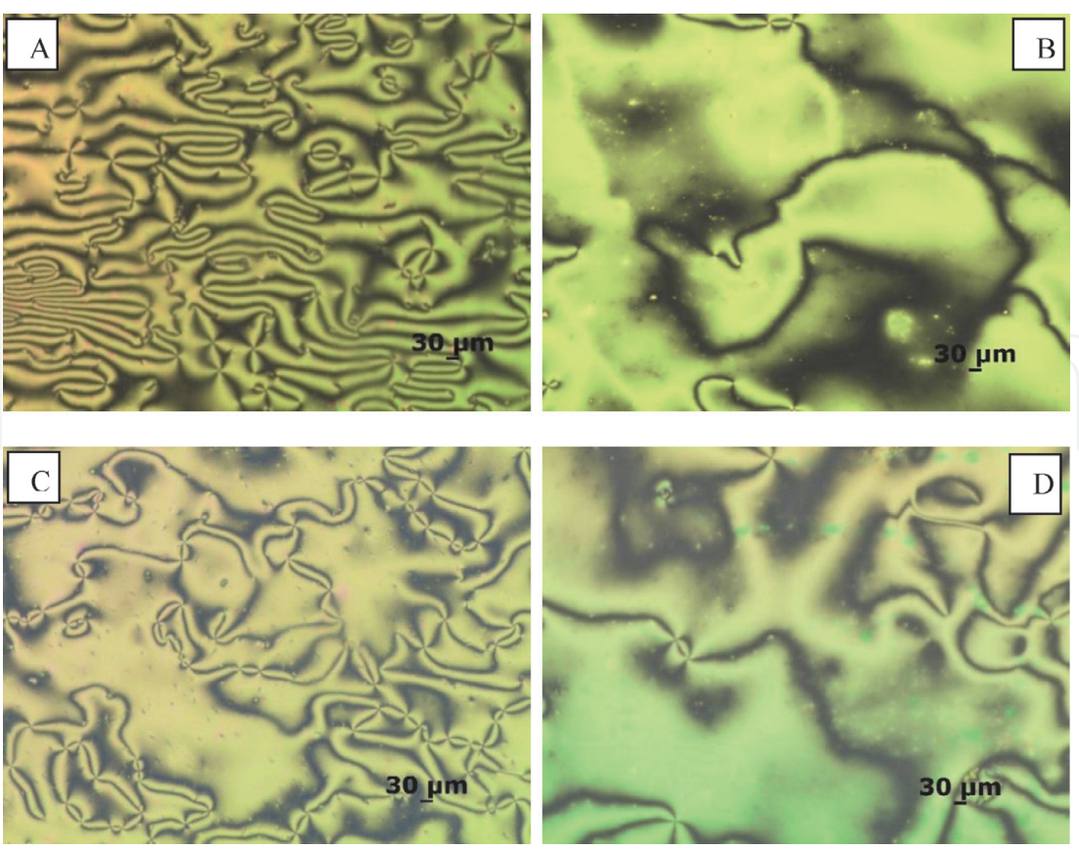

Figure 21.
POM images of homogenously aligned PSLC films: (A) antiparallel rubbing cured without any voltage, (B) antiparallel rubbing cured by applying 10 V, (C) 90° twist rubbing cured without any voltage and (D) 90° twist rubbing cured by applying 10 V, observed using 5× objective.

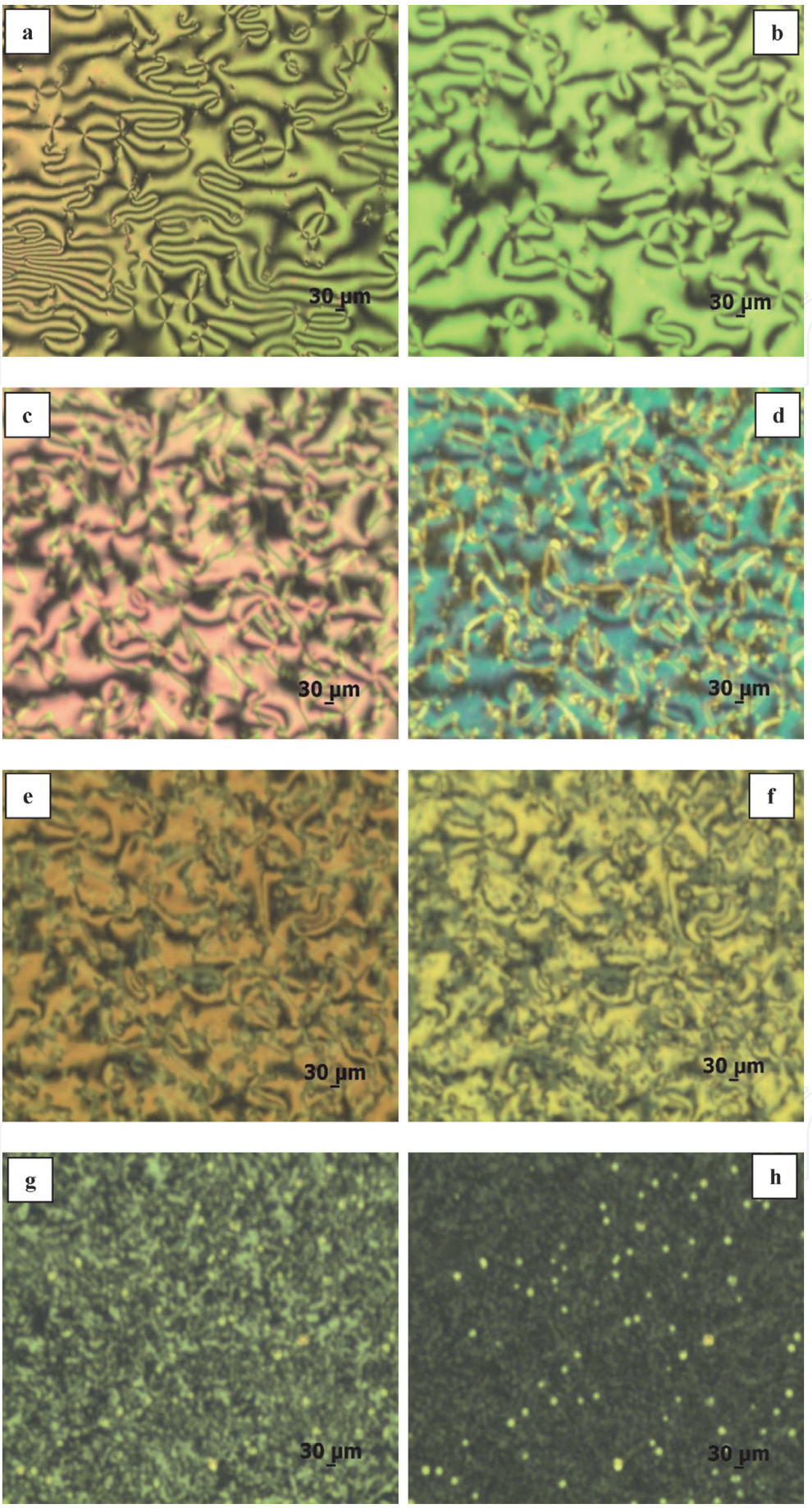

Figure 22.
Effect of voltage on homogenously aligned PSLC film sample A (anti-parallel rubbing; electric field absent during polymerization) observed at (a) 0 V, (b) 2 V, (c) 6 V, (d) 10 V, (e) 20 V (f) 40 V, (g) 60 V and (h) 80 V using 5× objective lens.

Figure 22 shows effect of electric field on sample A, prepared with antiparallel rubbing direction and in the absence of field. Upon application of low electric field of ~10 V, change in color was observed, which indicates change in refractive index. The change in refractive index is basically due to orientation of LC molecules in the domains. Also ~10 V vivid polymeric boundaries were made visible due to adsorption of LC molecules on frozen polymer network. On the application of high electric field of ~40 V and above, dark homeotropic state with the LC directors aligned perpendicular to the substrate surface was observed [83].

5.2 Voltage dependence of transmittance at fixed frequency

The voltage-transmittance curve (**Figure 23**) of PSLC film indicates that it follows an opposite trend to that of the PDLC films. It is clear from the graph that PSLC film has maximum transmittance (T_{OFF}) when no voltage is applied. Upon application of electric field, the LC orientation changes from planar to homeotropic state of alignment, and the transmission decreases rapidly for PSLC film.

At a particular voltage, transmittance of PSLC decreases by additional 10% of the OFF-state transmittance; this voltage is termed as threshold voltage (V_{TH}). With the further increase in voltage, the polarization state of light is perpendicular to the analyser which gives dark state or minimum transmittance (T_{ON}) state. A definite value of voltage at which PSLC film achieve T_{OFF} state is termed as ON-state voltage (V_{ON}) condition.

The ratio of maximum to minimum transmittance gives contrast ratio (CR) of the film, and difference between maximum and minimum transmittance gives transmittance difference (ΔT). Mathematically

$$\mathrm{CR} = \frac{T_{OFF}(\%)}{T_{ON}(\%)} \tag{11}$$

$$\Delta T(\%) = T_{OFF}(\%) - T_{ON}(\%) \tag{12}$$

Table 2 gives voltage-transmittance data of PSLC film prepared using monomer NOA-65 and LC BL036 in 95/5 wt/wt%.

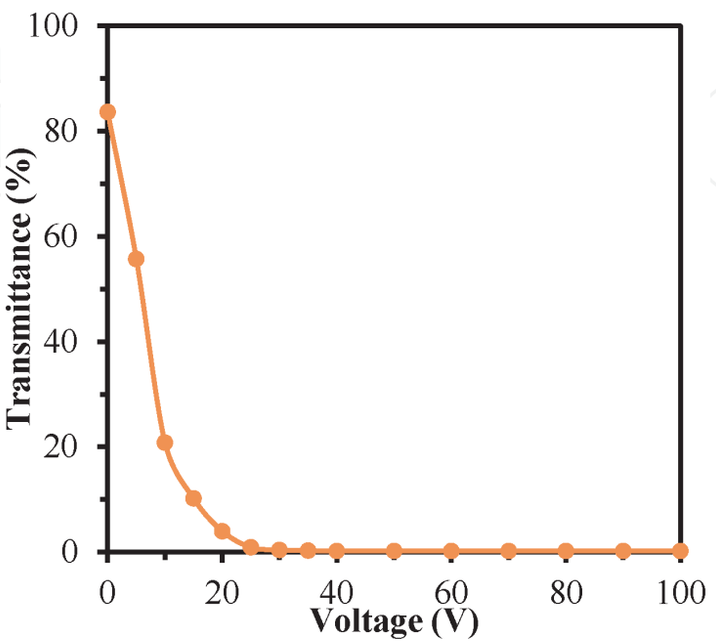

Figure 23.
Transmittance vs. voltage curve of PSLC film.

Sample	T_{OFF} (%)	T_{ON} (%)	ΔT (%)	CR	V_{TH} (V)	V_{ON} (V)
N36	83.6	0.20	83.4	418	2	25

Table 2.
Voltage-transmittance data of PSLC film prepared using monomer NOA-65 and LC BL036 in 95/5 wt/wt% ratio.

5.3 Hysteresis effect

In a scan up cycle, as voltage increases from 0 V to V_{max}, transmittance of PSLC films decreases from T_{OFF} to T_{ON}, whereas in scan down cycle as voltage decreases from V_{ON} to 0 V, transmittance increases from T_{ON} to T_{OFF}, but it does not follow the same path. The above observed phenomenon is termed as hysteresis and should be minimized for better electro-optic properties. It was observed that at a given voltage, transmittance for scan up cycle was higher than the transmittance for scan down cycle. A measure of hysteresis is given by the voltage width at half of maximum transmittance (ΔV_{50}). The hysteresis behaviour of a PSLC composite film is shown in **Figure 24**. Also, hysteresis effect was not observed at high fields because at higher voltages of scan down cycle, LC domains remain in the same state of orientation. However, when the applied field is reduced further, reorientation of LC domains begins, giving rise to hysteresis effect.

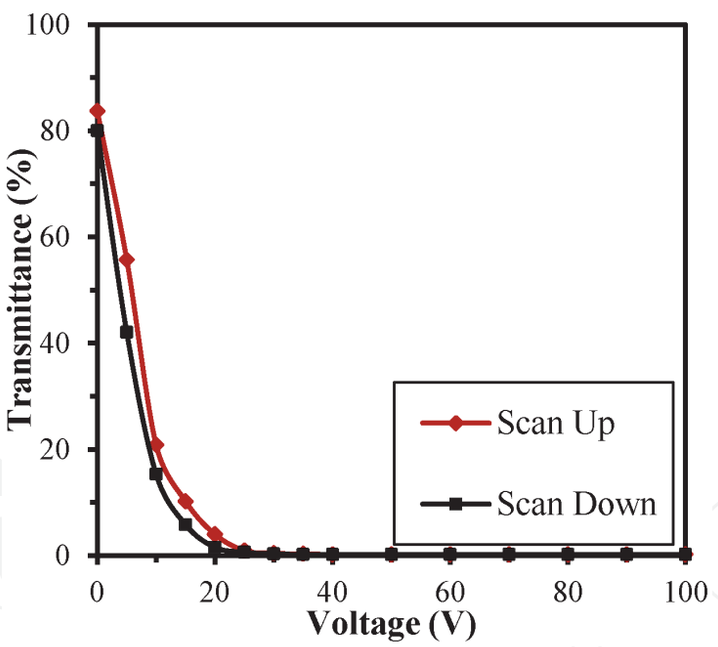

Figure 24.
Hysteresis curve of PSLC film.

5.4 Response time

Response time is the sum of rise time (τ_r) and decay time (τ_d). Upon application of electric field, LC molecules align along the field, and transmittance of film decreases in PSLC. The time in which transmittance of film reaches from 90–10% is termed as rise time. On the removal of field, these LC molecules relax back to their initial position. The time in which transmittance reaches from 10–90% is termed as decay time. Variation in rise and decay time of PSLC films with respect to applied voltage is shown in **Figure 25**. However, with the increase in voltage rise time shortens, but the trade-off is longer decay time [83, 84].

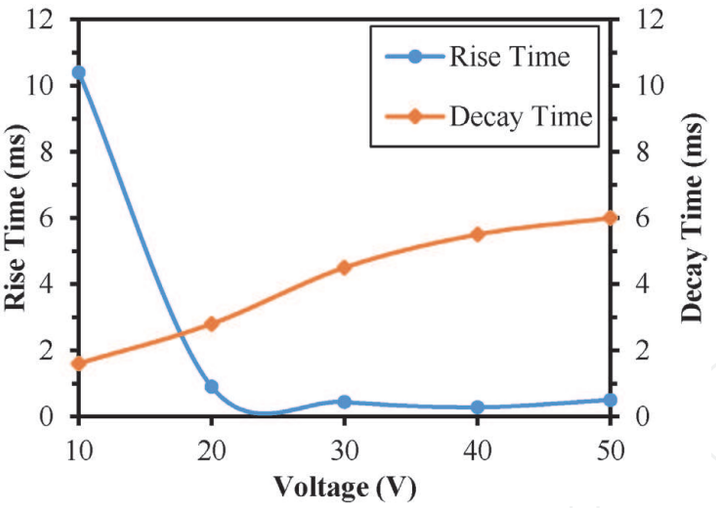

Figure 25.
Rise and decay time vs. voltage curve of PSLC film.

5.5 Dielectric properties of polymer-LC composite films

Polymer-LC composite films are complex heterogeneous system, holding intrinsic anisotropy of LC and polymer. In order to gather the information about the structure, alignment, phase transitions and intermolecular interactions of composite films, knowledge of their dielectric properties is essential [85, 86]. For this purpose dielectric relaxation spectroscopy (DRS) is one of the best methods to measure the dielectric constant and associated parameters with high accuracy and sensitivity in polymer-LC composites. It is based on a concept of "energy storage" and resulting "relaxation" per release of this energy by the system's individual components. By developing analogy between polymer-LC composites and passive electrical circuit, polymer-LC composite films can be conveniently illustrated as a parallel plate capacitor. Here, two ITO-coated glass plates act as a parallel electrode with plate separation d and plate area A, and polymer-LC material acts as a dielectric material as shown in **Figure 26(a)**. The effective circuit of polymer-LC cell is shown below (**Figure 26(b)**), where R_o is the resistance of electrodes and R_{LP} and C_{LP} are resistance and capacitance of polymer-LC layer, respectively.

The capacitance is measured, and the relative permittivity ε_r can be calculated from the formula given below:

$$C_p = \frac{\varepsilon_0 \varepsilon_r A}{d} \tag{13}$$

where $\varepsilon_0 = 8.854 \times 10^{-12}$ F/m is the permittivity of free space. Relative permittivity ε_r is complex quantity, also known as dielectric constant; it depends on parameters like temperature, pressure and frequency. To elucidate the frequency dependence of ε_r, we must understand the different polarization mechanisms that contribute to the dielectric constant (permittivity). In response to an applied electric field, various types of polarisations may arise, such as electronic, ionic, orientational and interfacial [87].

a. Electronic/atomic polarization: Electronic polarization occurs when the electric field displaces the centre of a negatively charged electron cloud relative to the positive nucleus of the atom and induces a dipole moment. It has been found to be independent of frequency and vanishes as soon as the electric field is removed [88, 89].

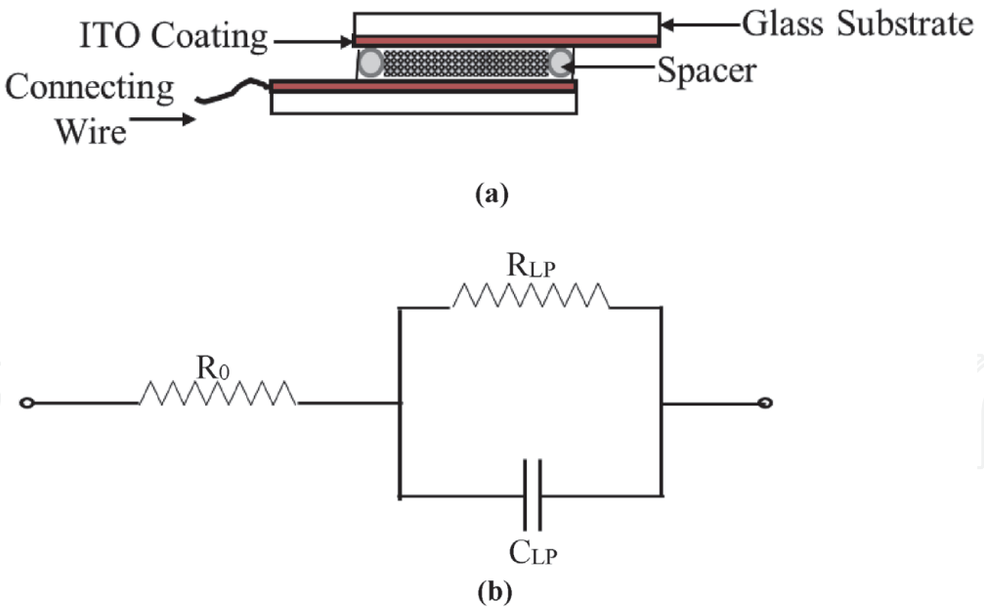

Figure 26.
(a) Schematic of polymer-LC composite film and (b) polymer-LC composite films as RC-circuit.

b. Ionic/displacement polarization: Ionic polarization also called as vibrational polarization occurs in ionic substances and is related to the displacement of atoms, causing the separation of charges [90, 91].

c. Dipolar/orientational polarization: Dipolar polarization usually occurs in materials with permanent dipoles. Under normal conditions, these materials exhibit zero net dipole moment and polarization, as the dipoles in these materials are randomly distributed/oriented. Upon application of an external electric field, the dipoles tend to orient along the direction of applied field, resulting a non-zero net dipole moment and polarization [90, 91].

d. Interfacial/translational polarization: Interfacial polarization is associated with migrating charges, by electrons or ions, over macroscopic distances in an applied field. These charges get trapped and accumulate at physical barriers such as defects, impurities, voids and grain or phase boundaries. The accumulation of charges distorts the local electric field and causes permittivity. Interfacial polarization is most prevalent in heterogeneous system like polymer-LC composites and is usually observed at lower frequencies. In general, a given dielectric material exhibits more than one polarization mechanism, and the average dipole moment in a given material is the sum of all polarization contributions. All four types of polarization occur at low frequency. Each of the above-mentioned polarization processes has specific features in the frequency and temperature dependence of the real and imaginary part of the complex dielectric permittivity. **Figure 27** shows the frequency dependence of various types of polarisations [90–92].

As frequency increases the contribution from each type of polarization successively decreases because polarization can no longer follow the variation in the field. As a result, there is a decrease in dielectric constant (relative permittivity) with the increasing frequency. The frequency dependence of dielectric constant reflects the fact that a material's polarization does not respond instantaneously to an applied field. The response must always arise after the applied field which can be

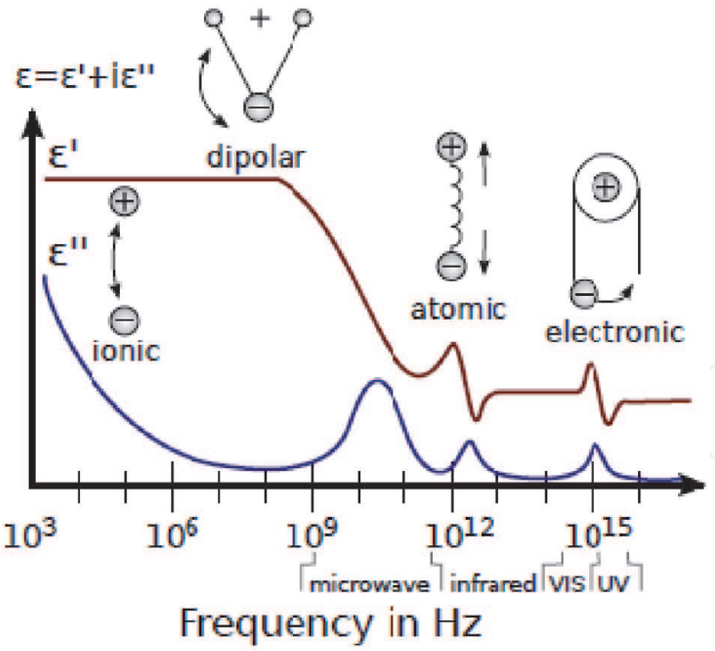

Figure 27.
A Dielectric constant Spectrum over a wide range of frequencies. ε′(ω) and ε′′(ω) denote real and imaginary part of the dielectric constant (relative permittivity) respectively.

represented by a phase difference. For this reason, dielectric constant is often treated as a complex function of the angular frequency (ω) of the applied field [93, 94].

5.5.1 Complex dielectric constant

The frequency-dependent permittivity characterizes amplitude and timescale (via the relaxation time) of the charge-density fluctuations within the sample. For the evaluation of relaxation time (time required for LC droplet reorientation), dielectric permittivity is expressed as a complex function of angular frequency (ω) of applied field:

$$\varepsilon^*(\omega) = \varepsilon'(\omega) - i\varepsilon''(\omega) \tag{14}$$

where $\varepsilon'(\omega)$ and $\varepsilon''(\omega)$ are real and imaginary parts of the complex dielectric constant.

Relaxation processes are characterized by a step-like decrease of the real part ε' and a peak in the imaginary part $\varepsilon''$of the complex dielectric function $\varepsilon^*(\omega)$ with increasing frequency. The real part is related to stored energy also called as dispersion, whereas imaginary part is related to loss of energy or dissipation called as absorption of the system. It is reasonable to introduce here a quantity "loss tangent", which is a measure of the energy dissipated due to oscillating field also known by dissipation factor "D" [21, 92, 95]:

$$tan\delta = \frac{\varepsilon''(\omega)}{\varepsilon'(\omega)} \tag{15}$$

For parallel plate capacitors with ideal dielectrics, the loss angle δ can be graphically expressed as shown in **Figure 28**.

Here, V is the applied voltage and I_c and I_R are the vector components of current I. The current I_c represents a non-lossy capacitive current proportional to the charge stored in the capacitor; it is frequency dependent and leads voltage by 90°. The current I_R is the alternating conduction current in phase with the applied voltage V, which represents the energy loss or power dissipated in the dielectric [96]. If ψ is the phase difference between the potential and current, then

$$\delta = 90 - \psi \tag{16}$$

To promote maximum energy storage in a capacitor, the dielectric loss, originating from interfacial, dipolar, distortional and conduction losses, should be minimal [87]. In general, dielectric loss increases with increase in humidity, temperature, frequency and amplitude of the applied voltage for most of the materials.

5.5.2 Macroscopic models for dielectric spectra

Dielectric relaxation processes are usually analyzed using model functions. Starting from the Debye function, several formulas for both the frequency and the time domain have been suggested to describe the experimentally observed spectra. The most important approaches are discussed below [97, 98].

a. Debye model: It is a method to study the dielectric behaviour of a material by measuring the complex dielectric permittivity versus frequency at constant temperature and ambient pressure. As the dielectric spectrum is obtained in a frequency domain, it is called as a frequency domain dielectric spectroscopy (FDDS). If a single relaxation is considered, it is known as Debye-type relaxation, and the time assumed for it is Debye relaxation time which is inversely related to the critical relaxation frequency. It is the point where dissipation factor is maximum. The relaxation frequency f is related to relaxation time τ by the relation

$$\tau = \frac{1}{\omega} = \frac{1}{2\pi f} \tag{17}$$

The dispersion and absorption terms for single relaxation as a function of the field angular frequency ω and relaxation time τ are given as

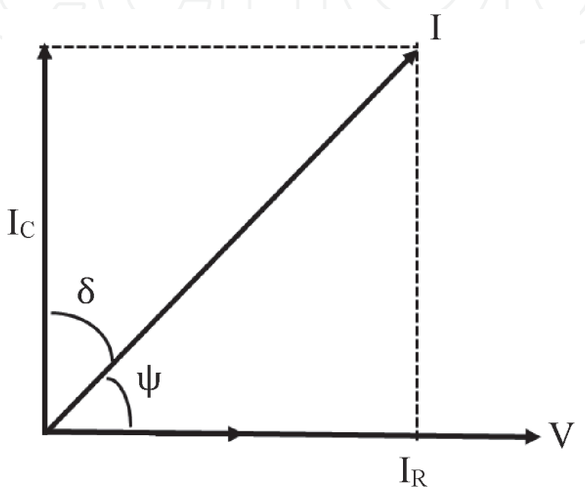

Figure 28.
Graphical representation of loss tangent.

$$\varepsilon'(\omega) = \varepsilon_\infty + \frac{(\delta\varepsilon')}{1+\omega^2\tau^2} \tag{18}$$

$$\varepsilon''(\omega) = \frac{(\delta\varepsilon')\omega\tau}{1+\omega^2\tau^2} \tag{19}$$

Debye relaxation is usually expressed in terms of the complex dielectric constant $\varepsilon^*(\omega)$ of a medium. On putting values from Eqs. (18) and (19) in (14), we get:

$$\varepsilon^*(\omega) = \varepsilon_\infty + \frac{(\delta\varepsilon')}{1+(i\omega\tau)} \tag{20}$$

where $\delta\varepsilon' = \varepsilon_s - \varepsilon_\infty$ is dielectric strength of the material, which is the voltage a material can withstand before breakdown occurs. ε_s and ε_∞ are static (at 20 Hz frequency) and optical (at relaxation frequency f) values of the relative dielectric constant, respectively, which were obtained by experimental relaxation spectra [91, 99–101]. The frequency dependence of real and imaginary components of complex dielectric constant of PSLC film is shown in **Figure 29(a)** and **(b)**, respectively.

b. Cole-Cole model: To describe secondary relaxations, Cole-Cole model has been used, given by the equation

$$\varepsilon^*(\omega) = \varepsilon'(\omega) - i\varepsilon''(\omega) = \varepsilon_\infty + \frac{(\delta\varepsilon')}{1+(i\omega\tau)^{1-\alpha}} \tag{21}$$

where α is known as the distribution parameter and other terms are the same as in Debye model. The exponent α characterizes the breadth of the relaxation time distribution and ranges from 0 (infinitely broad distribution) to 1 (Debye's single relaxation time limit), describing different spectral shapes. When α = 0, the Cole-Cole model reduces to the Debye model. The graph drawn between imaginary part ε'' and the real part ε' of the dielectric constant with frequency as a parameter, shown in **Figure 30**, is known as a Cole-Cole plot [102, 103]. It is useful for the interpretation of molecular dynamics of materials which possess one or more well-separated relaxation processes with comparable magnitudes. How well the ε' and ε'' are fitted to form semicircle is an indication of the nature of relaxation behaviour. All the above-mentioned parameters were determined from fitting the experimental data of dielectric spectra with

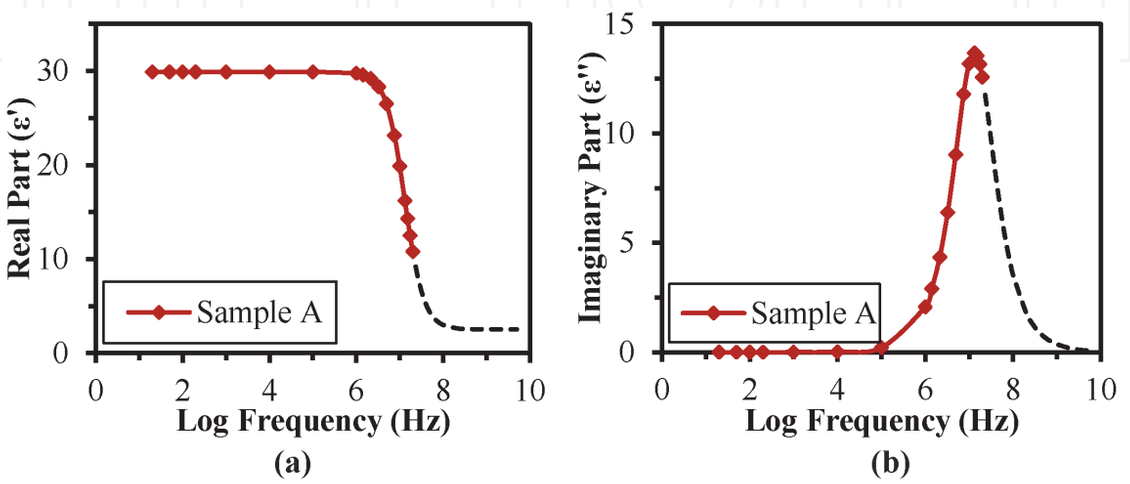

Figure 29.
Frequency dependence of (a) real component and (b) imaginary component of complex dielectric constant of PSLC film.

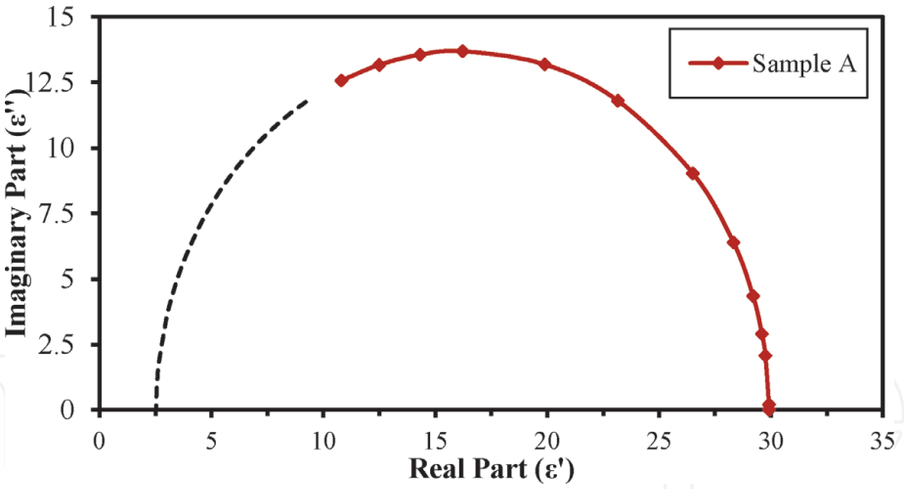

Figure 30.
Cole-Cole plot of PSLC film at 25°C temperature.

Sample	f (MHz)	ε_s	ε_∞	$\delta\varepsilon'$	τ (s)	α
A	13.2	29.9	2.53	27.4	1.21 E − 08	0.022

Table 3.
Fitting parameters of various PSLC films.

Cole-Cole approach of the Debye equation and are shown in **Table 3**. The frequency corresponding to the top point of this semicircle curve is the relaxation frequency f of orientational polarization of LC domains. At this point dielectric heating is maximum due to which dissipation factor is also maximum. The angle φ between arc radius and ε'-axis gives distribution parameter α:

$$\varphi = \frac{\alpha\pi}{2} \tag{22}$$

If the centre of the semicircle lies on the ε'-axis, then the distribution parameter $\alpha = 0$ (Debye type), and if the centre is below the ε'-axis, then $\alpha \neq 0$ (non-Debye type), while if $\alpha > 0.5$, there could be more than one relaxation process. The calculated value of α indicates that the PSLC film exhibits non-Debye-type relaxation process [104–106].

5.6 Conclusions of PSLC study

PSLC is a reverse to the conventional PDLC but identical to the twisted nematic liquid crystal cell having maximum and minimum transmittance under crossed polarizer in the OFF and ON states, respectively. However, the threshold voltages of PSLC are much lower than TNLC [107–109]. The PSLC are useful for bi-stable reflective displays and normal- and reverse-mode light shutters [68, 110]. In order to improve electro-optic responses of PSLC devices, LC material are doped with dye and nanoparticles [111, 112].

6. Polymer-dispersed liquid crystal

Polymer-dispersed liquid crystal is a smart, inhomogeneous thin composite film of micron-sized nematic LC droplets, randomly dispersed and embedded in

optically isotropic polymer matrix first introduced by Fergason in 1984 [61, 113, 114]. The composite of these two is technologically very important because it encompasses various unique properties of LCs, which are mechanically and structurally strengthened by polymer matrix. The operation of these composite films is based on birefringence property of LC. For LC with positive birefringence, $\Delta n>0$, in the OFF state as the LC droplets are randomly oriented, light repetitively refract/scatters at multiple polymer-LC interfaces. Due to which most of the light incident on PDLC device scatters, and the film becomes/appears opaque (**Figure 31(a)**). On the contrary, in the ON state as the directors in LC droplets align along the direction of electric field and if the RI, n_p of polymer matrix, matches with the ordinary RI, n_o of LC, most of the normally incident light on PDLC device behaves as an ordinary light and transmits through it, and the film becomes a transparent one [22, 115] (**Figure 31(b)**). In a similar manner, for LC with negative birefringence, $\Delta n < 0$, in the ON state extraordinary RI n_e comes into picture [34]. The LC droplet structure, their interaction with the polymer matrix and their optical and dielectric anisotropy play crucial role in shaping/modeling system properties. Although LC droplets are spherical in shape, they get deformed when embedded inside a polymer matrix. The polymer is supposed to act as a mere matrix for the LC aggregates, but their physical interactions can influence the formation of mesophases. The LC droplet morphology depends on many physical parameters such as refractive indices, conductivity, type and proportion of materials used, phase separation method, rate of diffusion, viscosity and solubility of the LC in the polymer, addition of dopant or dye molecules, etc. [116–121]. Unlike other LC technologies, PDLC do not require alignment layers and polarizers. This reduces cost; simplifies design; increases device lifetime in high-temperature and high-humidity conditions; increases transmittance, contrast ratio, flexibility and mechanical strength; and reduces response time. Also, the large surface-to-volume ratio of the composite film supports the construction of large area PDLC devices [19].

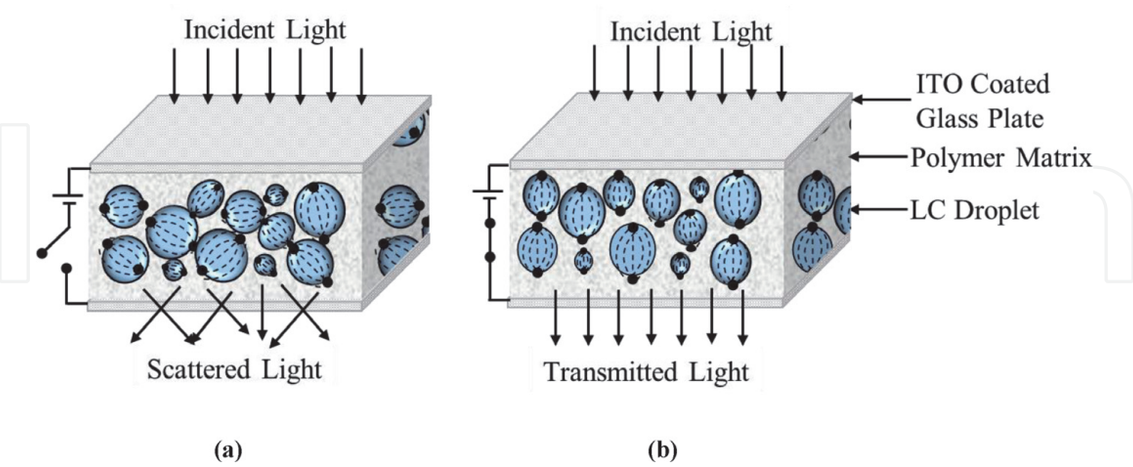

Figure 31.
PDLC in (a) OFF state and (b) ON state.

6.1 Fabrication of PDLC films

For the uniform dispersion of micron-sized nematic LC droplets inside polymer matrix, principally two methods have been enlisted, namely, phase separation and encapsulation.

6.1.1 Phase separation

The phase separation method starts with homogenous, isotropic solution of LC and polymer or prepolymer, followed by the formation of nucleated LC droplets (phase separation) and then finally solidification of polymer matrix pioneered by Doane and co-workers [122]. The morphology of a phase-separated PDLC film depends on the chemical nature of the LC and polymer constituents and kinetics of the processes driving the phase separation to occur, which ultimately control the electro-optic properties of device. Therefore, to obtain desired electro-optic properties in a device, systematically processed phase separation of LC and polymer is one of the key parameters. This technique is preferred where film moldability is required because during phase separation, polymer plasticization takes place. To induce phase separation in PDLC, generally any of the three routes, namely, polymerization-induced phase separation (PIPS), solution-induced phase separation (SIPS) and temperature-induced phase separation (TIPS), has been practised. Each method produces PDLC film with different properties and characteristics.

a. Polymerization-induced phase separation: It is usually an irreversible process, in which initially miscible, single-phased mixture of prepolymer (monomer or oligomer) and LC is filled into a prefabricated cell. On application of suitable energy in the form of heat, light or radiation, the polymerization is induced. The growing polymer chains phase separate LC droplets by forming an enclosing polymer matrix because LC is less soluble in polymer than in prepolymer. The phase-separated system has lower entropy than the mixed one. Polymerization may be initiated by heat, photo (UV irradiation) or free radicals. Generally, photopolymerization is preferred over the other two because it has low activation energy, has a good control over final properties of PDLC film and can occur in broader temperature range [120, 123, 124]. Phase separation process continues even if the UV exposure is interrupted during the cure process. Nowaday's photopolymerization technique is also applied in mask patterning.

b. Solution-induced phase separation: In this method, a polymer and LC are mixed and dissolved in a common organic solvent to form a single-phase homogeneous mixture. Such solution is then poured (using suitable technique) on an optically flat, transparent and conducting substrate for solvent evaporation. Evaporation of solvent causes phase separation between polymer and LC domains. Droplets start growing as the polymer and LC come out of solution and grow up till the polymer solidification. Another substrate (generally ITO) is laminated and annealed on the film using pressure and heat to form a PDLC cell. The electro-optic properties, which depend on LC droplet size and morphology, can be tailored by controlling evaporation rate. Droplet size and shape can be manipulated after the PDLC cell formation, by heating the sample cell till the clearing temperature of LC and then cooling. During heating LC get dissolved in polymer and again phase separates on cooling. By varying cooling rates, LC droplet size can be varied.

c. Temperature-induced phase separation: It is useful for thermoplastics which melt below their decomposition temperature. Thermoplastic and LC are heated until the clear solution is formed, such solution is filled into a prefabricated cell and then cooled. When the system is cooled, the LC phase separates from the solidifying polymer. Droplet size can be tailored by

controlling the rate of cooling. Droplet size (droplet numbers) shows inverse (direct) relation with rate of cooling. Methodically, it is a simple way of phase separation, but it is less preferred because the properties of TIPS films are difficult to reproduce, often sensitive to the processing history, and homogenous mixture of LC and thermoplastic is obtained at relatively higher temperature than in PIPS and SIPS techniques, which may worsen electro-optic properties of the PDLC device.

6.1.2 Encapsulation method

In contrast to phase separation method, encapsulation method starts from inhomogeneous solution. LC is dispersed by rapid stirring as an emulsion in an aqueous solution of a film-forming polymer such as PVA. This emulsion is then spin-coated or deposited onto a transparent conductive substrate like ITO-coated glass plate and dried. Thousands of non-uniform, sometimes interconnected LC capsules (droplets), surrounded by a solid layer of polymer are produced. Size of these droplets depends on stirring speed and time. Materials manufactured from this method are also known as nematic curvilinear aligned phase (NCAP). Encapsulation method is beneficial as LC is insoluble in aqueous solution; equilibrium phase separation is easily achieved as well as polymer plasticization is prevented. But it has limitation also; because of water evaporation, there is significant change in volume of film which tends to deform droplet structure, and only few polymers are appropriate for encapsulation with proper optical properties [120, 123, 124].

6.2 Nematic configurations in PDLC films

The nematic material confined in a droplet in a PDLC is in a particular arrangement, called the director configuration. LC droplets are usually spherical because of surface tension, but due to photopolymerization reaction the texture changes significantly to adopt different configurations. When LCs are confined to small cavities, curved surfaces deform the director field, inducing three basic Frank elastic deformations in the director structure, namely, splay, twist and bend. The contribution of each deformation to the overall energy density F is given by [19, 125]

$$F = \frac{1}{2}\left[K_{11}\left(\nabla.\vec{n}\right)^2 + K_{22}\left(\vec{n}.\nabla\times\vec{n}\right)^2 + K_{33}\left(\vec{n}\times\nabla\times\vec{n}\right)^2\right] \quad (23)$$

where the proportionality constants K_{11}, K_{22} and K_{33} are associated with splay, twist and bend deformations, respectively. It is usually not possible to pack the nematic director field into curvatures without creating one or more defects. These defects are responsible for the transformation of LC droplet from one configuration to another. Different defect structures are classified on the basis of their two-dimensional structure often known as "strength (s)" of the defect. "s" is defined by the rotation of the nematic director on a closed path around the defect; s indicates how many times of 2π the director rotates. Since $+n$ and $-n$ of the director are equivalent, half-integer values of s are allowed. The light scattering and dielectric properties of different droplet configurations can vary considerably, which is an important factor in the PDLC devices. Accordingly, the configuration of confined LCs is an area of both scientific and technological interest [19, 126]. The configuration adopted by the nematic director field within a droplet reflects the subtle interplay of a number of forces, such as shape and size of cavity containing LC

material, alignment properties of the LC at the polymer surface, elastic constants of the bulk nematic, temperature and the presence of external fields. Out of these factors, preferred alignment of the nematic at the surface of the polymer-LC interface determines the droplet configuration. If the anchoring energy is stronger than the elastic forces inside LC droplets, then the nematic director adopts a uniform tilt angle either (0° or 90°) at all points on the droplet surface, and the final configuration of nematic director within LC droplet is to minimize the total free energy. However, if the anchoring energy is weaker than the elastic forces inside LC droplets, then the tilt angle of the nematic varies spatially within the droplet to minimize curvature in the bulk of the droplet. Strong or weak anchoring conditions depend on the chemical nature of the polymer interface up to a certain degree. However, typically anchoring energy is more influential. Anchoring effects are magnified in small droplets, because of their shorter length scale and increased surface-to-volume ratio. Along with anchoring energy, balance of elastic constants is an imperative factor in determining the director configuration. Contribution of elastic constants to the system's free energy determines whether director configuration inside the droplet is simple or complex. The shape and size of cavity affects droplet structure. In submicron-sized droplets, the close proximity of surfaces and defects can distort the nematic structure throughout the droplet, whereas in large-sized droplets, it is easy to form multiple defect structures. The director configuration is isomorphic in a symmetric cavity and unpredictable in irregular-shaped cavity. The presence of external fields may influence the alignment direction of a nematic without altering the director configuration. Four commonly found director configurations in PDLCs [127–129] are illustrated in **Figure 32**.

a. Radial configuration (**Figure 32(a)**): In this configuration, director field is anchored perpendicular (homeotropic) to the droplet wall. A radial droplet possesses spherical symmetry, and the only elastic deformation present in this

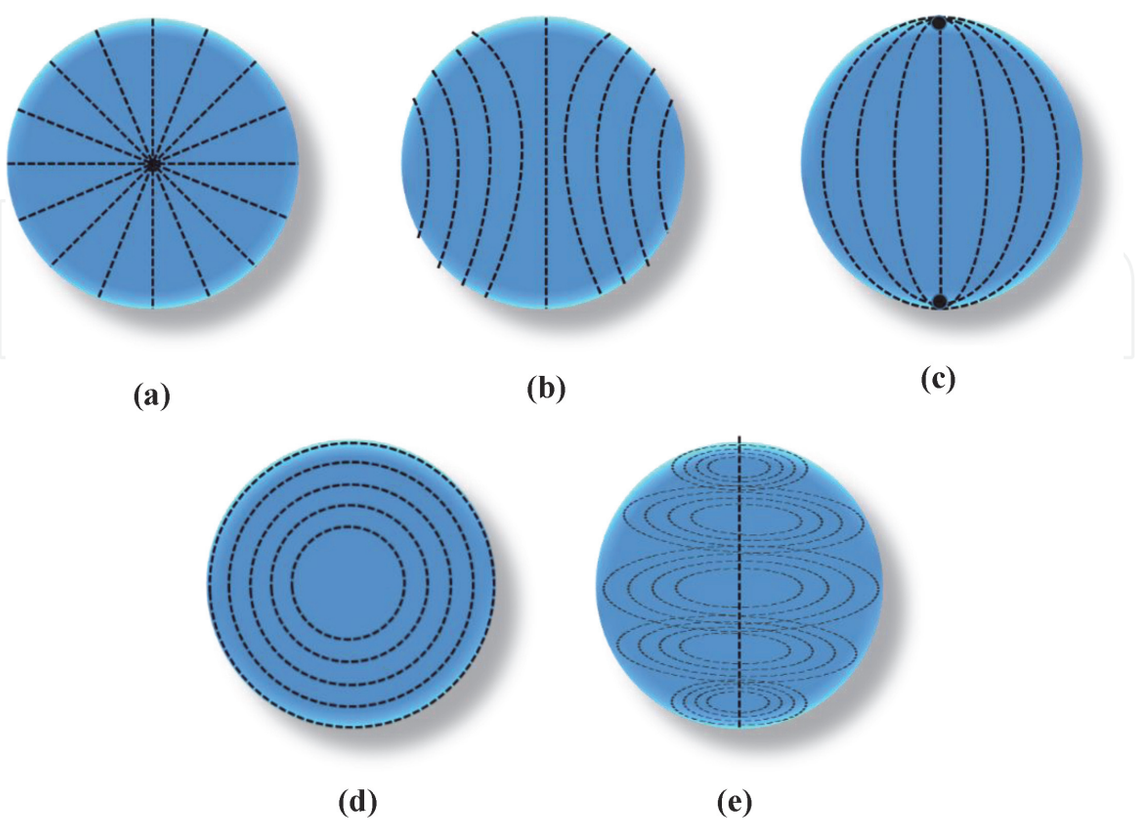

Figure 32.
Director configurations in a droplet of PDLC (a) radial, (b) axial, (c) bipolar, (d) toroidal and (e) three-dimensional view of the toroidal configuration.

structure is a splay deformation with a point defect (s = 1) in the volume centre known as hedgehog [19, 130]. This is shown in **Figure 33**. The defects (also known as disclinations) arise when the elastic energy density of a nematic grows sufficiently large, and the orientation of the nematic director becomes indistinct [131]. Radial structure is generally found by dispersing LC in low-surface energy fluids like polysiloxane or in glycerine containing a small amount of lecithin.

b. Axial configuration (**Figure 32(b)**): This configuration was found in director field which are weakly anchored perpendicular (homeotropic) to the droplet wall, smaller in radii than radial droplets and in those radial droplets which were exposed to electric or magnetic field [132]. The director field possesses cylindrical symmetry, with a line defect perpendicular to the preferred orientation direction at the droplet equator as shown in **Figure 32(b)**.

c. Bipolar configuration (**Figure 32(c)**): In this configuration, director field is anchored tangential (parallel or homogeneous) to the droplet wall. The director field possesses cylindrical symmetry, with the symmetry axis defined by two-point defects called *boojums*, which lie at opposite ends (poles) of the droplet. *Boojums* can exist only at the surface and cannot move into the volume of the droplet. In a bipolar droplet, both splay and bend deformations are present, with splay-type *boojums* located at the surface near the poles of the droplet, as shown in **Figure 33**. The bend deformation dominates throughout the rest of the drop along the lines connecting the two poles.

d. Toroidal configuration (**Figure 32(d)** and **(e)**): In the case of multiple elastic constants, the toroidal configuration exists when the splay energy becomes too large in comparison with the bend energy in the droplet. For a value of $K_{11}/K_{33} > 0.7$, a droplet with the toroidal configuration is a stable structure as it has a lower free energy than a bipolar structure. The toroidal structure possesses a line defect running along the droplet diameter, and the nematic director is everywhere perpendicular to this line arranged in a series of concentric circles.

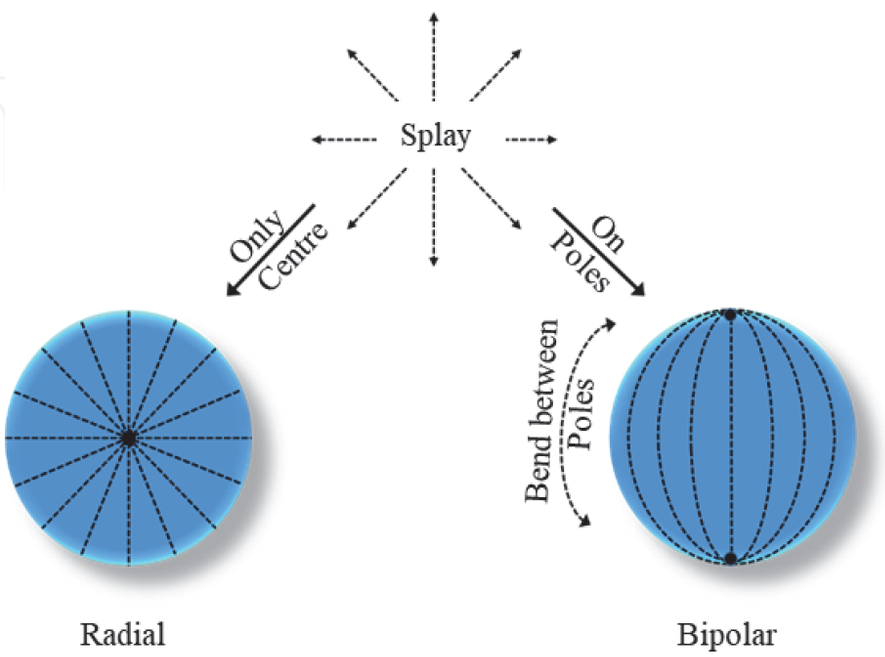

Figure 33.
A schematic illustration of splay and bend elastic deformations dictating the nematic ordering in radial and bipolar LC droplets.

6.3 Light scattering properties of PDLC films

Light scattering properties of PDLC films which can be controlled by electric field is a topic of great interest for scientific and technological reasons. The light scattering effects are insensitive to the initial polarization of light, and hence PDLC films can modulate light without the use of alignment layers or polarizers. The light scattering property of a PDLC film depends on many parameters such as LC droplet shape and size, droplet configuration, droplet density, refractive indices of LC and polymer, wavelength, etc. However, the nematic director orientation within the LC droplet dominates the light scattering properties of the films. Upon application of electric field, directors can be oriented along the direction of electric field causing transformation from highly scattering to highly transparent film. For simplicity, to explain the scattering and/or propagation of light at different voltage levels, we have developed a single droplet model [116, 133, 134].

In the absence of electric field, the different droplets will have different orientations. The droplet under investigation (**Figure 34(a)**) will scatter the light at polymer-LC interface. When a little voltage, below threshold voltage V_{TH} (defined later) (**Figure 34(b)**) is applied, because of the strong anchoring at interface, the alignment of LC droplet directors will not change much except the internal portion of the droplet. The internal portion experiences the electric field effect and aligns LC directors along the direction of the field. When the field (**Figure 34(c)**) is further increased up to the intermediate level, the majority of the LC droplets gets oriented along the direction of applied electric field, except the LC directors, which are on the polymer-LC interface, experiencing enough anchoring forces. At adequately high electric field (**Figure 34(d)**), i.e. above saturation voltage V_{ON} (defined later), all the directors get aligned along the direction of electric field. In such situation, light encounters only ordinary RI of LC, which is very close with the RI of the polymer. Therefore, a clear transparent film is observed at sufficiently high voltages.

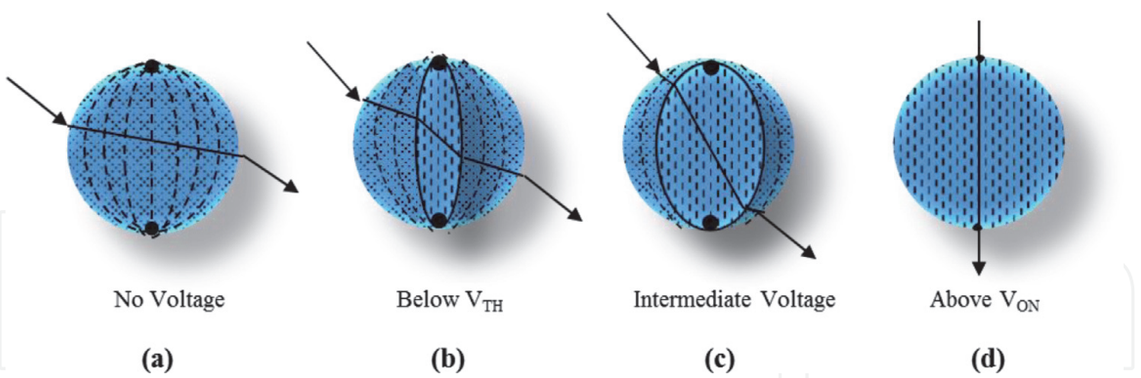

Figure 34.
Single LC droplet model: (a) V=0, (b) $V<V_{TH}$, (c) $V_{TH} \leq V \leq V_{ON}$, (d) $V>V_{ON}$.

6.4 Electro-optic properties of PDLC films

6.4.1 OFF-state transmittance (scattering) (T_{OFF})

In the absence of field, i.e. OFF state, the directors of LC droplet are randomly aligned. In this situation, most of the light incident normal to the film surface gets scattered giving opaque appearance to the film. The reason behind this is the mismatch of RI (a) between two adjacent droplets, (b) between a LC droplet and polymer and (c) within a LC droplet [135]. The OFF-state transmittance of a PDLC film depends on the birefringence of the LC. To minimize the value of OFF-state transmittance, the difference between LC extraordinary and ordinary refractive indices $\Delta n = n_e - n_o$ must be as large as possible.

6.4.2 ON-state transmittance (T_{ON})

In the ON state, when sufficient voltage is applied across the PDLC which overcome the anchoring at polymer-LC interface, the LC droplets attain minimum free energy by completely aligning themselves parallel to the field direction by the action of dielectric torque. In such a situation, light incident normal to the film surface experiences RI, $n_p = n_o$, and gets transmitted through the film.

6.4.3 Contrast ratio (CR)

Contrast ratio is the term used to evaluate display properties of PDLC films. It is the ratio of the ON- to OFF-state transmittance:

$$CR = \frac{T_{\mathrm{ON}}(\%)}{T_{\mathrm{OFF}}(\%)} \tag{24}$$

6.4.4 Transmittance difference (ΔT)

Another term used to evaluate the efficiency of PDLC films is transmittance difference (ΔT); it is difference of ON- and OFF-state transmittance:

$$\Delta T(\%) = T_{\mathrm{ON}} - T_{\mathrm{OFF}} \tag{25}$$

6.4.5 Switching voltages

One of the most important parameters of PDLC films is the voltage required to achieve an electro-optic effect. Initially the LC droplets are randomly oriented in PDLC films. When low electric field is applied, LC droplets starts orienting along the field; the voltage required to increase the transmittance of PDLC film by additional 10% of OFF-state transmittance (T_{OFF}) is termed as threshold voltage (V_{TH}). The theoretical model for threshold voltage has been developed by balancing the elastic forces, surface interaction and applied electric force and is mathematically derived as [136, 137]:

$$V_{\mathrm{TH}} = \frac{d}{3a}\left[\frac{\rho_p}{\rho_{LC}} + 2\right]\left[\frac{k\left(l^2 - 1\right)}{\Delta\varepsilon}\right]^{\frac{1}{2}} \tag{26}$$

where d is the film thickness; ρ_p and ρ_{LC} are the resistivities of polymer and LC, respectively; k is the elastic constant; the aspect ratio $l = a/b$, where a and b are the length of the major and minor axes of LC droplet, respectively; and $\Delta\varepsilon$ is the dielectric anisotropy of the LC. With further increase in voltage, more and more LC align along the field. When sufficient voltage is applied across the PDLC which overcome the anchoring at polymer-LC interface, the LC droplet attains minimum free energy by completely aligning itself parallel to the field direction. At this stage film becomes fully transparent, and corresponding voltage is termed as saturation voltage or ON-state voltage (V_{ON}).

6.4.6 Response time

Another decisive factor in evaluating the performance of the polymer-LC composite film is its dynamic response to an applied electric field. Quick response of a

PDLC film is critical in many applications. Response time is the time required by the LC molecules to align along the electric field upon application of field and to relax to their initial orientation when the electric field is removed. It generally depends on the relative strength of the applied field and the elastic reorientation forces. It can be affected by the degree of phase separation between nematic and polymer phase. Polymer-LC material properties and film morphology which include droplet size, shape, multiple scattering processes, etc. have high impact on response time of composite film [138, 139]. Erdmann observed reduced values of response time for elongated LC droplets [128]. It is calculated by balancing an elastic torque (Γ_{d}), electric torque (Γ_{e}) and viscous torque (Γ_{v}). It is the sum of rise time (τ_{r}) and decay time (τ_{d}). Rise and decay times are usually defined in terms of an optical response. Rise time is the time in which transmittance of film reaches from 10 to 90% on application of electric field. Similarly decay time is the time in which transmittance reaches from 90 to 10% on removal of electric field [115]. Mathematically

$$\frac{1}{\tau_r} = \frac{1}{\gamma_1}\left[\Delta\varepsilon \times V^2 + \frac{k\left(l^2-1\right)}{a^2}\right] \tag{27}$$

and

$$\tau_d = \frac{\gamma_1 \times a^2}{k\left(l^2-1\right)} \tag{28}$$

where $\gamma_1$is the rotational viscosity of LC and other symbols manifest same meaning defined earlier.

For higher electric fields

$$\tau_r = \frac{\gamma_1}{\Delta\varepsilon \times V^2} \tag{29}$$

An analysis of the above equation indicates that τ_r is predominantly a function of the applied voltage, where τ_d typically depends on the configuration of LC domain and their anchoring energy with polymer wall. A good estimation of rise and decay times can be attained by understanding the director direction inside LC droplet.

6.4.7 Hysteresis effect

During the study of electro-optic properties, a well-known hysteresis phenomenon was observed in PDLC films [138]. The hysteresis is a known problem, which must be addressed for practical application of the display material. It has been found that the transmittance values obtained at various voltages during scan down cycle do not follow the same path as that of the scan up cycle. A measure of hysteresis is given by the voltage width at half of maximum transmittance (ΔV_{50}). The lag of transmittance during scan down cycle may trace on any of the three paths as shown in **Figure 35**:

1. Hysteresis: Hysteresis occurs in intermediate voltage range, and the transmission at a given voltage depends on the previous voltage state. The situation when a higher transmission at a given voltage is observed during the scan down cycle as compared to the transmission at the same voltage during the scan up cycle is termed as hysteresis effect.

2. Persistence: The phenomenon when the film does not return to its complete scattering state immediate after removal of field is termed as persistence. The reason behind persistence is high interconnectivity between LC droplets which creates defect structure in any of the droplet. Then the other connected droplets may get trapped in the high field and remain in the same state even after the removal of field, until the defect escapes from the trap.

3. Memory effect: It is a semi-permanent persistence because film remains permanently in the transparent state even after removal of field. The reason for memory effect is weak anchoring force which develops between the boundaries of polymer network and LC domain upon application of field.

There are some common factors in hysteresis, persistence and memory effect in PDLC films. Persistence and memory effects are due to predominance of some specific factor.

The sources which give rise to hysteresis phenomenon have been studied by various researchers [117, 135, 138, 140, 141]. Hysteresis depends on the rate at which fields are applied and removed. For quickly (period of microseconds) varying voltages, hysteresis are more as compared to slowly varying (period of seconds) voltages in a same film [19]. It has been proposed that the orientation mechanism of the LC droplet director is a crucial factor responsible for hysteresis. Upon application and removal of field, there is substantial difference in the director direction of LC molecules, which are at the polymer-LC interface and which are inside the LC droplet [138]. The orientation-reorientation of LC directors depends on the polymer-LC compatibility and induced interfacial polarization, influencing the distribution of the relaxation time [136]. Hysteresis might be due to the presence of defect structure within a LC droplet [138, 141]. Depolarization effects might contribute to hysteresis through the generation of electric fields inside the PDLC films [142]. It has been suggested that hysteresis might be due to the residual electric charge (on field removal) which serves as a capacitor during the scan down cycle [84, 135]. On analysing **Figure 35**, it is clear that hysteresis effect is not observed at high fields because at higher voltages of scan down cycle, LC droplets

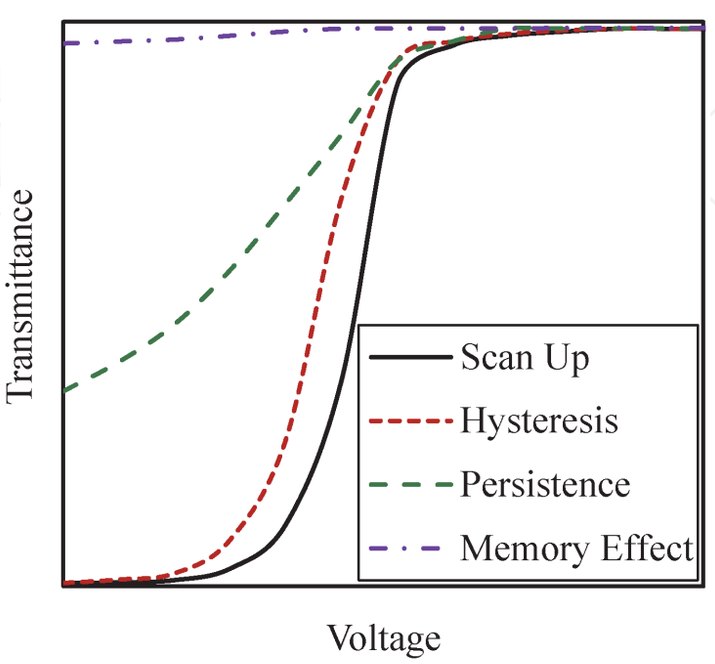

Figure 35.
Schematic of hysteresis, persistence and memory effect in a PDLC film.

remain in the same state of orientation. However, when the applied field is reduced further, reorientation of LC droplets director begins, giving rise to hysteresis effect [143].

There is a much scope of improvement in the optical and dielectric properties of PDLC devices, by reducing operating voltages, quickening switching and relaxation times, enhancing image contrast, etc. Before photopolymerization, PDLC films are a homogeneous mixture composed of monomer and LC which transforms into heterogonous system consisting LC droplets embedded in polymer matrix after photopolymerization.

Several groups have suggested that to augment the PDLC film properties, we can alter:

1. Film preparation conditions, such as, reaction temperature, UV irradiation intensity, curing time and film thickness

2. Properties of monomer unit such as their structure, functionality, concentration in LC, etc.

3. Physical properties of LC such as optical and dielectric parameters, rotational viscosity, temporal characteristics, molecular dynamics, etc. [76, 119, 120, 123, 144–149].

To enhance the properties of PDLC films, LC properties are modified suitably by addition of nanoparticles, dyes, polymers and carbon nanotubes. The inclusion of new additives can add new functionalities to the obtained devices. To obtain the desired result from the host LC material, proper selection of size, shape and structure of guest/additive particle is an imperative factor. In has been proved that due to the inherent dipole moment, LC materials respond radically when doped and anchored with elongated species.

The incorporation of small quantity of dye molecules to the LC is one suitable solution, which has been studied by several researchers.

6.5 Operating principle of DPDLC composite films

DPDLC films are also named as guest-host polymer-dispersed liquid crystal (GHPDLC) composite films. The LC phase acts as the host and dye molecules doped in LC act as the guest. Once the geometrically anisotropic dye molecules are added/dissolved in LC, the long molecular axis of dye molecule tends to align along the LC director; this is called as guest-host interaction. Dyes used for LC media must have high dichroic ratio, high-order parameter, high stability and good compatibility and solubility with LC but not with monomer unit or polymer matrix. It must be a positive type, i.e. the absorption transition dipole is along the long molecular axis. When the polarization of the incident light is perpendicular to the long axis of the dye molecules, the light is weakly absorbed. When the polarization of the incident light is parallel to the long axis of the dye molecules, the light is strongly absorbed, as shown in **Figure 36**. Considering all the above-mentioned points, dichroic azo dyes, which are N═N substance and absorb light of certain wavelength more along one direction than the other, have been used.

Similar to the PDLC films, the dispersion of the droplets can also be achieved using polymerization-induced phase separation method, in which the dye and LC mixture separate from the polymer binder. These DPDLC films possess controllable

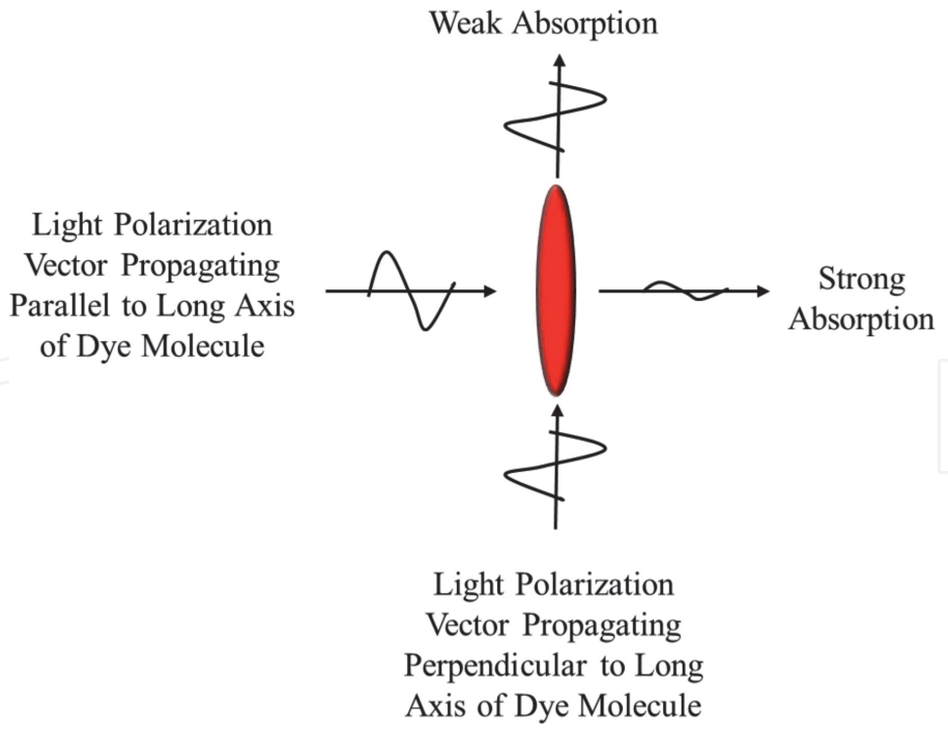

Figure 36.
A schematic representation of direction dependent absorption of dichroic dye molecule.

scattering as well as controllable absorbance, modulated by the liquid crystal molecule. The large transition moment of the rod-shaped dye molecules is modulated by the symmetry axis of the LC molecule in the OFF and ON states of electric field [150–153]. In the field "OFF state", dye molecules are randomly oriented along with the LC droplets. The unpolarised incident light is scattered as well as absorbed due to LC droplets and dissolved dye molecules. Due to the scattering of light, the optical path length of light increases, and hence enhancement in absorption has been noticed. In the field "ON state," LC droplets and dissolved dye molecules get aligned along the field direction, making the film feebly absorbing; hence, most of the light is transmitted through the film. **Figure 37** shows the schematic of DPDLC film in the OFF and ON states of applied electric field [61, 125].

LC droplets in all the composite films exhibit predominantly bipolar (LC droplet with cylindrical symmetry axis defined by two-point defects at opposite ends)-type morphology with some radial (LC droplet with spherical symmetry and the only point defect in the volume centre) structures. No preferred orientation of LC droplets was found, which is responsible for the scattering of light. Upon addition of dichroic dye molecule, significant morphological changes arise in LC droplet. The dye, polymer and LC are chosen such that the solubility of dye is high in LC but very low in polymer. **Figure 38** shows POM image of DPDLC film (O36N), prepared using LC BL036 and prepolymer NOA65 in wt/wt% with varying disperse Orange 25 dye concentration. As the dye concentration increases from 0–1%, there is noticeable increase in droplet size from submicron to ~10 μ. The reason is dye molecules dissolved in LC absorb some of the UV radiations provided for photopolymerization, which reduces rate of polymerization and in turn influences droplet growth. At lower dye content, faster polymerization rate produces smaller and denser LC droplets. At higher dye content, slow polymerization rate preserves polymer in a liquid state for an extended period, thus allowing the growth and coalescence of small LC droplets to form bigger ones. There is more number of bipolar droplets in the high dye-doped film

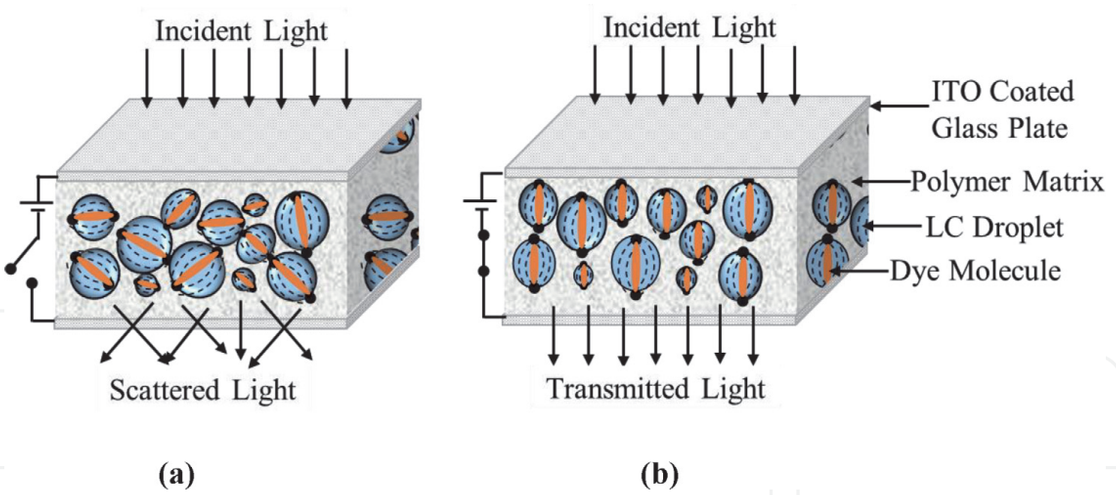

Figure 37.
Schematic of DPDLC in (a) OFF state and (b) ON state.

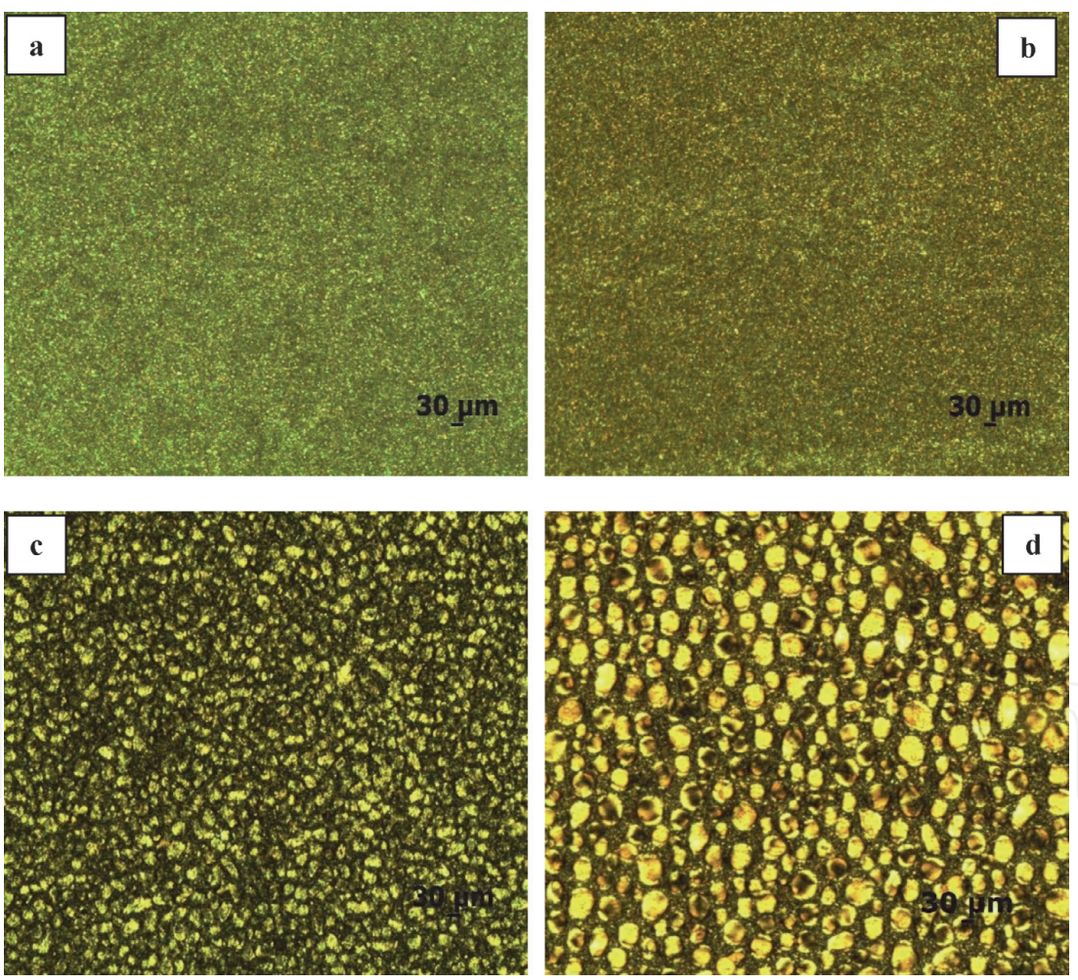

Figure 38.
POM images of O36N DPDLC film with dye concentrations (a) 0%, (b) 0.015%, (c) 0.25% and (d) 1%.

(**Figure 38(d)**) showing relatively higher affinity for the polymer and thus aiding strong anchoring at the polymer-LC interface than the low dye-doped composite films. Altogether, the addition of dye increases the viscosity of polymer-LC mixture, especially at low temperatures, which increases droplet size and hence optical path length [143, 154–158].

The high dye-doped PDLC film emerges with more number of bipolar droplets, as shown in **Figure 38(d)**. This can be interpreted as high dye-doped LC molecules

show relatively higher affinity for the polymer than the low dye-doped LC molecules and hence facilitating strong anchoring conditions at the interface of polymer and LC molecules [155].

Figure 39 shows effect of electric field on the morphology of DPDLC film O36S prepared using disperse Orange 25 dye, LC BL036 and Prepolymer SAM-114. The LC and prepolymer are taken here in 45/55 wt/wt%. In the ON state, when the electric field is low (10–20 V) (**Figure 39(b)**), there is substantial difference in the director direction of molecules which are near the polymer-LC interface and which are inside the LC droplet, and point defects are still at their initial position. On increasing the voltage (higher than anchoring energy at polymer-LC interface) (30 V and above) (**Figure 39(c)** and **(d)**), small and big LC droplets acquire maltese-type structure and twisted arrangement with director direction parallel to field, respectively. The appearance of maltese crosses is due to the interference (recombination) of the two refracted waves at higher fields [125, 159, 160].

The voltage dependence of transmittance for DPDLC composite film (O00N), prepared using dye disperse Orange 25+ LC HPC850100–100 + prepolymer NOA-65, at a constant frequency of 200 Hz is shown in **Figure 40**. LC and prepolymer are taken in 40/60 wt/wt% ratio, respectively, with dye content varying from 0 to 1%. The parameters such as T_{OFF}, T_{ON}, CR, ΔT, V_{TH} and V_{ON} calculated from graph (**Figure 40**) are summarized in **Table 4**.

From the above graph (**Figure 40**) and **Table 4**, it is clear that the DPDLC film with lowest dye concentration (0.007%) is the optimum one. This film has low value of T_{OFF} and high value of T_{ON}, which results in high CR and high ΔT. The value of V_{TH} and V_{ON} is remarkably low, desired for good EO devices.

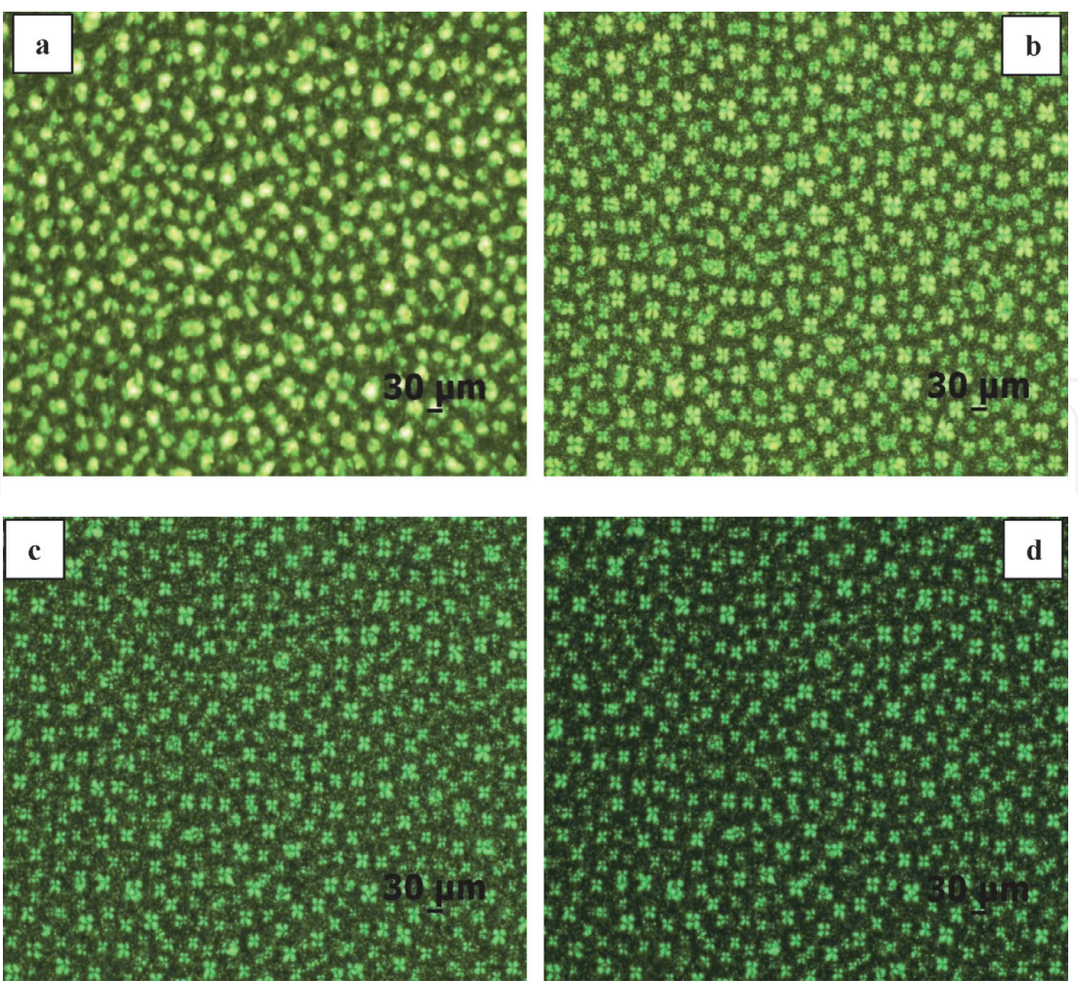

Figure 39.
Droplet structure of 0.015% O36S DPDLC film at (a) 0 V, (b) 20 V, (c) 40 V and (d) 60 V.

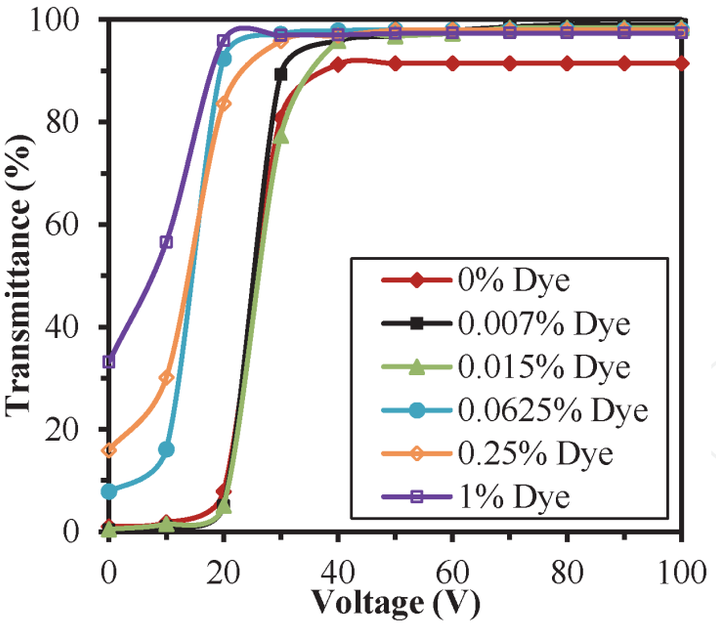

Figure 40.
Transmittance vs. voltage curve of various dye concentrations OooN DPDLC films at 200 Hz frequency and 25°C temperature.

Dye concentration (wt%)	T_{OFF} (%)	T_{ON} (%)	ΔT (%)	CR	V_{TH}	V_{ON}
0.0	1.02	91.43	90.41	90	3.5	40
0.007	**0.41**	**98.98**	**98.57**	**241**	**1.1**	**40**
0.015	0.51	98.37	97.86	193	1	40
0.0625	7.86	97.96	90.1	12	1.5	29
0.25	15.52	97.96	82.44	6	1.3	33
1	33.16	97.40	64.24	3	1.5	29

The significance of bold values are the optimum parameters for the given film.

Table 4.
Voltage-transmittance data of various dye concentrations OooN DPDLC films.

The variation in rise time and decay time of DPDLC composite films (O36S) prepared using LC BL036+ Prepolymer SAM-114 in 45/55 wt/wt% ratio and doped with disperse orange dye, at 40 V, is given in **Table 5**.

Generally, the rise time of all composite films decreases with the increase in voltage, whereas decay time is independent of voltage. This observed phenomenon is in good agreement with Eqs. (27) and (28). However, sometimes, there is small increase in decay time with voltage indicating longer transparent state even after field removal. Also, at higher voltages, rise time is of the order of microseconds indicating quick switching of the films. **Table 5** indicates lower value of rise time for low dye concentration DPDLC film. The proposed reason is increased dipole

Dye concentration (wt%)	Rise time (ms)	Decay time (ms)
0	0.4	6.8
0.007	0.2	6.6
0.015	0.3	6.7
1	0.8	8.3

Table 5.
Rise time and decay time of DPDLC film O36S at 40 V.

moment of LC droplet due to addition of dye molecules, contributing in LC droplet quick orientation, hence low rise time. With the further increase in dye concentration, rise time increases because of increase in viscosity of LC+ dye mixture. Altogether, at higher dye concentration, LC molecules expel dye towards polymer surface creating additional surface anchoring. Upon removal of field, LC droplets of low dye concentration DPDLC film quickly reorients as compared to the un-doped film. In high dye concentration DPDLC film, LC droplets took more time to reorient because of the additional surface anchoring between dye-doped LC droplet and polymer walls. During application of field, charge gets stored in dye-doped LC droplet, which serves as capacitor even after removal of external field affecting relaxation time of LC droplet.

For the analysis of experimental data and qualitative evaluation of distribution of relaxation time, Cole-Cole plot is drawn for imaginary part ε'' vs. real part ε' of the dielectric constant. For O00N (dye Orange 25+ LC HPC850100–100 + prepolymer NOA65) DPDLC film, Cole-Cole plot is shown in **Figure 41**. Dielectric parameters calculated using Cole-Cole plot are summarized in **Table 6**. The zero value of α listed in **Table 6** clearly shows that DPDLC films show Debye type behaviour. The 0.007% DPDLC film has very high value of dielectric strength.

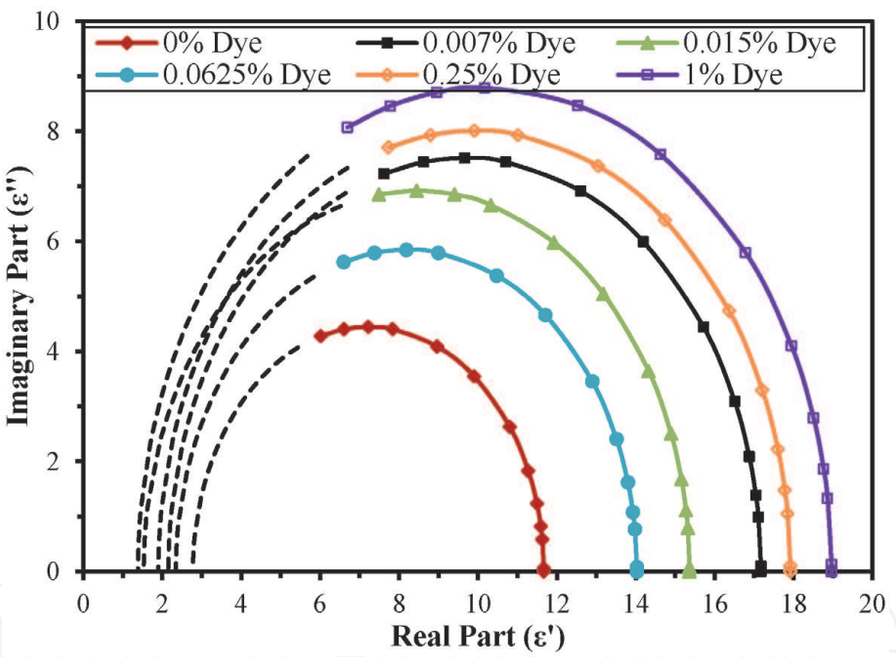

Figure 41.
Cole-Cole plots of various dye concentrations O00N DPDLC films at 25°C temperature.

Dye concentration (wt%)	f (MHz)	ε_s	ε_∞	$\delta\varepsilon'$	τ (s)	α
0.0	15.1	11.66	2.77	8.89	$1.05\ E^{-8}$	0
0.007	**15.1**	**17.17**	**2.15**	**15.02**	**$1.05\ E^{-8}$**	**0**
0.015	17.4	15.36	1.53	13.83	$9.15\ E^{-9}$	0
0.0625	15.1	14.03	2.34	11.69	$1.05\ E^{-8}$	0
0.25	15.1	17.91	1.89	16.02	$1.05\ E^{-8}$	0
1	13.2	18.96	1.38	17.58	$1.21\ E^{-8}$	0

Table 6.
Fitting parameters of various dye concentrations O00N DPDLC films.

In order to improve the performance of PDLC films, similar to DPDLC films, LC can be doped with nano-particles or carbon nanotubes. One such example is multiwalled carbon nanotubes (MWCNT)-doped PDLC (CPDLC) film, which is discussed here.

6.6 Operating principle of CPDLC composite films

Similar to the DPDLC composite films, in CPDLC films, LC phase acts as the host and MWCNT doped in LC act as the guest entity. MWCNTs are physically and environmentally stable, mechanically strong, chemically inert and thermally and electrically conducting material with high aspect ratio. MWCNT is also self-organizing, like LC material, but strong attractive Van der Waals forces between adjacent MWCNT lead them to cluster and form unorganized bundles [161]. It is very difficult to disperse MWCNT in a medium, but small percentage of MWCNT can be dispersed well in LC fluid. Till date any experimental confirmations regarding the interaction between MWCNT and LC are unavailable, but on analyzing their structure, π-π interaction (aromatic interaction) between MWCNT walls and phenyl rings of LC molecules is evident. As MWCNT is insoluble in LC, this type of interaction is quite weak to cause any LC director deformation. The well-dispersed MWCNT are generally orientated with their cylindrical axis parallel to the director direction of nematic LC. After the sufficiently stable dispersion of MWCNT in LC, both host LC and guest MWCNT share their intrinsic properties with each other, which are listed below:

1. Due to the dipolar nature of LC material, asymmetric charges are induced on MWCNT producing permanent dipole moment on MWCNT.

2. Nematic LC solvent provides partial orientational order to MWCNT.

3. MWCNT impart their electrical conductivity to the LC molecules.

Because of this sharing of inherent properties with each other, properties of CPDLC films get affected significantly. Similar to the DPDLC films, in CPDLC films also the dispersion of the LC droplets has been achieved using PIPS method, but in CPDLC films even after completion of polymerization process, MWCNT are found to be well separated entity from LC droplets embedded in polymer matrix. Since MWCNT do not absorb any light, hence operating principle of CPDLC films is based only on controllable scattering of light from randomly dispersed LC droplets. In the absence of field, i.e. "OFF state", MWCNT and LC droplets are separately and randomly oriented inside polymer matrix as shown in **Figure 42(a)**. The unpolarised incident light is scattered because of LC droplets. Upon application of field, i.e. "ON state", LC droplets get aligned along the direction of field, and MWCNT also get partially oriented as shown in **Figure 42(b)** and may form conducting channel at higher MWCNT concentration.

Figure 43(a)–(d) shows SEM images of some representative CPDLC films (C00N) prepared using LC HPC850100–100 and prepolymer NOA-65 doped with MWCNT concentration 0, 0.005, 0.05 and 0.5%. Here, LC and prepolymer are taken in 60/40 wt/wt% ratio. As MWCNT are insoluble in LC and do not participate in photopolymerization kinetics, therefore, the size of the LC droplets remains invariant upon addition of MWCNT. On analysing SEM images of 0% and 0.005% CPDLC films (**Figure 43(a)** and **(b)**), it is clear that the size of cavities is of few microns. Increase in MWCNT concentration (0.05 and 0.5% CPDLC film) does not affect the size of LC droplets but because of clustering of MWCNT, few bigger size cavities are formed as shown in **Figure 43(c)** and **(d)**.

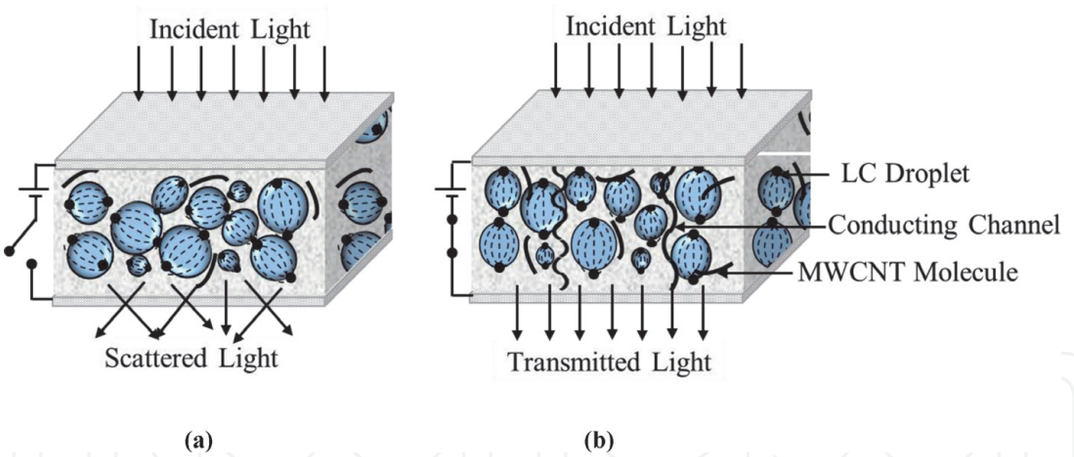

Figure 42.
Schematic of CPDLC in (a) OFF state and (b) ON state.

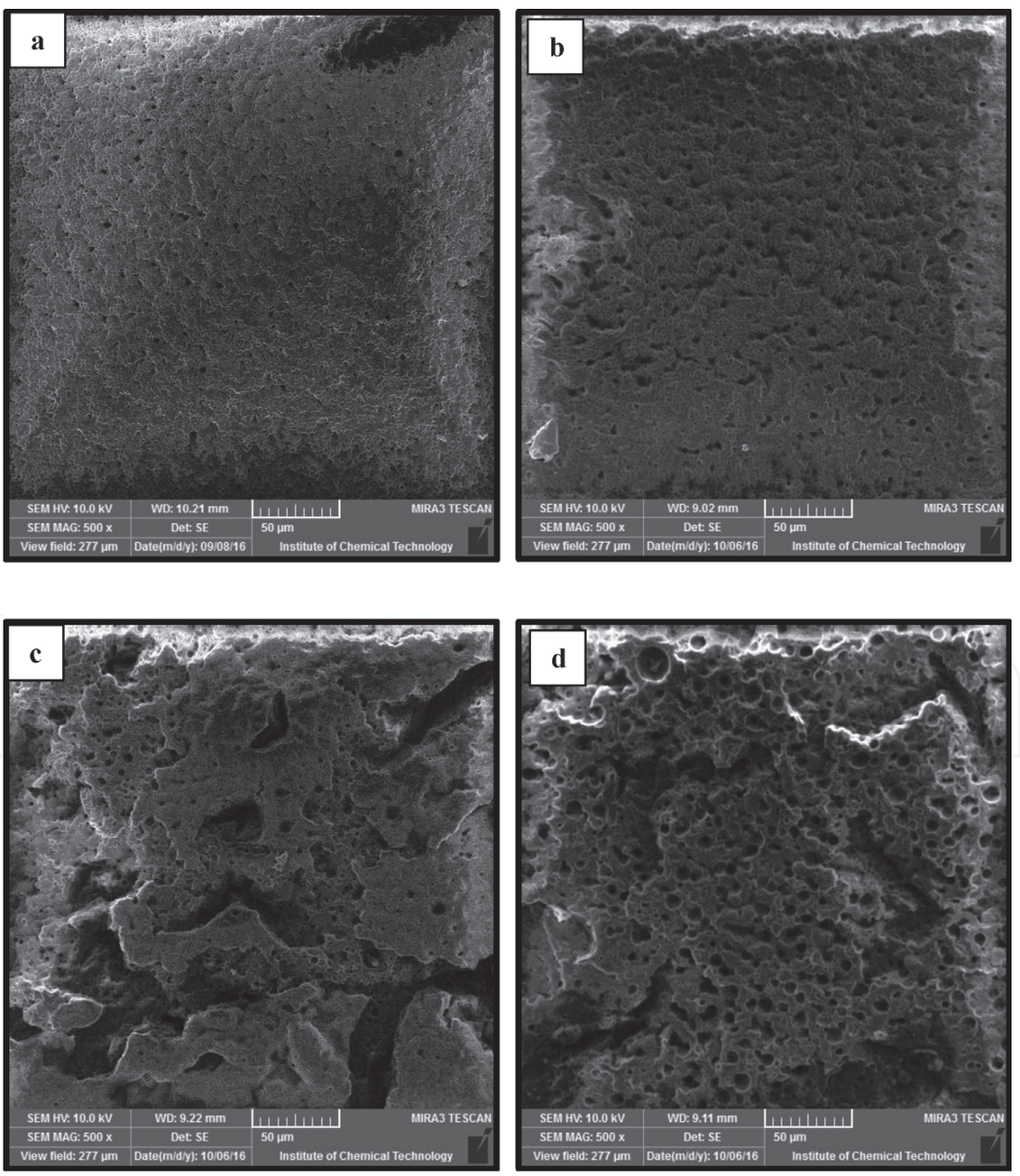

Figure 43.
Cavities formed after removal of LC from (a) 0%, (b) 0.005%, (c) 0.05% and (d) 0.5%, C00N CPDLC films.

The voltage dependence of output transmittance for CPDLC films with MWCNT content varying from 0 to 0.5% is shown in **Figure 44**. The parameters such as T_{OFF}, T_{ON}, CR, ΔT, V_{TH} and V_{ON} calculated from this graph are summarized in **Table 7**.

From the above graph (**Figure 44**) and **Table 7**, it is clear that the CPDLC film with lowest MWCNT concentration (0.005%) is optimum one. This film has low value of T_{OFF} and high value of T_{ON}, which results in high *CR* and high ΔT. The value of V_{TH} and V_{ON} is remarkably low, desired for good EO devices.

In order to understand the effect of temperature on other dielectric parameters such as dielectric strength and relaxation process, Cole-Cole plot can be drawn between real and imaginary parts of complex dielectric constant. **Figure 45** shows Cole-Cole plots of 0.005% MWCNT-doped C36N CPDLC film (LC BL036 and prepolymer NOA-65 in 50/50 wt/wt % ratio) at different temperatures. It is clear from graphs that the value of dielectric strength {difference of relative dielectric constant at static (at 20 Hz) and optical (at relaxation) frequency *f*} increases up to 40°C and then starts decreasing because small increase in temperature weakens intermolecular interaction and hence relaxes orientation-reorientation process of dipoles, whereas at high temperatures, thermal agitation becomes more predominant than intermolecular interaction which produces randomization of dipoles.

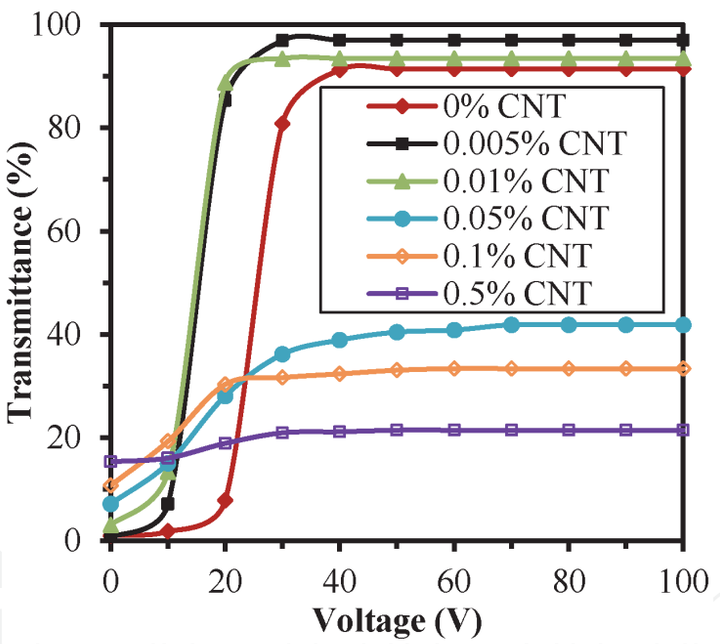

Figure 44.
Transmittance vs. voltage curve of various MWCNT concentrations CooN, CPDLC films at 200 Hz frequency and 25°C temperature.

MWCNT concentration (wt %)	T_{OFF} (%)	T_{ON} (%)	ΔT (%)	CR	V_{TH}	V_{ON}
0.0	1.02	91.42	90.4	90	3.5	40
0.005	**0.71**	**97.02**	**96.31**	**137**	**0.1**	**30**
0.01	3.06	93.46	90.4	31	0.4	24
0.05	7.14	41.83	34.69	6	1.0	32
0.1	10.71	33.36	22.65	3	1.3	20
0.5	15.3	21.42	6.12	1	7.4	30

Table 7.
Voltage-transmittance data of various MWCNT concentrations CooN CPDLC films.

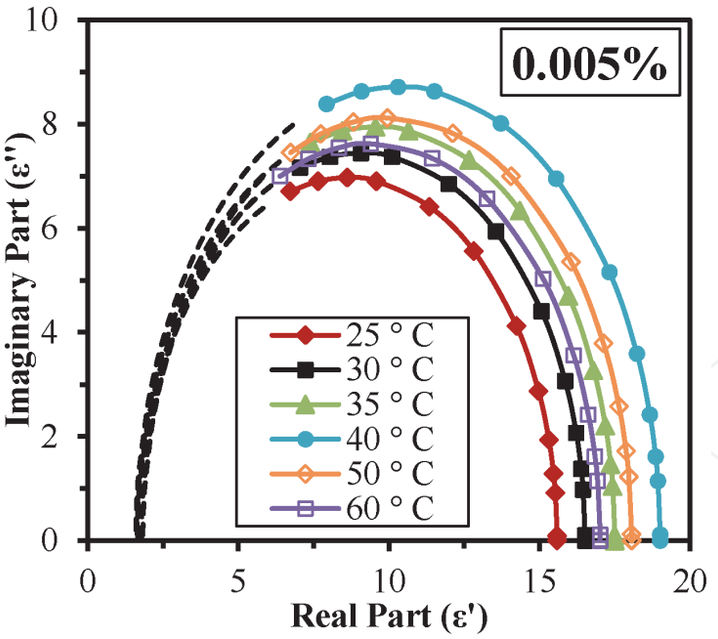

Figure 45.
Cole-Cole plots of 0.005% MWCNT concentration C36N, CPDLC film at different temperatures.

The value of distribution parameter α (not shown here) calculated for all Cole-Cole plots drawn for CPDLC films at different temperatures was zero, revealing Debye type relaxation [162].

6.7 Conclusions of PDLC study

The phenomenal optical and dielectric anisotropy of LC has been exploited in various display devices/LC technologies, and one such example is polymer-dispersed liquid crystal films. To improve the optical efficiency of PDLC device, with reduced operating voltages, faster switching time and high image contrast, properties of LC have been modified by doping it with some foreign entity. To obtain the desired result from the host LC material, proper selection of size, shape and structure of guest is an imperative factor. In all cases it has been proven that LC responds radically when doped and anchored to elongated species due to their inherent dipole moment. Therefore, host LC can be doped with dichroic dye guest molecules. Dye molecules tend to line up with the LC director, and dye absorbance is modulated by the alignment of nematic director with an external electric field. The controlled absorption and scattering of light through these materials make them promising candidates for various potential devices. Also the self-organizing properties of nematic LCs can be used to align carbon nanotubes (CNT) dispersed in them. CNT not only well integrate in the matrix but also, even at very low concentration, have a detectable effect on the LC properties that can be very attractive for display applications.

7. Holographic polymer-dispersed liquid crystal

When monomer concentration is high around 60–70%, nanosized LC droplets are formed and embedded inside the polymer matrix, this kind of polymer-LC composite films is named as HPDLC films. In PDLC films LC droplets are randomly distributed in polymer matrix, whereas in HPDLC films, alternate polymer-rich and LC-rich regions exist. As the size of the LC droplets is much smaller than the wavelength of visible light, composite films, free from scattering effect and with

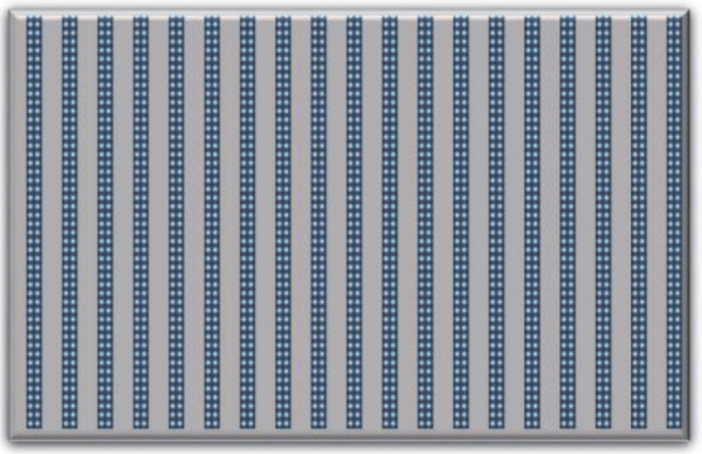

Figure 46.
Schematic of HPDLC film.

faster response time, have been obtained. Similar to the PDLC composite films, no surface alignment layer is needed in HPDLC films. **Figure 46** shows schematic of HPDLC film.

7.1 Operating principle

When a mixture of LC, monomer and photoinitiator (PhI) is exposed under the standing wave, formed from the interference of two or multiple coherent laser beams, it generates periodic dark and bright fringes. These periodic fringes regulate polymerization and hence phase separation process. High polymerization rate in the bright region (diffusion of monomer from dark to bright region) and low polymerization rate in the dark region (diffusion of LC from bright to dark region) create Bragg grating with alternate polymer-rich and LC-rich regions. Similar to the PDLC, the polymer and LC material are chosen such that the RI of the polymer should match with the ordinary RI of LC. Upon application of electric field, HPDLC film becomes optically transparent/homogenous, and the grating is in its OFF state. When the electric field is removed, LC molecules return to their original random state, and grating is in its ON state. This HPDLC grating reflects light of a particular wavelength and transmits light of all other wavelengths [163]. Morphology and diffraction properties of grating depends upon writing set-up, materials, diffusion rate, curing conditions and phase separation process [164, 165]. The particular wavelength that is reflected is a function of the refractive index difference and the width of the layers in the grating. When a voltage is applied, the liquid crystals align with the field, and their new refractive index matches that of the polymer, causing the grating to become transparent.

7.2 Material used and sample preparation of HPDLC films

HPDLC composite films are also prepared by mixing LC, monomer, photoinitiator and dopant (if any) in a desired ratio.

7.2.1 LC material

The optical and dielectric anisotropy of nematic LC make them suitable candidate for HPDLC films. Similar to the PDLC composite films, the operation of these composite films is based on birefringence property of LC. Nematic LCs are

optically uniaxial materials, i.e. they have two direction-dependent refractive indices, (ordinary RI, n_o, and extraordinary RI, n_e) with birefringence $\Delta n = n_e - n_o$ and average RI, $n_{av} = \sqrt{\frac{1}{3}\left(n_e^2 + 2n_o^2\right)}$. The value of Δn may be positive or negative [34, 37, 38]. The polymer and LC are chosen such that the refractive index of the polymer (n_p) should match with ordinary refractive index (n_o) of the LC, typically $n_e \gg n_o \sim n_p$.

7.2.2 Monomer unit

In HPDLC films two types of monomer can be used:

a. Acrylate-based monomer: A wide range of acrylate-based monomers with different functionalities are available such as phthalic diglycol diacrylate (PDDA), 2-ethylhexyl acrylate (EHA), polyurethane acrylate oligomers (PUA), etc. But these multifunctional acrylates carry some drawbacks in HPDLC gratings, such as: (i) Because of early gelation and subsequent vitrification, monomer conversion is low, and polymerization can continue for prolonged periods, even in the dark; (ii) during exposure considerable shrinkage was also observed; (iii) larger interfacial area increases unwanted optical scattering; and (iv) interconnectivity in LC droplets and variety in LC droplet configuration decreases prompt electrical switching.

b. Thiol-ene-based monomer: Thiol-ene-based monomers are composed of multifunctional aliphatic thiols and vinyl monomers comprising ene groups. These monomers have high conversion efficiency, good stability, less shrinkage and more elastic; therefore they are preferably used for constructing HPDLC composite films. Norland optical adhesives are good examples of these kinds of monomers. Earlier these monomers could only be cured by UV light, but now new materials were synthesized, which can be cured under visible light.

7.2.3 Photoinitiator and co-initiators

Along with LC material and monomer, to induce photopolymerization, PhI and co-initiators are also required. Choice of PhI depends on the wavelength of laser beam employed for writing. Sometimes chain extenders are also incorporated into the mixture to optimize grating morphologies.

7.2.4 Sample preparation

Empty sample cell is prepared by two ITO-coated glass substrate (ITO coating facing each other) separated by suitable spacers. Mixture of LC, monomer, photoinitiator and dopant (if any) is stirred for homogenization. Mixture is filled into ITO cell and then exposed under suitable light depending upon the PhI. Generally, for curing sample cell is placed under the interference pattern formed by coherent laser beams. Samples are again placed under UV lamp for postcuring if needed [166].

7.3 Types of HPDLC gratings

Different writing set-ups produce different types of HPDLC gratings, named as transmission grating and reflection grating. If the writing beams are incident on

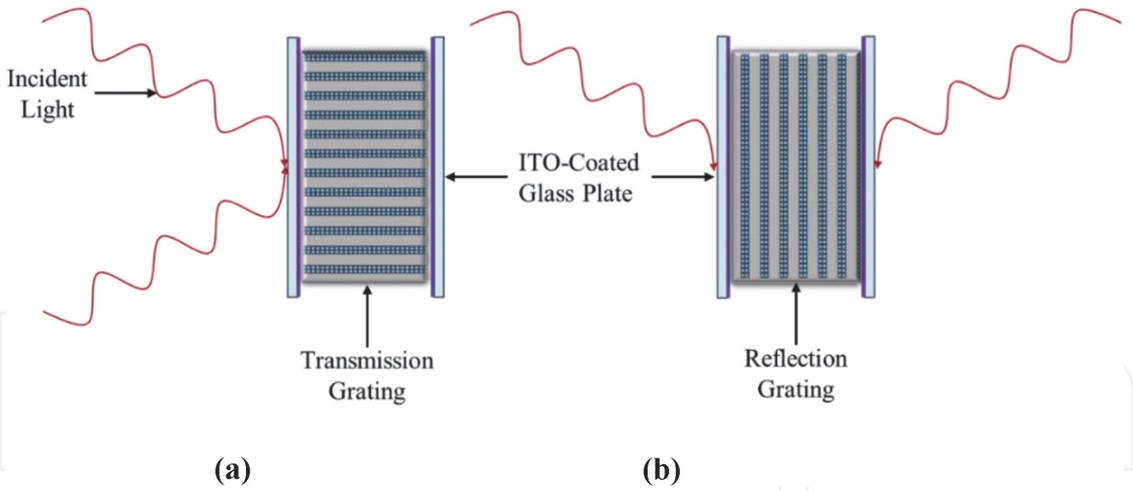

Figure 47.
Types of HPDLC grating: (a) transmission grating and (b) reflection grating.

the same side of sample cell, transmission grating will be formed, with grating planes perpendicular to the sample cell surface as shown in **Figure 47(a)**. If the writing beams are incident from both sides of the samples, reflection grating will be formed, with grating planes parallel to the sample cell surface as shown in **Figure 47(b)**.

7.4 HPDLC grating parameters

7.4.1 Grating period/grating pitch

The grating period depends on the writing wavelength and intersection beam angle:

$$\Lambda = \frac{\lambda}{2\overline{n}\ \sin\left(\theta_i/2\right)} \tag{30}$$

Here, Λ is the grating period, λ is the writing wavelength and $\overline{n}$ is the average refractive index of the material mixture. A grating with varied period can be obtained by inserting a refractive cylindrical lens in conventional double interference optical path. It varies the angle of incidence of one of the two interference laser beams [167].

7.4.2 Cook-Klein parameter

This parameter depends on the grating period and thickness of grating:

$$Q = 2\pi \frac{\lambda d}{\overline{n}\Lambda^2} \tag{31}$$

Here, λ is the wavelength of incident light, and d is the thickness of the grating.

If the value of $Q < 1$, then it is a Raman-Nath-type grating. It is thin grating and multiple diffraction orders can be found.

If the value of $Q > 1$, then it is Bragg-type grating. It is thick or volume grating, and only zero order or first order of diffraction can be found. Since the optical losses are low in Bragg-type-grating, it is preferred for practical applications.

7.5 HPDLC morphology

Different materials and varying curing conditions produce different types of polymer-LC morphologies in HPDLC composite films. Mainly, HPDLC morphologies can be categorized into three types.

7.5.1 LC droplet-like morphology

Generally, this type of morphology has been found in transmission or reflection grating (**Figure 48**). These types of gratings are made up of acrylate- or thiol-ene-based monomers. During PIPS process, because of fast curing process (intense curing light and small curing time) and high effective functionality of monomer, LC molecules get diffuse and configure themselves into distinct and elongated LC droplets. These LC droplets, embedded into the polymer matrix, are distinguished in SEM image (**Figure 48(b)**). Here, light scattering is more because the size of the LC droplets is comparable to the wavelength of the visible light [164, 168].

7.5.2 Polymer scaffolding morphology

In transmission gratings prepared from acrylate-based material systems under slow curing process, polymer scaffolding morphology can be obtained (**Figure 49**). Here instead of small LC droplets, large LC domains or LC layer is obtained. If the curing process is relatively slow as compared to that in "LC droplet-like morphology", transverse polymer filaments are obtained in polymer-rich region, in between

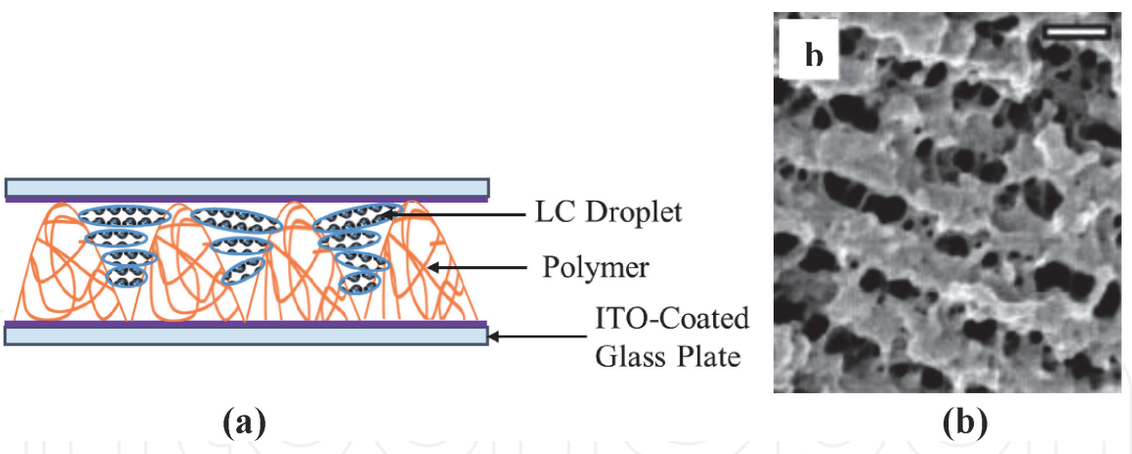

Figure 48.
LC droplet-like morphology: (a) schematic and (b) SEM image of HPDLC film [164, 168].

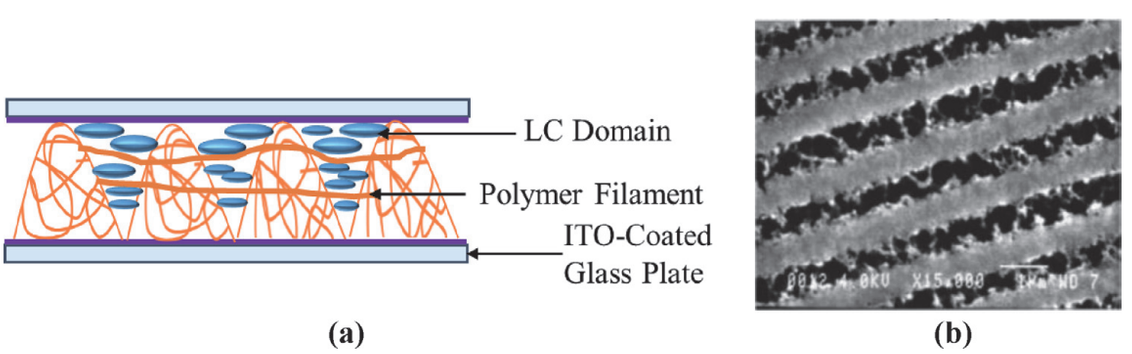

Figure 49.
Polymer scaffolding morphology: (a) schematic and (b) SEM image of HPDLC film [164, 169].

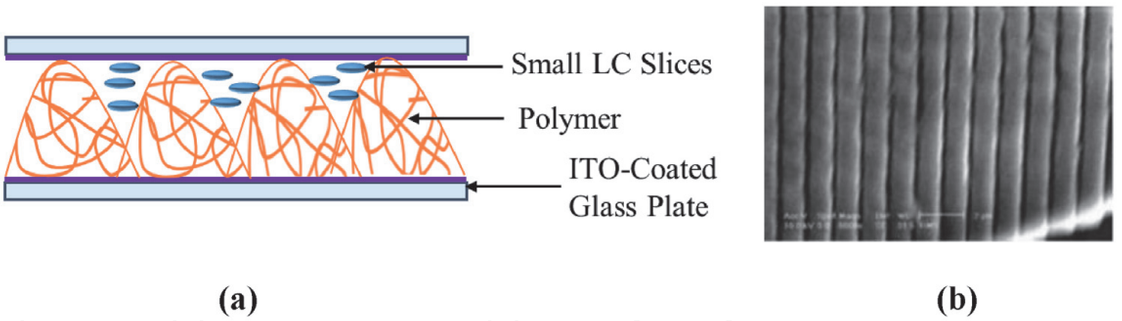

Figure 50.
Sliced polymer morphology: (a) schematic and (b) SEM image of HPDLC film [164, 170].

two LC domains/layers, as shown in SEM image (**Figure 49(b)**). As LC droplets are absent, scattering losses are low [164, 169].

7.5.3 Sliced polymer morphology (policryps)

In this type of morphology, transmission gratings are prepared from thiol-ene-based monomers, under slow curing process and above nematic-isotropic temperature T_{NI} of LC (**Figure 50**). In this type of grating, polymer slices are well separated from aligned nematic slices. From the SEM image (**Figure 50(b)**), it is clear that as the concentration of LC is low than the polymer, thickness of the LC slices is also small as compared to polymer slices. The high phase separation degree produces smooth polymer layers and aligned LC layers, which in turn minimizes scattering losses [164, 170].

7.6 Conclusions of HPDLC study

Similar to the PDLC films, HPDLC films are based on the scattering and transmittance effect of light from polymer-LC composite film. High monomer concentration and formation of interference pattern during photopolymerization give rise to alternate polymer-rich and LC-rich regions. Depending upon writing set-ups, two types of HPDLC gratings can be formed. Variation in materials and curing conditions can produce different types of morphology in HPDLC composite films. Simple configuration, easy fabrication process and their integration with other optical devices make them suitable for practical applications.

8. Applications

Polymer-LC composite film-based devices are switchable and tunable. The RI of LC droplets embedded in polymer matrix can be tuned using external fields; therefore they can be used for a wide range of display and non-display applications. The low monomer concentration polymer-LC composite film termed as PSLC films can be used for bi-stable reflective displays and haze-free normal- and reverse-mode light shutters with quick response [68, 110].

The PDLC composite films with the intermediate monomer concentration are distinguished because of their flexibility as well as mechanical strength. The comprehensive list of applications of PDLC film includes haze-free light shutter devices; switchable windows; high-definition Fuoss-Kirkwood spatial light modulators; flat-panel and large area flexible displays; light valves; color projectors; thermal, optical and strain sensors; electrically tunable focusing lenses; etc. [171].

When the monomer concentration is higher than the LC concentration, HPDLC films get formed. HPDLC films are known to be a promising technology because they can be used in 3D display, fiber optics, data storage, zoom lenses, image capture systems, beam vibration sensor, etc. [172].

It can be concluded that the LC's inherent optical and dielectric anisotropy can be effectively used in a display as well as non-display devices.

9. Summary

This chapter encompasses a wide range of LC-related subject matter. It begins with the basics of LC materials, such as definition, history, types, phases and properties of LCs. Information about properties of LC materials offer deep insight in choosing LC material for particular application and also benefit in innovating new applications. Initially applications of LC materials are limited to display world only; now it is finding scope in a non-display world too. A brief outline about applications of LC devices has been followed by an extensive study of polymer-LC composites. The three types of composite films reported in this chapter are as follows:

1. Low monomer concentration composite: PSLC film

2. Moderate monomer concentration composite: PDLC film

3. High monomer concentration composite: HPDLC film

The detailed study of each of the above composite films is about the following:

1. Fabrication technique using the most suited phase separation process.

2. Morphological analysis, which portrays their size, shape, configuration and defects in LC droplet/domain structure.

3. Electro-optic study: It comprises definition and formulation of various electro-optic parameters, such as transmittance difference, contrast ratio, hysteresis, threshold and saturation voltages and response time, with examples.

4. Dielectric study: Calculation of relaxation frequency, distribution parameter and breakdown strength using Debye and Cole-Cole plots is incorporated in this study.

Precisely, this chapter gives a deep and comprehensive knowledge about LC and some of their applications.

IntechOpen

Author details

Anuja Katariya Jain and Rajendra R. Deshmukh*
Department of Physics, Institute of Chemical Technology, Mumbai, India

*Address all correspondence to: rr.deshmukh@ictmumbai.edu.in; rajedeshmukh@rediffmail.com

References

[1] Woltman SJ, Crawford GP, Jay GD. Liquid Crystals: Frontiers in Biomedical Applications. Singapore: World Scientific; 2007

[2] Chandrasekhar S. Liquid Crystals. Cambridge: Cambridge University Press; 1992

[3] Reinitzer F. Zur Kenntnis des Cholesterins. Monatshefte für Chemie. 1888;**9**:421-441

[4] Dierking I. Textures of Liquid Crystals. Wiley-VCH Verlag: Weinheim; 2003

[5] Lehmann O. Uber fliessende Krystalle. Zeitschrift für physikalische Chemie. 1889;**4**:462-472

[6] Friedel G. The mesomorphic states of matter. Annales de Physique. 1922;**18**: 273-474

[7] Vorlander D. Chemische Kristallographie der Flussigkeiten: Kurze Anleitung zur Synthese und Untersuchung Polymorpher und Kristallinflüssiger Substanzen. Leipzig: Akademische Verlagsgesellschaft; 1924

[8] Herrmann K. Inclinations of molecules in some crystalline-fluid substances. Transactions of the Faraday Society. 1933;**29**:972-976

[9] Demus D, Goodby J, Gray GW, Spiess HW, Vill V. Handbook of Liquid Crystals-I. Wiley-VCH Verlag: Weinheim; 1998

[10] Jeu WHD. On the role of spherical symmetry in the Maier-Saupe theory. In: Cladis P, Palffy-Muhoray P, editors. Dynamics and Defects in Liquid Crystals: A Festschrift in Honor of Alfred Saupe. The Netherlands: Gordan and Breach; 1998

[11] Maier Z, Saupe A. Eine einfache molekular-statistische Theorie der nematischen kristallinflüssigen phase. Teil II. Zeitschrift für Naturforschung A. 1960;**15**:287-292

[12] Coates D, Gray GW. Optical studies of the amorphous liquid-cholesteric liquid crystal transition: The "blue phase". Physics Letters A. 1973;**45**: 115-116

[13] Demus D, Richter L, Rurup CE, Sackmann H, Schubert H. Synthesis and liquid crystalline properties of 4,4′-disubstituted biphenyls. Le Journal de Physique Colloques. 1975;**36**:349-354

[14] Luckhurst GR, Gray GW. The Molecular Physics of Liquid Crystal. London: Academic Press; 1979

[15] Andrienko D. Introduction to Liquid Crystals [Online]. 2006. Available from: www.mpip-ainz.mpg [Accessed: 11 July 2015]

[16] Demus D, Sackmann H. The problems of polymorphism in Liquid crystals. Molecular Crystals and Liquid Crystals. 1988;**21**:239-273

[17] LiqCryst Database. June 2010. Available from: www.lcipublisher.com/liqcryst.html [Accessed: 14 February 2019]

[18] Madsen LA, Dingemans TJ, Nakata M, Samulski ET. Thermotropic biaxial nematic liquid crystals. Physical Review Letters. 2004;**92**:145505-145514

[19] Drzaic PS. Liquid Crystal Dispersions. World Scientific: Singapore; 1995

[20] Collings PJ, Hird M. Introduction to Liquid Crystals. Bristol: Taylor & Francis; 1997

[21] De Gennes PG, Prost J. The Physics of Liquid Crystals. Oxford: Clarendon Press; 1993

[22] Bahadur B, editor. Liquid Crystals: Applications and Uses. Vol. I. Singapore: World Scientific; 1990

[23] Armitage D, Price FP. Calorimetry of liquid crystal phase transitions. Le Journal de Physique Colloques. 1975;**36**: 133-136

[24] Seideman T. The liquid-crystalline blue phases. Reports on Progress in Physics. 1990;**53**:659-705

[25] Crooker PP. Blue phases. In: Kitzerow HS, Bahr C, editors. Chirality in Liquid Crystals Partially Ordered System. New York: Springer; 2001. pp. 375-432

[26] Papon P, Lebond J, Meijer PHE. The Physics of Phase Transitions. Berlin Heidelberg: Springer-Verlag; 2006

[27] Largerwell ST. Comments on liquid crystal terminology, nomenclature and conventions. Ferroelectrics. 1988;**85**: 497-501

[28] Meiboom S, Sethna JP, Anderson PW, Brinkman WF. Theory of blue phase of cholesteric liquid crystals. Physical Review Letters. 1981;**46**: 1216-1219

[29] Brooks JD, Taylor GH. The formation of graphitizing carbons from the liquid phase. Carbon. 1965;**3**: 185-199

[30] Chandrasekhar S, Sadashiv BK, Suresh KA. Liquid crystals of disc like molecules. Pramana. 1977;**9**:471-480

[31] Desimpel, C. Liquid Crystals & Photonics Group, 2006. Available from: https://lcp.elis.ugent.be/tutorials/lc [Accessed: 01 December 2015]

[32] Pelzl G, Diele S, Weissflog W. Banana shaped compounds—A new field of liquid crystals. Advanced Materials. 1999;**11**:707-714

[33] Petrov AG. The Lyotropic State of Matter. Gordon & Breach: New York; 1999

[34] Stegemayer H. Liquid Crystals. New York: Springer; 1994

[35] Blinov LM, Cigrinov VG. Electro-Optic Effects in Liquid Crystal Materials. New York: SpringerVerlag; 1994

[36] Collings PJ. Liquid Crystals: Nature's Delicate Phase of Matter. Princeton: Princeton University Press; 1990

[37] Kedzierski J, Garbat K, Raszewski Z, Kojdecki MA, Kowiorski K, Jaroszewicz LR, et al. Optical properties of a liquid crystal with small ordinary and extraordinary refractive indices and small optical anisotropy. Opto-Electronics Review. 2014;**22**:162-165

[38] Mckenna L, Miller LS, Peterson IR. Polymer dispersed liquid crystal films for modulating infra-red radiation. Polymer. 2004;**45**:6977-6984

[39] Pasechnik SV, Chigrinov VG, Shmeliova DV. Liquid Crystals: Viscous and Elastic Properties. Wiley-VCH Verlag: Weinheim; 2009

[40] Singh S. Liquid Crystals Fundamentals. Singapore: World Scientific; 2002

[41] Taherian R. Application of conducting composite in dielectrics. In: Reza Taherian R, Kausar A, editors. Electrical Conductivity in Polymer-Based Composites: Experiments, Modelling and Applications. Oxford: William Andrew, Applied Science Publishers; 2019. pp. 73-90

[42] Leslie FM. Continuum theory for nematic liquid crystals. Continuum Mechanics and Thermodynamics. 1992; **4**:167-175

[43] Ge Z, Wu ST. Transflective Liquid Crystal Display. Chichester, UK: Wiley; 2010

[44] Kang H, Park JS, Sohn EH, Kang D, Rosenblatt C, Lee JC. Polyimide blend alignment layers for control of liquid crystal pretilt angle through baking. Polymer. 2009;**50**:5220-5227

[45] Mauguin MC. Sur les cristaux liquides de Lehmann. Bulletin de la Société Française de Minéralogie et de Cristallographie. 1911;**34**:71-117

[46] Varghese S. Patterned alignment of liquid crystal by microrubbing-A new route towards wide viewing angle flat panel displays [PhD thesis]. The Eindhoven University of Technology; 2005

[47] Shibaev VP. Polymers as Electrooptical and Photooptical Active Media. Heidelberg, Berlin: Springer-Verlag; 1996

[48] Acharya BR, Kim JH, Kumar S. Material independent determination of anchoring properties on rubbed polyimide surfaces. Physical Review E. 1999;**60**:6841-6846

[49] Janning JL. Thin film surface orientation for liquid crystals. Applied Physics Letters. 1972;**21**:173-174

[50] Porte G. Tilted alignment of MBBA induced by short-chain surfactants. Journal of Physics (France). 1976;**37**: 1245-1252

[51] Kim SH. Fast switching polymer stabilized liquid crystal devices: Morphological and electro-optical properties [PhD thesis]. Kent State University; 2004

[52] Van-Aerle NAJM, Toi AJW. Molecular reorientation in rubbed polyimide alignment layers used for liquid crystal display. Macromolecules. 1994;**27**:6520-6526

[53] Jeng SC, Hwang SJ. Controlling the alignment of polyimide for liquid crystal devices. In: Abadie MJM, editor. High Performance Polymers—Polyimides Based—from Chemistry to Applications. Rijeka: IntechOpen; 2012

[54] Yoon HG, Kang SW, Lehmann M, Park JO, Srinivasrao M, Kumar S. Homogenous and homeotropic alignment of bent core uniaxial and biaxial nematic liquid crystals. Soft Matter. 2011;**7**:8770-8775

[55] Kim JW, Kim H, Lee M, Magda JJ. Interfacial tension of a nematic liquid crystal/water Interface with homeotropic surface alignment. Langmuir. 2004;**20**:8110-8113

[56] Paek SH. Comparative study of effects of rubbing parameters on polyimide alignment layers and liquid crystal alignment. Journal of Industrial and Engineering Chemistry. 2001;**7**: 316-325

[57] Sonin AA. The Surface Physics of Liquid Crystals. Gordon and Breach: Luxembourg; 1995

[58] Bahadur B. Liquid crystals display. Molecular Crystals and Liquid Crystals. 1984;**109**:3-93

[59] Guyon, E., Urbach W. Anchoring properties and alignment of liquid crystals Kmetz, AR, von Willisen FK, editors. Non-Emissive Electro-optic Displays. Plenum Press: New York, 1976.

[60] Khoo IC. Liquid Crystals. Wiley: New Jersey; 2007

[61] Yang DK, Wu ST. Fundamentals of Liquid Crystal Devices. Chichester, UK: Wiley; 2006

[62] Lueder E. Liquid Crystal Display: Addressing Schemes and Electro-Optical Effects. Chichester, UK: Wiley; 2010

[63] Maini AK, Agrawal V. Electronic Devices and Circuits. New Delhi: Wiley; 2009

[64] Fergason JL. Display devices utilizing liquid crystal light modulation. US Patent 3731986, 1971.

[65] Helfrich W, Schadt M. Optical device. Swiss Patent 532261. 1970.

[66] Heilmeier GH, Zanoni LA. Guest-host interactions in nematic liquid crystals. Applied Physics Letters. 1968; **13**:91-92

[67] Scheffer TJ, Nehring J. Guets-host displays. In: The Physics and Chemistry of Liquid Crystal Devices. Springer: New York; 1980. pp. 173-180

[68] Crawford GP, Svensek D, Zumer S. Some aspects of polymer dispersed and polymer stabilized chiral liquid crystals. In: Kitzerow HS, Bahr C, editors. Chirality in Liquid Crystals Partially Ordered System. New York: Springer; 2001. pp. 375-432

[69] Jeon YJ, Bingzhu Y, Rhee JT, Cheung DL, Jamil M. Applications and new developments in polymer-dispersed liquid crystal simulation studies. Macromolecular Theory and Simulations. 2007;**16**:643-659

[70] Karapinar R. Electro-optic response of a polymer dispersed liquid crystal film. The Turkish Journal of Physics. 1998;**22**:227-235

[71] Spruce G, Pringle RD. Polymer dispersed liquid crystal (PDLC) films. Electronics & Communication Engineering Journal. 1992;**4**:91-100

[72] Liu YJ, Sun XW. Holographic polymer-dispersed liquid crystals: Materials, formation, and applications. Advances in OptoElectronics. 2008; **2008**:1-52

[73] Crawford GP, Zumer S. Liquid Crystals in Complex Geometries. London: Taylor & Francis; 1996

[74] Hicks SE. Polymer dispersed and polymer stabilized liquid crystals [PhD thesis]. Kent State University; 2012

[75] Zou J, Fang J. Director configuration of liquid-crystal droplets encapsulated by polyelectrolytes. Langmuir. 2010;**26**: 7025-7028

[76] Crawford NJ, Dadmun MD, Bunning TJ, Natarajan LV. Time-resolved light scattering of the phase separation in polymer-dispersed liquid crystals formed by photo-polymerization induced phase separation. Polymer. 2006;**47**:6311-6321

[77] Dierking I. Polymer network stabilized liquid crystals. Advanced Materials. 2002;**12**:167-181

[78] Fung YK, Yang DK, Ying S, Chien LC, Zumer S, Doane JW. Polymer networks formed in liquid crystals. Liquid Crystals. 1995;**19**:797-801

[79] Kumar R, Raina KK. Enhanced ordering in polymer stabilised ferroelectric liquid crystal guest-host composites: Evidence by polarised fluorescence spectroscopy. Liquid Crystals. 2014;**41**:694-700

[80] Deshmukh RR, Katariya-Jain A. Effect of anti-parallel and twisted alignment techniques on various properties of polymer stabilized Liquid crystal (PSLC) films. Liquid Crystals. 2016;**43**:436-447

[81] Moheghi A, Nemati H, Yang DK. Polarizing light waveguide plate from polymer stabilized liquid crystals. Optical Materials Express. 2015;**5**: 217-1223

[82] Serra F, Buscaglia M, Bellini T. The emergence of memory in liquid crystals. Materials Today. 2011;**14**:488-490

[83] Malik MK, Deshmukh RR. Electro-optics of homogenously aligned Nematic Liquid crystals stabilized by a

polymer network. International Journal of ChemTech Research. 2014;**6**:1833-1835

[84] Deshmukh RR, Malik MK. Effects of the composition and nematic-isotropic phase transition on the electro-optical responses of unaligned polymer-dispersed liquid crystals. I. Composites of poly(methyl methacrylate) and E8. The Journal of Applied Polymer Science. 2008;**108**:3063-3072

[85] Dixit S. Liquid crystals: Dielectric and electro-optic study. [PhD thesis]. Lucknow: University of Lucknow; 2013

[86] Parab SS, Malik MM, Deshmukh RR. Dielectric relaxation and electro-optical switching behavior of nematic liquid crystal dispersed in poly(methyl methacrylate). Journal of Non-Crystalline Solids. 2012;**358**:2713-2722

[87] Thakur VK, Kessler MR. Polymer nanocomposites: New advanced dielectric materials for energy storage applications. In: Tiwari A, Valyukh S, editors. Advance Material Energy. Salem, MA: Scrivener Publishing LLC-Wiley; 2014

[88] Dissado LA, Fothergill LC. Electrical Degradation and Breakdown in Polymers. London, UK: Peter Peregrins; 1992

[89] Malik NH, Al-Arainy AA, Qureshi MI. Electrical Insulation in Power System. Boca Raton: CRC Press; 1998

[90] Bunget I, Popescu M. Physics of Solid Dielectrics. Amsterdam, The Netherlands: Elsevier; 1984

[91] Raju GG. Dielectrics in Electric Fields. New York: CRC Press; 2003

[92] Jonscher AK. Dielectric Relaxation in Solids. Chelsea Dielectric Press: London; 1983

[93] Ding H. A study of dielectric and electro-optical response of liquid crystal in confined systems. [PhD thesis]. Kent State University; 1996

[94] Seekola DL. Dielectric response of polymer dispersed liquid crystal films [PhD thesis]. Kent State University; 1992

[95] Deshmukh RR, Parab SS, Malik MK. Effect of host polymer matrices on electro optical and dielectric behaviour of polymer dispersed liquid crystal system. Advances in Materials Research. 2012;**584**:531-535

[96] Lee DG, Suh NM. Axiomatic Design and Fabrication of Composite Structures: Applications in Robots, Machine Tools, and Automobiles. New York: Oxford University Press; 2006

[97] Kremer F, Schonhals A. Broadband Dielectric Spectroscopy. Berlin Heidelberg: Springer-Verlag; 2003

[98] Wrobel S. Dielectric relaxation spectroscopy. In: Haase W, Wrobel S, editors. Relaxation Phenomena: Liquid Crystals, Magnetic Systems, Polymers, High-Tc Superconductors, Metallic Glasses. Berlin, Heidelberg: Springer-Verlag; 2003

[99] Lvovich VF. Impedance Spectroscopy Applications to Electrochemical and Dielectric Phenomena. Wiley: New Jersey; 2012

[100] Parab SS, Malik MK, Bhatia PG, Deshmukh RR. Investigation of liquid crystal dispersion and dielectric relaxation behavior in polymer dispersed liquid crystal composite films. Journal of Molecular Liquids. 2014;**199**: 287-293

[101] Parab SS, Malik MM, Deshmukh RR. Investigation of dielectric properties of poly(methyl methacrylate)-E7 composite films. International Journal of ChemTech Research. 2014;**6**:1836-1839

[102] Cole KS, Cole RH. Dispersion and absorption in dielectrics-I alternating

current characteristics. The Journal of Chemical Physics. 1941;**9**:341-351

[103] Cole KS, Cole RH. Dispersion and absorption in dielectrics-I alternating current characteristics. The Journal of Chemical Physics. 1942;**10**:98-105

[104] Al-Refaie SN. A generalized formula to determine the relaxation time distributions in dielectrics. Applied Physics A: Materials Science & Processing. 1991;**52**:234-236

[105] Parab SS, Malik MK, Dabrowski R, Deshmukh RR. Thermodynamic and bias field characterization of quickly operating antiferroelectric liquid crystal. Journal of Molecular Liquids. 2013;**183**: 20-25

[106] Pevzner B. Transport and dielectric properties of thin fullerene (C60) films [PhD thesis]. Massachusetts: Massachusetts Institute of Technology; 1995

[107] Gray GW, Kelly SM. Liquid crystals for twisted nematic display devices. Journal of Materials Chemistry. 1999;**9**:2037-2050

[108] Hale PS, Shapter JG, Voelcker NH, Ford MJ, Waclawik ER. Liquid-crystal displays: Fabrication and measurement of a twisted nematic liquid-crystal cell. Journal of Chemical Education. 2004;**81**: 854-860

[109] Rajaram CV, Hudson SD. Morphology of polymer stabilized Liquid crystal. Chemistry of Materials. 1995;**7**:2300-2308

[110] Zhang T, Cong Y, Zhang B, Zhao W. Preparation and characterisation: PSCLC film doping with FexNiy nanoparticles. Liquid Crystals. 2015;**42**: 167-173

[111] Sun H, Xie Z, Ju C, Hu X, Yuan D, Zhao W, et al. Dye-doped electrically smart windows based on polymer-stabilized liquid crystal. Polymer. 2019;**11**: 694-703. DOI: 10.3390/polym11040694

[112] Yan X, Zhou Y, Liu W, Liu S, Hu X, Zhao W, et al. Effects of silver nanoparticle doping on the electro-optical properties of polymer stabilized liquid crystal devices. Liquid Crystals. 2019;**46**:1-8. DOI: 10.1080/02678292.2019.1641754

[113] Fergason JL. Encapsulated liquid crystal and method. US Patent 4435047, 1984.

[114] Fergason JL. Polymer encapsulated nematic liquid crystals for display and light control applications. Society for Information Display Technical Digest. 1985;**85**:68-70

[115] Doane JW, Golemme A, West JL, Whitehead JB Jr, Wu BG. Polymer dispersed liquid crystals for display application. Molecular Crystals and Liquid Crystals. 1988;**165**:511-532

[116] Deshmukh RR. Electro-optic and Dielectric properties in PDLC composite systems. In: Thakur VK, Kessler MR, editors. Liquid Crystalline Polymers-II, Processing and Applications. Switzerland: Springer International Publishing; 2015. pp. 169-195

[117] Kalkar AK, Kunte VV. Electro-optical studies on polymer dispersed liquid crystal composite films. II. Composites of PVB/E44 and PMMABA/E44. Molecular Crystals and Liquid Crystals. 2002;**383**:1-25

[118] Li W, Cao Y, Cao H, Kashima M, Kong L, Yang H. Effects of the structures of polymerizable monomers on the electro-optical properties of UV cured polymer dispersed liquid crystal films. Journal of Polymer Science Part B: Polymer Physics. 2008;**46**:1369-1375

[119] Liu F, Cao H, Mao Q, Song P, Yang H. Effects of monomer structure on the morphology of polymer networks and

the electro-optical properties of polymer-dispersed liquid crystal films. Liquid Crystals. 2012;**39**:419-424

[120] Lu Y, Wei J, Shi Y, Jin O, Guo J. Effects of fabrication condition on the network morphology and electro-optical characteristics of polymer-dispersed bistable smectic a liquid crystal device. Liquid Crystals. 2013;**40**:581-588

[121] West JL, Ondris R, Erdmann M. Dichroic dye containing polymer-dispersed liquid crystal films. Proceedings of SPIE. 1990;**1257**:76-83

[122] Doane JW, Vaz NA, Wu BG, Zumer S. Field controlled light scattering from nematic microdroplets. Applied Physics Letters. 1986;**48**: 269-271

[123] Bulgakova SA, Mashin AI, Kazantseva IA, Kashtanov DE, Jones MM, Tsepkov GS, et al. Influence of the composition of the polymer matrix on the Electrooptical properties of films with a dispersed liquid crystal. Russian Journal of Applied Chemistry. 2008;**81**: 1446-1451

[124] Higgins DA. Probing the mesoscopic chemical and physical properties of polymer-dispersed liquid crystals. Advanced Materials. 2000;**12**: 251-264

[125] Kumar P. Preparation and characterization of dichroic polymer dispersed liquid crystals [PhD thesis]. Patiala: Thapar University; 2007

[126] Frank FC. Liquid crystals. On the theory of liquid crystals. Transactions of the Faraday Society. 1958;**25**:19-28

[127] Drzaic PS. a new director alignme nt for droplets of nematic liquid crystal with low bend-to-splay ratio. Molecular Crystals and Liquid Crystals. 1988;**154**: 289-306

[128] Erdmann JH, Zumer S, Doane JW. Configuration transition in a nematic liquid crystal confined to a small spherical cavity. Physical Review Letters. 1990;**64**:1907-1910

[129] Golemme A, Zumer S, Allender DW, Doane JW. Continuous nematic-isotropic transition in submicron-size liquid-crystal droplets. Physical Review Letters. 1988;**61**:2937-2940

[130] Volovik GE, Lavrentovich OD. Topological dynamics of defects: Boojums in nematic drops. Soviet Physics—Journal of Experimental and Theoretical Physics. 1983;**58**:1159-1166

[131] Brinkman WF, Cladis PE. Defects in liquid crystals. Physics Today. 1982; **35**:48-54

[132] Candau S, Le Roy P, Debeauvais F. Magnetic field effects in nematic and cholesteric droplets suspended in an isotropic liquid. Molecular Crystals and Liquid Crystals. 1973;**23**:283-297

[133] He J, Yan B, Yu B, Wang S, Zeng Y, Wang Y. The effect of molecular weight of polymer matrix on properties of polymer-dispersed liquid crystals. European Polymer Journal. 2007;**43**: 2745-2749

[134] Deshmukh RR, Katariya-Jain A. Novel techniques of PDLC film preparation furnishing manifold properties in a single device. Liquid Crystals. 2016;**43**:256-267

[135] Malik MK, Bhatia PG, Deshmukh RR. Effect of nematic liquid crystals on optical properties of solvent induced phase separated PDLC composite films. Indian Journal of Science and Technology. 2012;**5**:3440-3452

[136] Kalkar AK, Kunte VV, Bhamare SA. Electrooptic studies on polymer-dispersed liquid-crystal composite films. III. Poly(methyl methacrylate-Co-butyl acrylate)/E7 and poly(methyl methacrylate-Co-butyl acrylate)/E8 composites. The Journal of Applied Polymer Science. 2008;**107**:689-699

[137] Wu BG, West JL, Doane JW. Angular discrimination of light transmission through polymer-dispersed-liquid-crystal films. Journal of Applied Physiology. 1987;**62**:3925-3931

[138] Drzaic PS. Reorientation dynamics of polymer dispersed nematic liquid crystal films. Liquid Crystals. 1988;**3**: 1543-1559

[139] Wu BG, Erdmann JH, Doane JW. Response times and voltages for PDLC light shutters. Liquid Crystals. 1989;**5**: 1453-1465

[140] Deshmukh RR, Malik MK. Effect of temperature on the optical and electro-optical properties of poly (methyl methacrylate)/E7 polymer-dispersed Liquid crystal composites. Journal of Applied Polymer Science. 2008;**109**:627-637

[141] Reamey RH, Montoya W, Wong A. Video microscopy of NCAP films: The observation of LC droplet in real time. Proceedings of SPIE. 1992;**1665**:2-7

[142] Hirai Y, Niiyama S, Ooi Y, Kumai H, Wakabayashi T, Gunjima T. Recent development in polymer dispersed LCDS. Society for Information Display Technical Digest. 1994;**25**:833-836

[143] Deshmukh RR, Katariya-Jain A. The complete morphological, electro-optical and dielectric study of dichroic dye doped polymer dispersed liquid crystal. Liquid Crystals. 2014;**41**: 960-975

[144] Han JW, Kang TJ, Park G. Effects of composition, curing-time, and temperature on the electro-optical characteristics of polymer-dispersed liquid crystal films. Journal of the Korean Physical Society. 2000;**36**: 156-163

[145] Neeraj, Raina KK. Multiwall carbon nanotubes doped ferroelectric liquid crystal composites: A study of modified electrical behavior. Physica B. 2014; **434**:1-6

[146] Sadovoy AV, Nazvanov VF. Optical transmission of polymer dispersed liquid crystals doped with carbon nanotubes. Physics Letters. 2006;**32**:659-660

[147] Song P, Cao H, Wang F, Liu F, Yang H. The influence of the structure of curable epoxy monomers on the electro-optical properties of polymer dispersed liquid crystal devices prepared by UV initiated cationic polymerization. Liquid Crystals. 2012; **39**:433-440

[148] Wang JH, Zhang BY, Qu WZ, Chu HS, Li H. The kinetics of photo-polymerization in the fabrication of polymer-dispersed liquid crystals doped with nano-graphite. Liquid Crystals. 2010;**37**:1-11

[149] Yadav SP, Pandey KK, Misra AK, Dixit S, Manohar R. Molecular dynamics in weakly polar nematic liquid crystal doped with dye. Canadian Journal of Physics. 2011;**89**:661-665

[150] Bauman D, Hasse W. Dielectric measurements of guest-host systems. Molecular Crystals and Liquid Crystals. 1989;**168**:155-168

[151] Drzaic PS. Recent progress in dichroic polymer-dispersed liquid crystal materials. Pure and Applied Chemistry. 1996;**68**:1435-1440

[152] Malik P, Raina KK. Dichoic dye - dependent studies in guest-host polymer dispersed liquid crystal films. Physica B: Condensed Matter. 2010;**405**: 161-166

[153] Masutani A. Guest-host effect of dyes in polymer dispersed liquid crystals [PhD thesis]. Durham: Durham University; 2002

[154] Kumar P, Raina KK. Morphological and electro-optical responses of dichroic

polymer dispersed liquid crystal films. Current Applied Physics. 2007;**7**: 636-642

[155] Deshmukh RR, Malik MK. A method for estimating interfacial tension of liquid crystal embedded in polymer matrix forming PDLC. The Journal of Applied Polymer Science. 2014;**131**:41137 (1–6)

[156] Deshmukh RR, Malik MK. Effect of dichroic dye on phase separation kinetics and electro-optical characteristics of polymer dispersed liquid crystals. Journal of Physics and Chemistry of Solids. 2013;**74**:215-224

[157] Deshmukh RR, Malik MK. Photopolymerisation kinetics and electro-optical properties in mixtures of dichroic dye doped nematic liquid crystal and photocurable polymer. Liquid Crystals. 2013;**40**:1050-1059

[158] Deshmukh RR, Malik MK, Parab SS. Dichroic dye induced nonlinearity in polymer dispersed Liquid crystal materials for display devices. Advances in Materials Research. 2012;**584**:79-83

[159] Carlton RA. Pharmaceutical Microscopy. Springer: New York; 2011

[160] Katariya-Jain A, Deshmukh RR. Influence of a guest dichroic azo dye on a host liquid crystal dispersed in polymer matrix. International Journal of ChemTech Research. 2014;**6**:1813-1816

[161] Lagerwall JPF, Scalia G. Carbon nanotubes in liquid crystals. Journal of Materials Chemistry. 2008;**18**:2890-2898

[162] Katariya-Jain A, Deshmukh RR. Electro-optical and dielectric study of multi-walled carbon nanotube doped polymer dispersed liquid crystal films. Liquid Crystals. 2019;**46**:1191-1202

[163] Domash LH, Crawford GP, Ashmead AC, Smith RT, Popovich MM, Storey J. Holographic PDLC for photonic applications. Proceedings of SPIE. 2000;**4107**:46-58

[164] Ma J, Huang W, Xuan L, Yokoyama H. Holographic polymer-dispersed liquid crystals: From materials and morphologies to applications. In: Vaibhav Jain V, Kokil A, editors. Optical Properties of Functional Polymers and Nano Engineering Applications. Boca Raton: CRC Press, Taylor & Francis Group; 2015

[165] Villa-Manríquez JF, Ortiz-Gutiérrez M, Pérez-Cortés M, Ibarra-Torre JC, Arturo Olivares-Pérez M. Holographic gratings recorded in PDLC mixed with crystal violet dye. Optik. 2017;**144**:219-223

[166] Sutherland RL, Natarajan LV, Tondiglia VP. Bragg gratings in an acrylate polymer consisting of periodic polymer-dispersed liquid-crystal planes. Chemistry of Materials. 1993;**5**:1533-1538

[167] Wang K, Zheng J, Liu Y, Gao H, Zhuang S. Electrically tunable two-dimensional holographic polymer-dispersed liquid crystal grating with variable period. Optics Communication. 2017;**392**:128-134

[168] Jakubiak R, Bunning TJ, Vaia RA, Natarajan LV, Tondiglia VP. Electrically switchable, one-dimensional polymeric resonators from holographic photopolymerization: A new approach for active photonic Bandgap materials. Advanced Materials. 2003;**15**:241-244

[169] Sarkar MD, Gill NL, Whitehead JB, Crawford GP. Effect of monomer functionality on the morphology and performance of the holographic transmission gratings recorded on polymer dispersed liquid crystals. Macromolecules. 2003;**36**:630-638

[170] Caputo R, Veltri A, Umeton C, Sukhov AV. Kogelnik-like model for the

diffraction efficiency of POLICRYPS gratings. Journal of the Optical Society of America B: Optical Physics. 2005;**22**: 735-742

[171] Coates D. Polymer dispersed liquid crystals. Journal of Materials Chemistry. 1995;**5**:2063-2072

[172] Liu Y, Zheng J, Shen T, Wang K, Zhuang S. Diffusion kinetics investigations of nano Ag-doped holographic polymer dispersed liquid crystal gratings. Liquid Crystals. 2019; **46**:1050-1059